

Supplementary Tables

Table S1: 95% quantiles of the $U_{A,B,C}$ statistic in a 40 kb window, under different demographic scenarios and archaic allele frequency cutoffs in the outgroup (A) and target (B) population panels. The demographic scenarios correspond to scenarios A, B, C and G from Figure 2. The bottlenecks were 5X and lasted 200 generations.

Max. outgroup freq.	Min. target freq.	Scenario	95% quantile under neutrality
0.01	0.8	Admixture (2%)	0
0.01	0.8	Admixture (10%)	0
0.01	0.8	Admixture (25%)	0
0.01	0.8	Ancestral Structure (strong mig.)	0
0.01	0.8	Ancestral Structure (medium mig.)	1
0.01	0.8	Ancestral Structure (weak mig.)	18
0.01	0.8	Admixture (2%), then bottleneck	0
0.01	0.8	Admixture (10%), then bottleneck	0
0.01	0.8	Admixture (25%), then bottleneck	0.05
0.01	0.8	Bottleneck, then admixture (2%)	0
0.01	0.8	Bottleneck, then admixture (10%)	0
0.01	0.8	Bottleneck, then admixture (25%)	0
0.01	0.5	Admixture (2%)	2
0.01	0.5	Admixture (10%)	2
0.01	0.5	Admixture (25%)	5
0.01	0.5	Ancestral Structure (strong mig.)	0
0.01	0.5	Ancestral Structure (medium mig.)	5
0.01	0.5	Ancestral Structure (weak mig.)	22
0.01	0.5	Admixture (2%), then bottleneck	2
0.01	0.5	Admixture (10%), then bottleneck	2
0.01	0.5	Admixture (25%), then bottleneck	8
0.01	0.5	Bottleneck, then admixture (2%)	2
0.01	0.5	Bottleneck, then admixture (10%)	2
0.01	0.5	Bottleneck, then admixture (25%)	6
0.01	0.2	Admixture (2%)	6
0.01	0.2	Admixture (10%)	13
0.01	0.2	Admixture (25%)	29.05
0.01	0.2	Ancestral Structure (strong mig.)	0
0.01	0.2	Ancestral Structure (medium mig.)	9.05
0.01	0.2	Ancestral Structure (weak mig.)	25
0.01	0.2	Admixture (2%), then bottleneck	6
0.01	0.2	Admixture (10%), then bottleneck	17
0.01	0.2	Admixture (25%), then bottleneck	30
0.01	0.2	Bottleneck, then admixture (2%)	8
0.01	0.2	Bottleneck, then admixture (10%)	13.05
0.01	0.2	Bottleneck, then admixture (25%)	29
0.01	0	Admixture (2%)	24
0.01	0	Admixture (10%)	37
0.01	0	Admixture (25%)	39
0.01	0	Ancestral Structure (strong mig.)	3
0.01	0	Ancestral Structure (medium mig.)	12.05
0.01	0	Ancestral Structure (weak mig.)	27
0.01	0	Admixture (2%), then bottleneck	21
0.01	0	Admixture (10%), then bottleneck	34
0.01	0	Admixture (25%), then bottleneck	38
0.01	0	Bottleneck, then admixture (2%)	28
0.01	0	Bottleneck, then admixture (10%)	34.05
0.01	0	Bottleneck, then admixture (25%)	37.05
0.1	0.8	Admixture (2%)	0
0.1	0.8	Admixture (10%)	2
0.1	0.8	Admixture (25%)	2
0.1	0.8	Ancestral Structure (strong mig.)	0
0.1	0.8	Ancestral Structure (medium mig.)	11
0.1	0.8	Ancestral Structure (weak mig.)	23.05

0.1	0.8	Admixture (2%), then bottleneck	0
0.1	0.8	Admixture (10%), then bottleneck	2
0.1	0.8	Admixture (25%), then bottleneck	2
0.1	0.8	Bottleneck, then admixture (2%)	1
0.1	0.8	Bottleneck, then admixture (10%)	2
0.1	0.8	Bottleneck, then admixture (25%)	2
0.1	0.5	Admixture (2%)	5
0.1	0.5	Admixture (10%)	6
0.1	0.5	Admixture (25%)	12
0.1	0.5	Ancestral Structure (strong mig.)	0
0.1	0.5	Ancestral Structure (medium mig.)	17
0.1	0.5	Ancestral Structure (weak mig.)	29
0.1	0.5	Admixture (2%), then bottleneck	6
0.1	0.5	Admixture (10%), then bottleneck	7
0.1	0.5	Admixture (25%), then bottleneck	12
0.1	0.5	Bottleneck, then admixture (2%)	6
0.1	0.5	Bottleneck, then admixture (10%)	6.05
0.1	0.5	Bottleneck, then admixture (25%)	12
0.1	0.2	Admixture (2%)	12
0.1	0.2	Admixture (10%)	18.05
0.1	0.2	Admixture (25%)	35
0.1	0.2	Ancestral Structure (strong mig.)	4
0.1	0.2	Ancestral Structure (medium mig.)	21
0.1	0.2	Ancestral Structure (weak mig.)	32.05
0.1	0.2	Admixture (2%), then bottleneck	14
0.1	0.2	Admixture (10%), then bottleneck	22
0.1	0.2	Admixture (25%), then bottleneck	37
0.1	0.2	Bottleneck, then admixture (2%)	14
0.1	0.2	Bottleneck, then admixture (10%)	20
0.1	0.2	Bottleneck, then admixture (25%)	37
0.1	0	Admixture (2%)	29
0.1	0	Admixture (10%)	44
0.1	0	Admixture (25%)	45
0.1	0	Ancestral Structure (strong mig.)	11
0.1	0	Ancestral Structure (medium mig.)	25
0.1	0	Ancestral Structure (weak mig.)	34
0.1	0	Admixture (2%), then bottleneck	28
0.1	0	Admixture (10%), then bottleneck	40
0.1	0	Admixture (25%), then bottleneck	44
0.1	0	Bottleneck, then admixture (2%)	35
0.1	0	Bottleneck, then admixture (10%)	41
0.1	0	Bottleneck, then admixture (25%)	45

Table S2: 95% quantiles of the $Q95_{A,B,C}$ statistic in a 40 kb window, under different demographic scenarios and archaic allele frequency cutoffs in the outgroup (A) population panel. The demographic scenarios correspond to scenarios A, B, C and G from Figure 2.

Max. outgroup freq.	Scenario	95% quantile under neutrality
0.01	Admixture (2%)	0.28
0.01	Admixture (10%)	0.37
0.01	Admixture (25%)	0.54
0.01	Ancestral Structure (strong mig.)	0.04
0.01	Ancestral Structure (medium mig.)	0.67
0.01	Ancestral Structure (weak mig.)	1
0.01	Admixture (2%), then bottleneck	0.31
0.01	Admixture (10%), then bottleneck	0.44
0.01	Admixture (25%), then bottleneck	0.6
0.01	Bottleneck, then admixture (2%)	0.28
0.01	Bottleneck, then admixture (10%)	0.42
0.01	Bottleneck, then admixture (25%)	0.55
0.1	Admixture (2%)	0.47
0.1	Admixture (10%)	0.51
0.1	Admixture (25%)	0.63
0.1	Ancestral Structure (strong mig.)	0.25
0.1	Ancestral Structure (medium mig.)	0.91
0.1	Ancestral Structure (weak mig.)	1
0.1	Admixture (2%), then bottleneck	0.53
0.1	Admixture (10%), then bottleneck	0.58
0.1	Admixture (25%), then bottleneck	0.67
0.1	Bottleneck, then admixture (2%)	0.47
0.1	Bottleneck, then admixture (10%)	0.53
0.1	Bottleneck, then admixture (25%)	0.66

Table S3: 40 kb windows that lie in the highest 99.9% quantile of both $U_{A,B,Nea,Den}$ and $Q95_{A,B,Nea,Den}$ for various outgroup panels A and target panels B, using an outgroup maximum frequency cutoff of 1%, and using different target allele frequency cutoffs (20%, 50%). For each region, we also show other statistics indicative of AI for reference. We partitioned the 1000 Genomes panels into outgroup panel A and target panel B in different ways (column “Mode”), depending on the signals we were looking for. These modes of partitioning are as follows. “Populations” = outgroup panel was the combination of all the populations that were not the target panel. “PopulationsB” = outgroup panel was the combination of all African panels (excluding admixed African-Americans), while target panel was one of the non-African panels. “Continents” = target panel was either the EUR continental panel (in which case the outgroup was AFR+EAS) or the EAS continental panel (in which case the outgroup was AFR+EUR). “ContinentsB” = target panel was the EUR continental panel (in which case the outgroup was AFR+EAS+SAS) or the EAS continental panel (in which case the outgroup was AFR+EUR+SAS) or the SAS continental panel (in which case the outgroup was AFR+EUR+EAS). “Eurasia” = target panel was EUR+EAS, while outgroup panel was AFR.

https://www.dropbox.com/s/p9k94i2c50rincq/Extreme_gene_table.xlsx?dl=0

Supplementary Figures

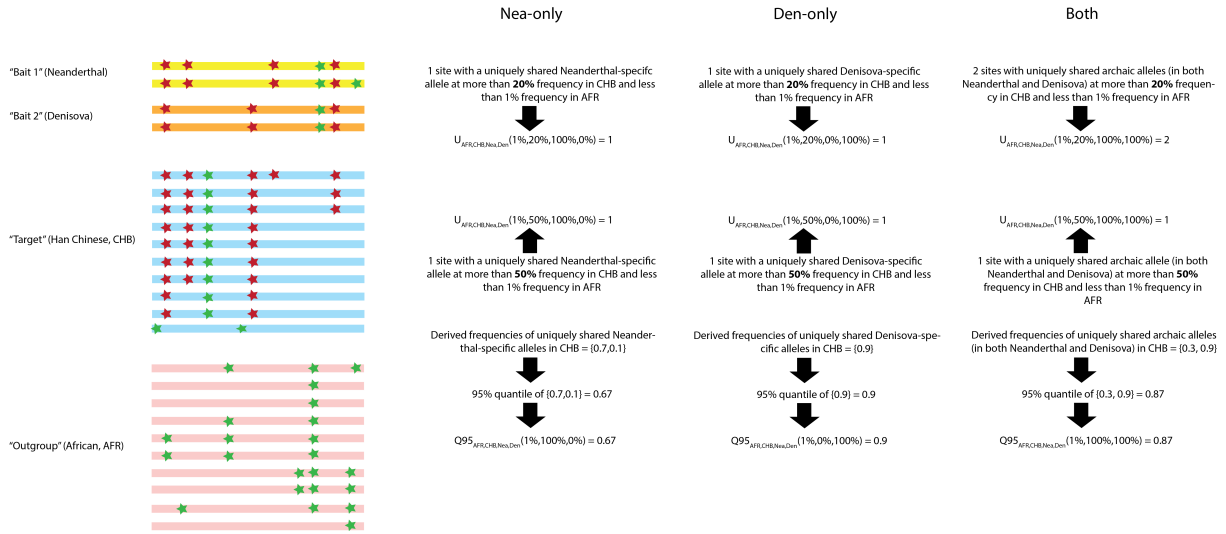


Figure S1: Schematic illustration of the way the $U_{A,B,C,D}$ and $Q95_{A,B,C,D}$ statistics are calculated.

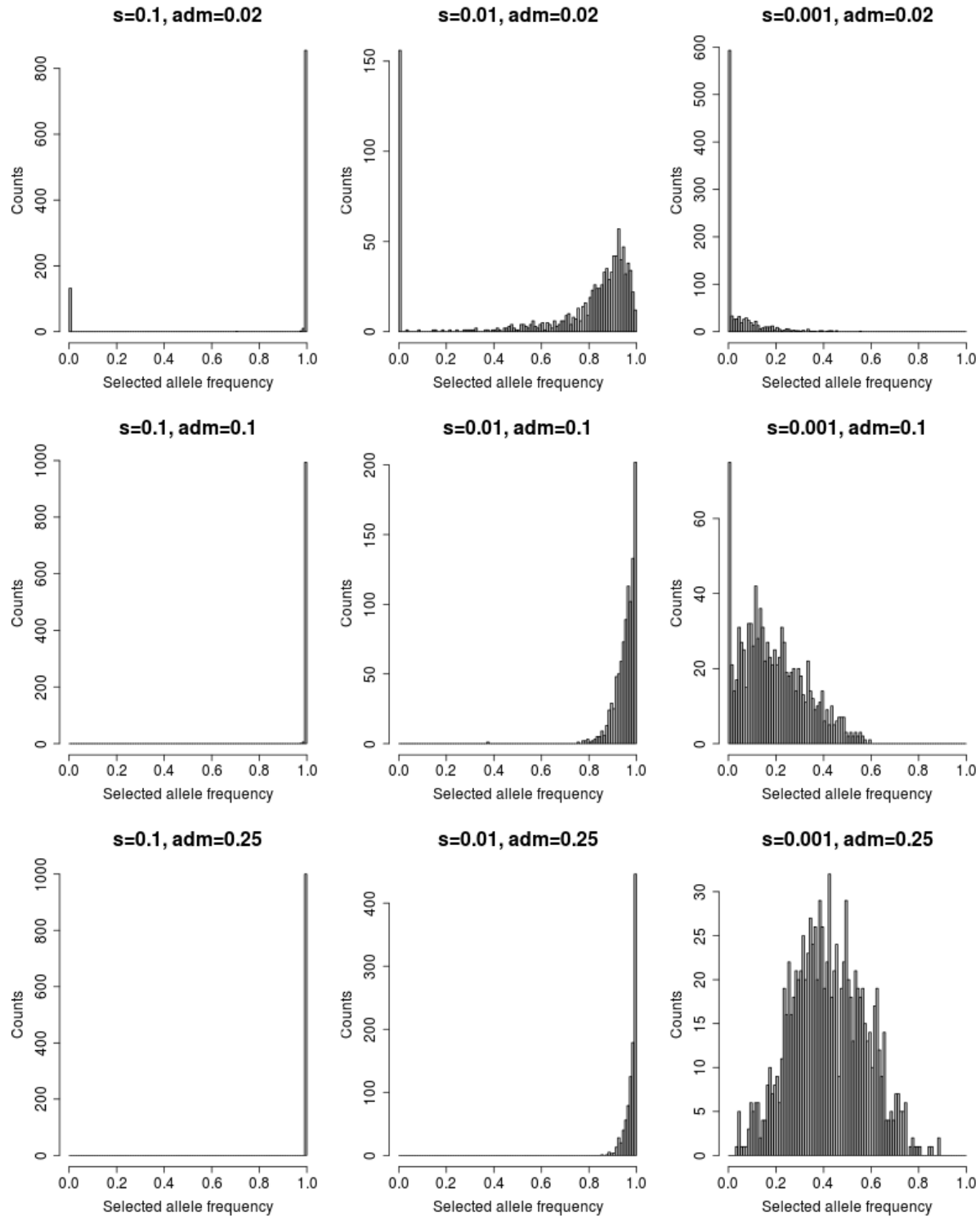


Figure S2: Histograms of the frequencies of the selected allele in the introgressed population in the present, for each AI scenario under constant population sizes.

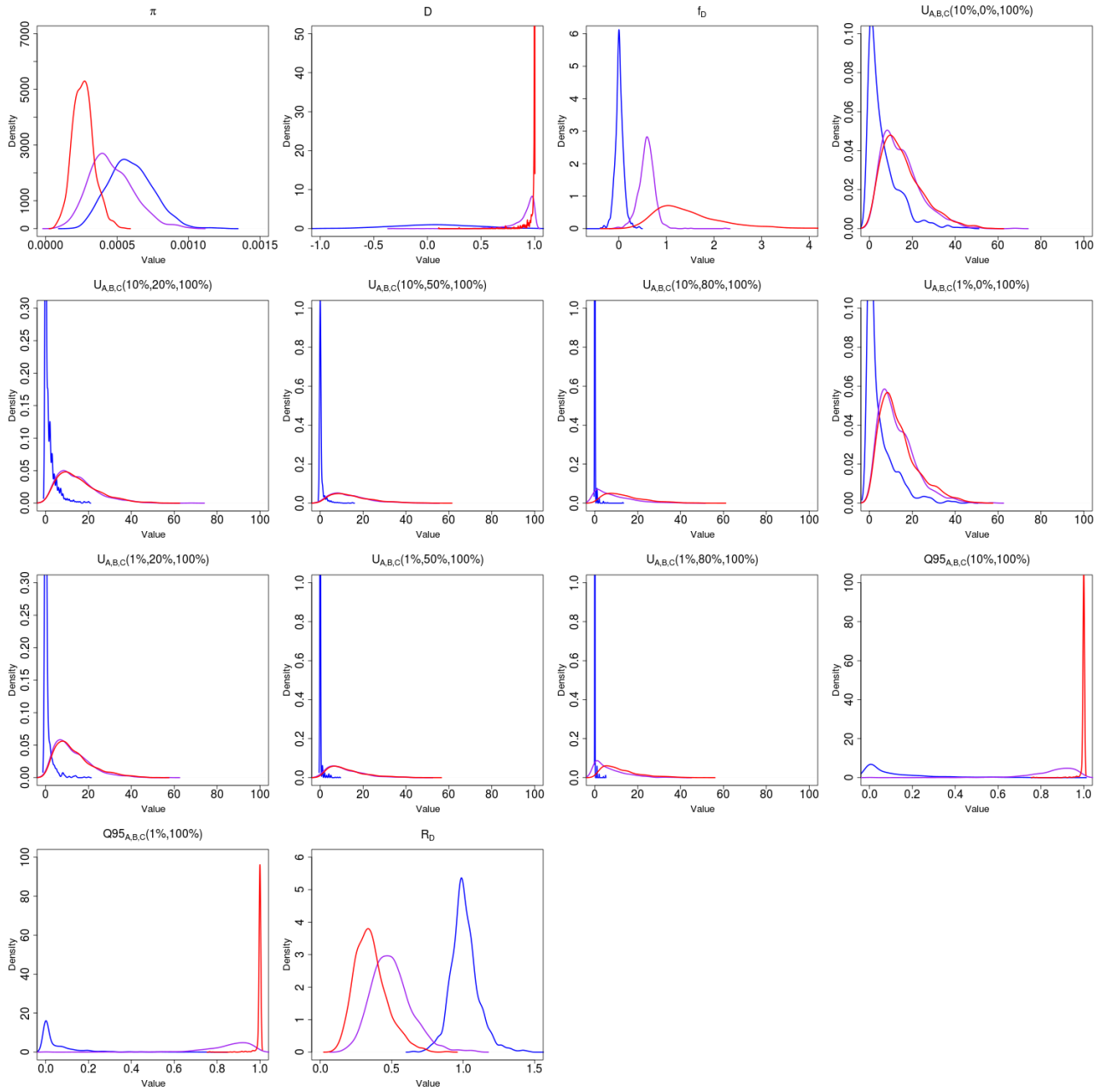


Figure S3: Density of various statistics meant to detect genetic patterns left by adaptive introgression, for three scenarios: neutrality ($s=0$) in blue, weak adaptive introgression ($s=0.01$) in purple and strong adaptive introgression ($s=0.1$) in red. The demography was the same as in Figure 3 and the admixture rate was set at 2%. See Table 1 for a definition of the statistics shown.

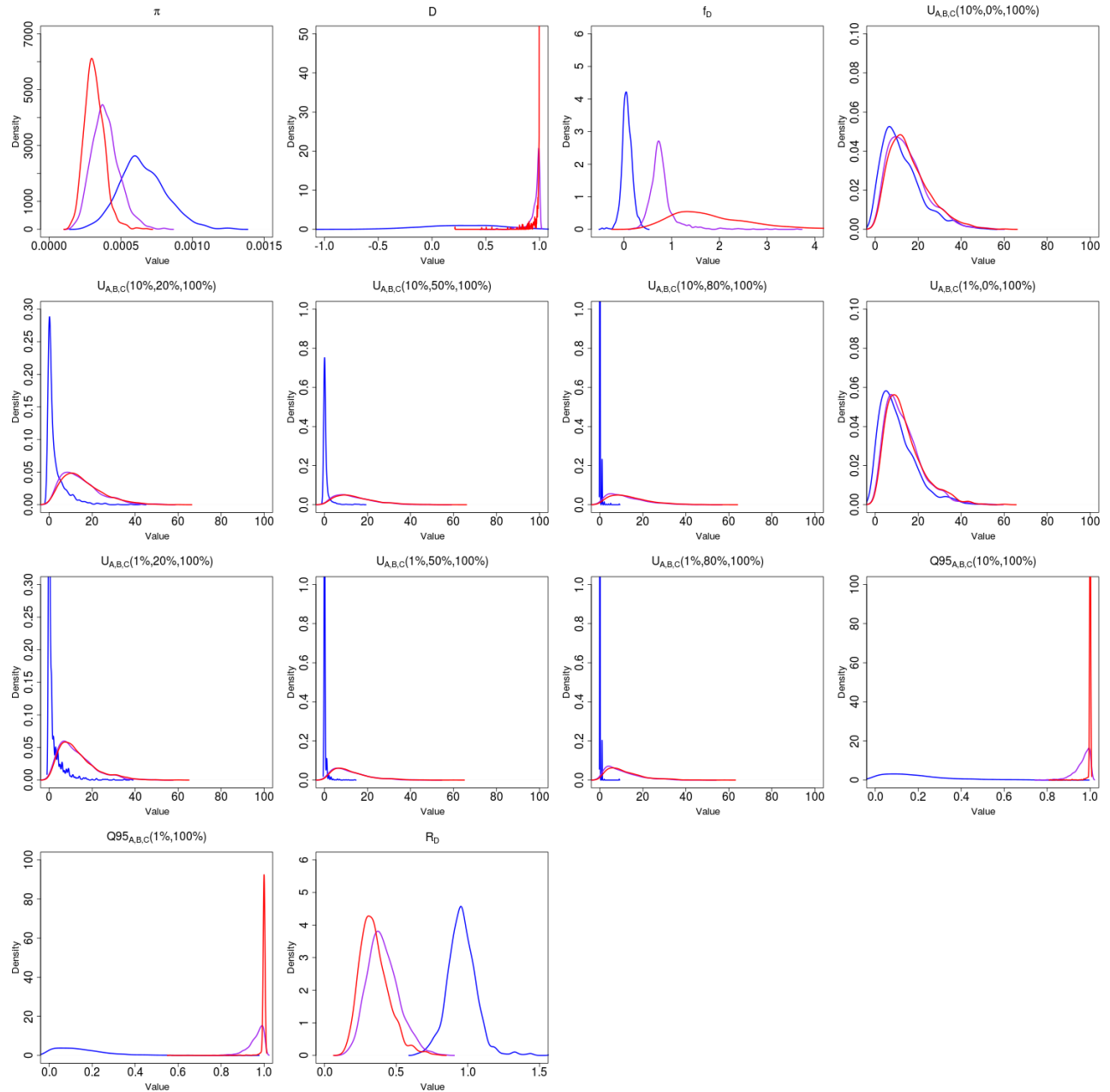


Figure S4: Density of various statistics meant to detect genetic patterns left by adaptive introgression, for three scenarios: neutrality ($s=0$) in blue, weak adaptive introgression ($s=0.01$) in purple and strong adaptive introgression ($s=0.1$) in red. The demography was the same as in Figure 3 and the admixture rate was set at 10%. See Table 1 for a definition of the statistics shown.

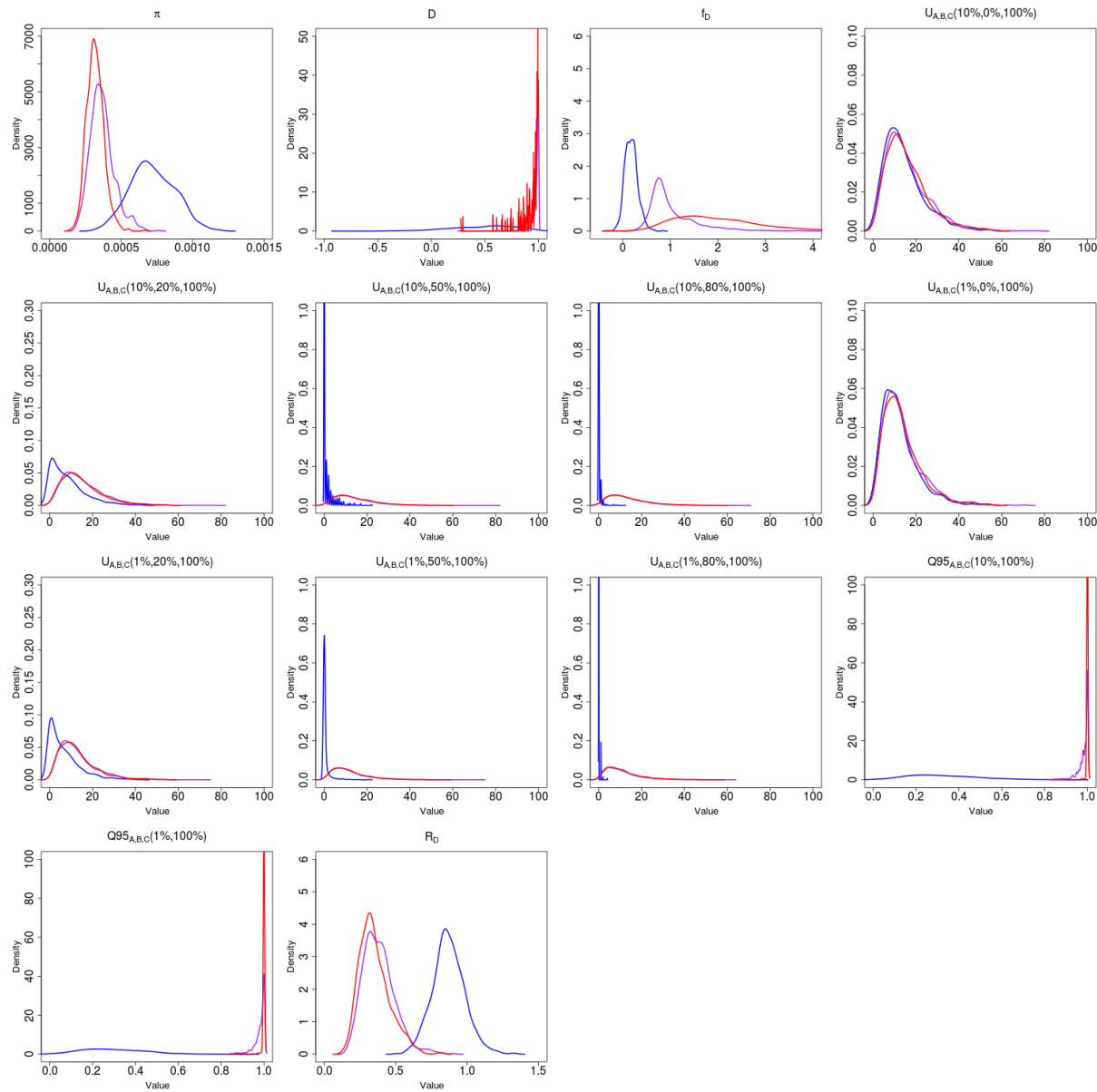


Figure S5: Density of various statistics meant to detect genetic patterns left by adaptive introgression, for three scenarios: neutrality ($s=0$) in blue, weak adaptive introgression ($s=0.01$) in purple and strong adaptive introgression ($s=0.1$) in red. The demography was the same as in Figure 3 and the admixture rate was set at 25%. See Table 1 for a definition of the statistics shown.

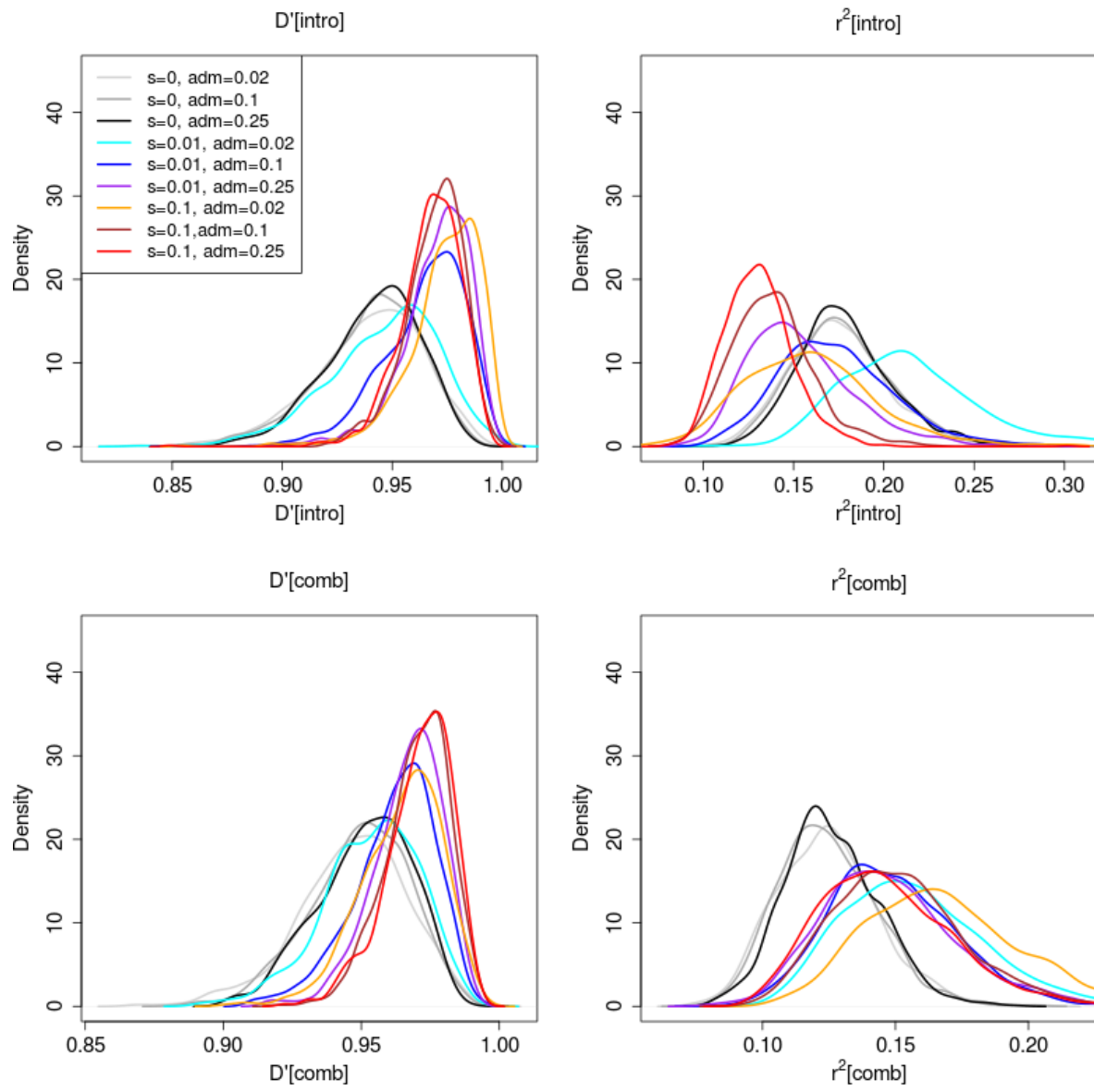


Figure S6: Density of statistics that detect patterns of linkage disequilibrium for various neutral and adaptive introgression scenarios. See Table 1 for a definition of the statistics shown.

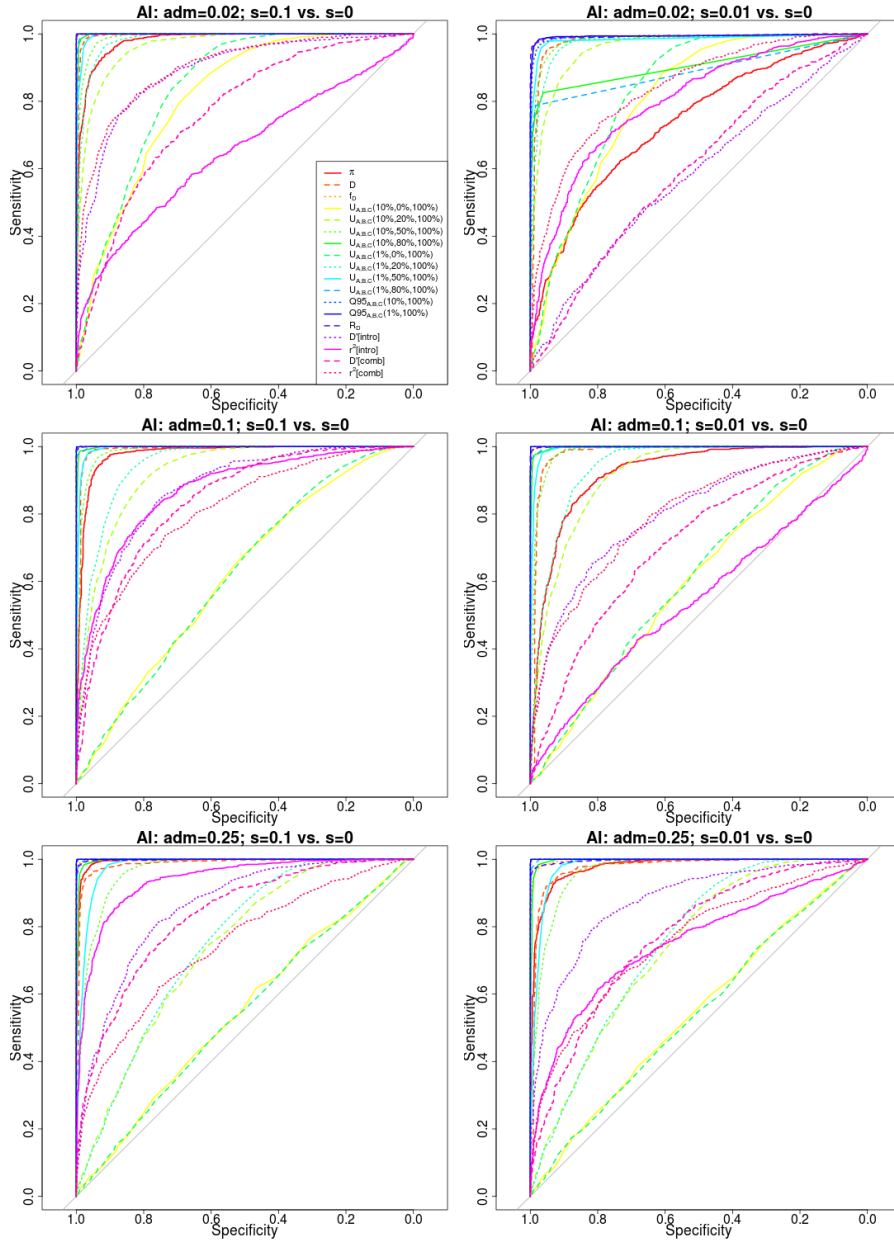


Figure S7: Receiver operating characteristic curves for adaptive introgression with constant population size, using 1,000 simulations of adaptive introgression, under various selection ($s=0.1$, $s=0.01$) and admixture rate (2%, 10%, 25%) regimes. Populations A and B split from each other 4,000 generations ago, and their ancestral population split from population C 16,000 generations ago. Population sizes were set at $2N = 20,000$. The admixture event occurred 1,600 generations ago from population C into population B,

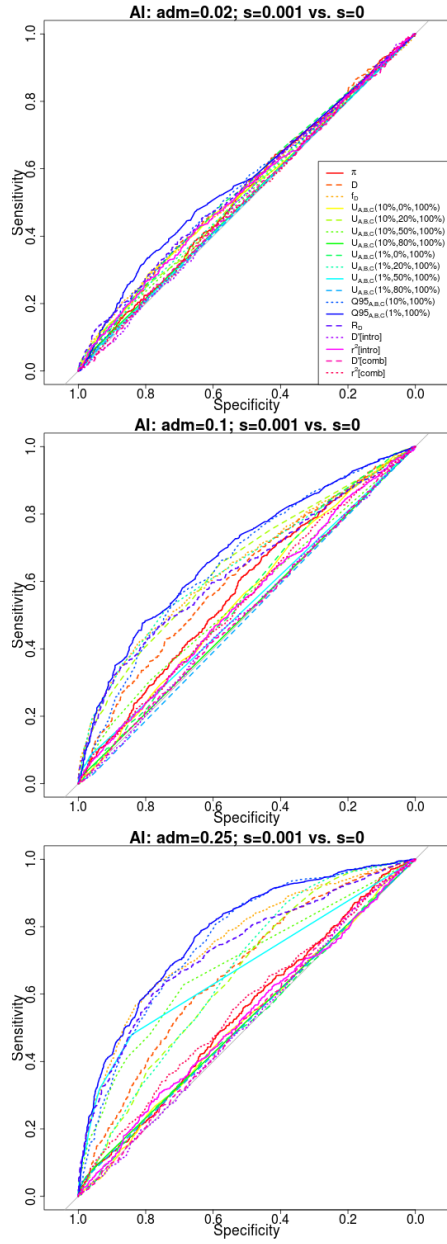


Figure S8: Receiver operating characteristic curves for adaptive introgression with constant population size, using 1,000 simulations of adaptive introgression, under weak selection ($s=0.001$) and different admixture rate (2%, 10%, 25%) regimes. Populations A and B split from each other 4,000 generations ago, and their ancestral population split from population C 16,000 generations ago. Population sizes were set at $2N = 20,000$. The admixture event occurred 1,600 generations ago from population C into population B,

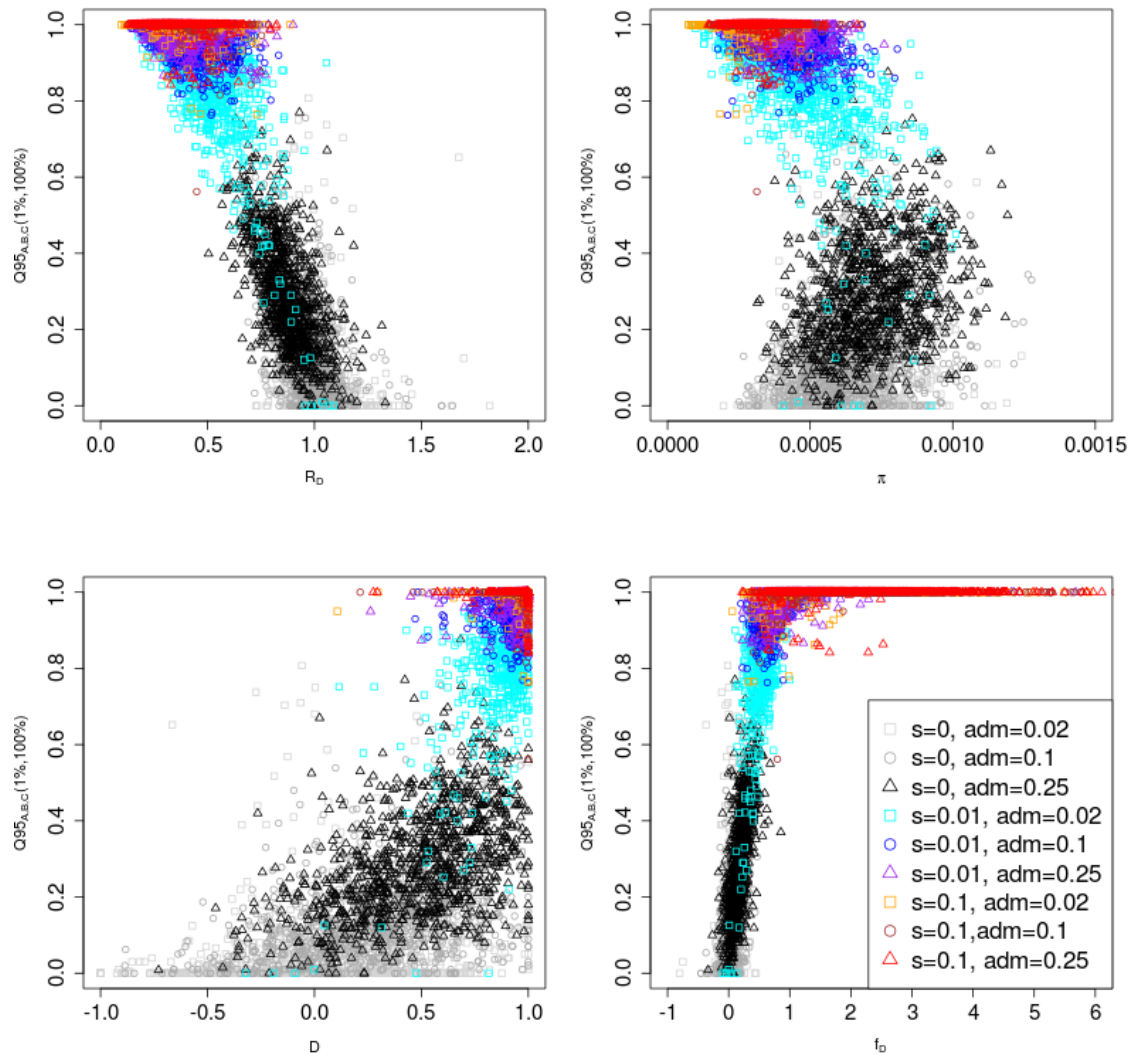


Figure S9: Joint distribution of $Q95_{A,B,C}(1\%, 100\%)$ and other statistics (R_D , π , D and f_D). 100 individuals were sampled from panel A, 100 from panel B and 2 from panel C. The demographic parameters were the same as in Figure 3.

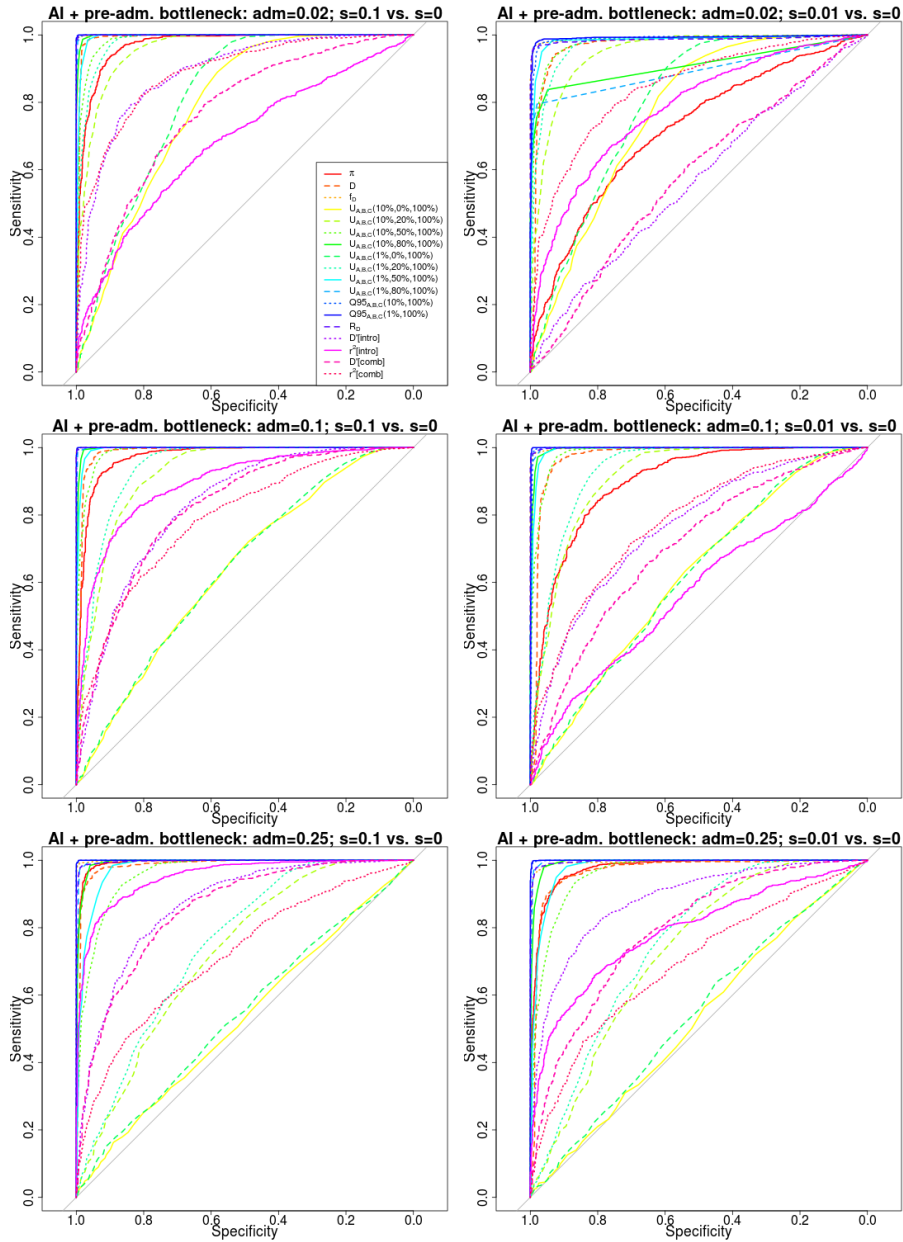


Figure S10: Receiver operating characteristic curves for adaptive introgression with a pre-admixture bottleneck, using 1,000 simulations under adaptive introgression. We simulated the same demography as in Figure 3, but also included a 5X bottleneck in population B before the introgression event, starting 3,000 generations ago and finishing 2,800 generations ago.

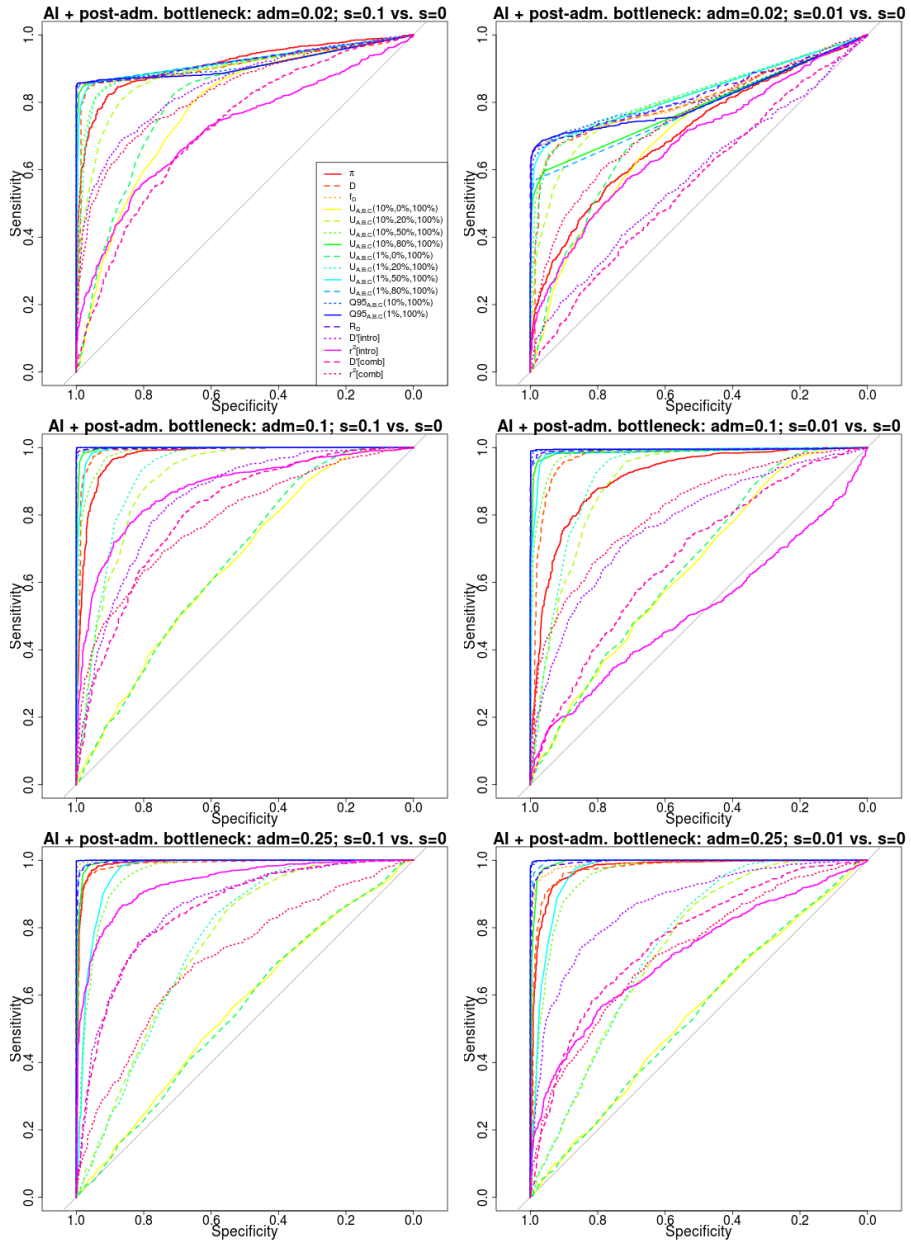


Figure S11: Receiver operating characteristic curves for adaptive introgression with a post-admixture bottleneck, using 1,000 simulations under adaptive introgression. We simulated the same demography as in Figure 3, but also included a 5X bottleneck in population B after the introgression event, starting 1,400 generations ago and finishing 1,200 generations ago.

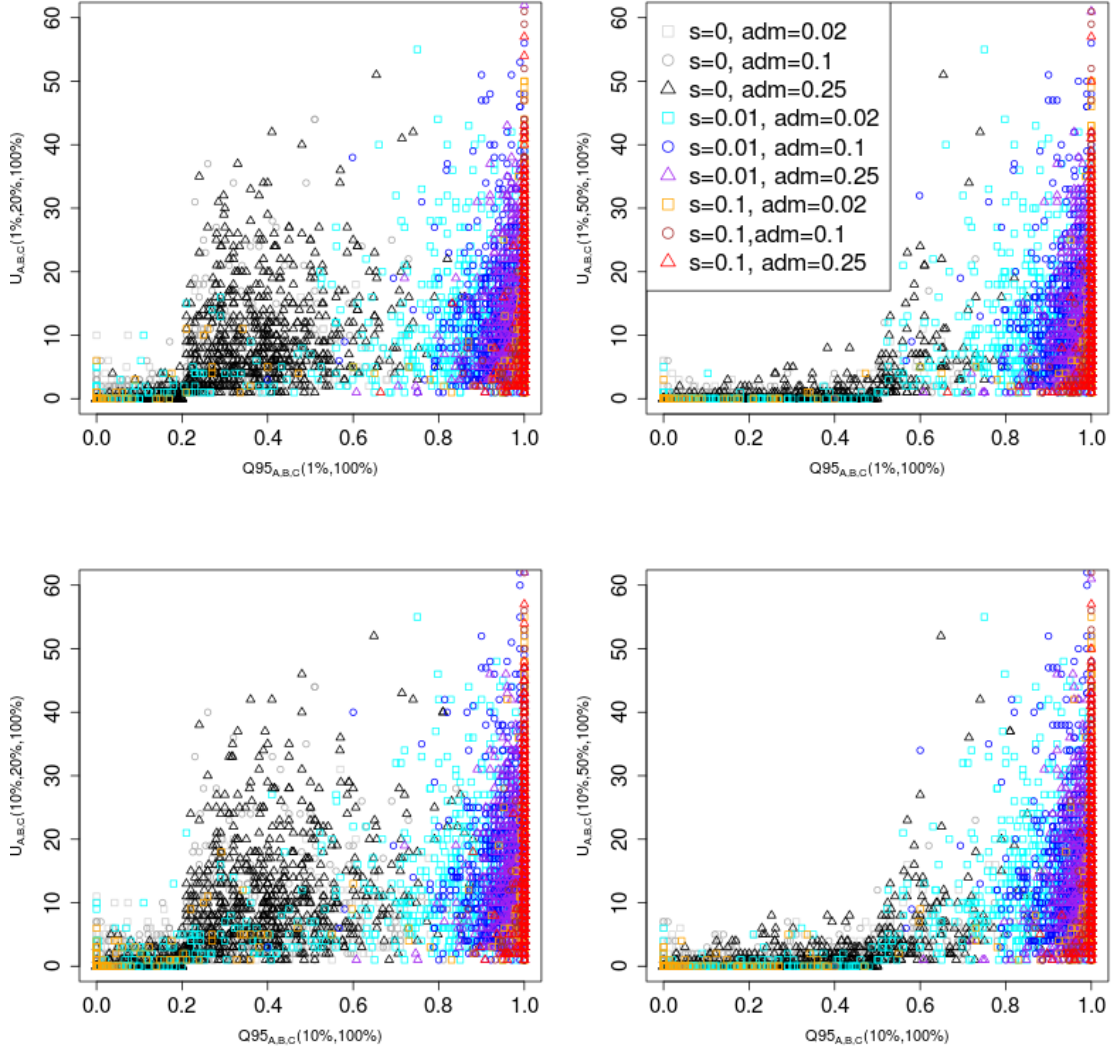


Figure S12: Joint distribution of $Q95_{A,B,C}(w, y)$ and $U_{A,B,C}(w, x, y)$ for different choices of w (1%, 10%) and x (20%, 50%). We set y to 100% in all cases. 100 individuals were sampled from panel A, 100 from panel B and 2 from panel C. In this case, we included a 5X bottleneck in population B after the introgression event, starting 1,400 generations ago and finishing 1,200 generations ago.

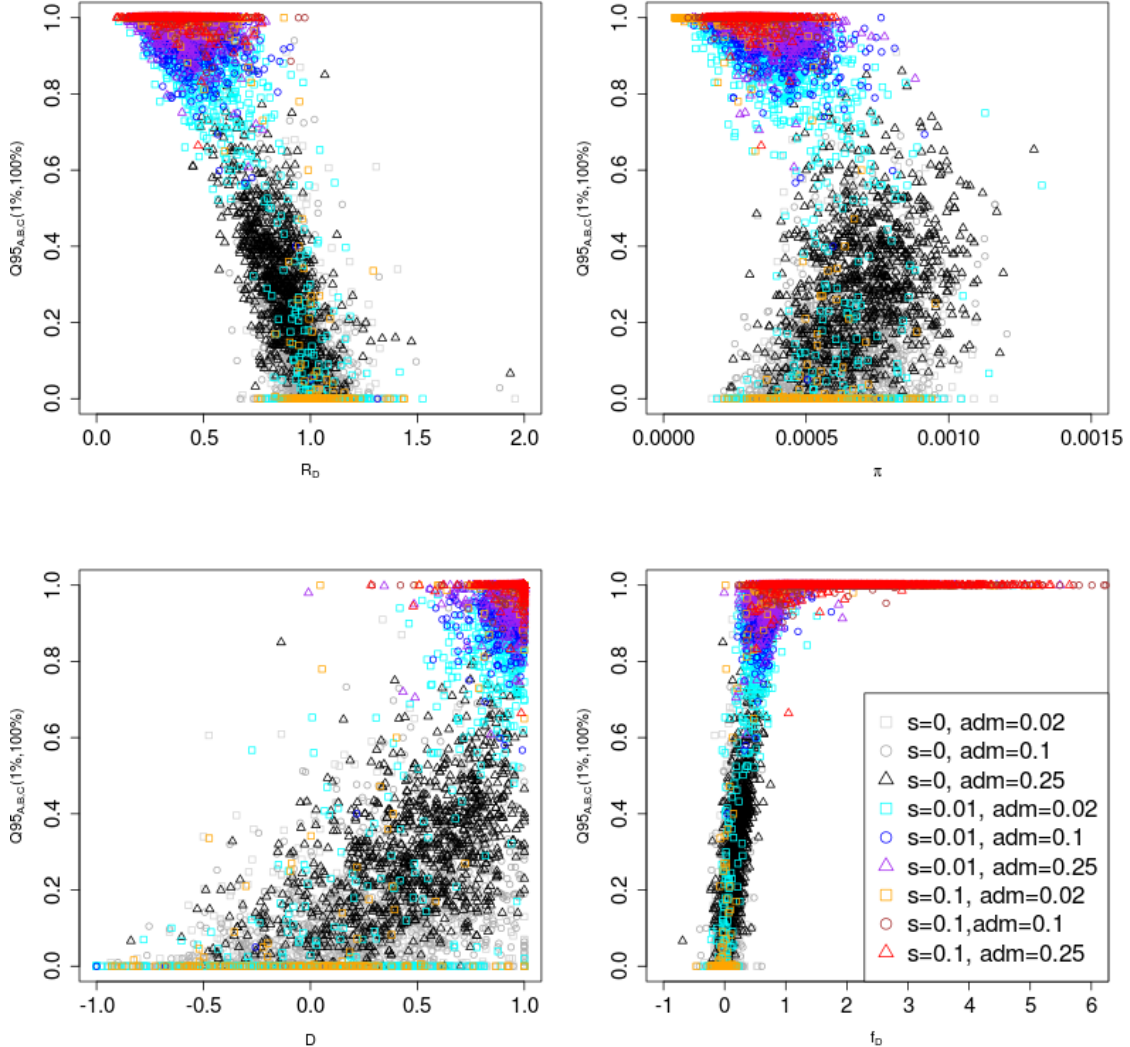


Figure S13: Joint distribution of $Q95_{A,B,C}(1\%, 100\%)$ and other statistics (R_D , π , D and f_D). 100 individuals were sampled from panel A, 100 from panel B and 2 from panel C. In this case, we included a 5X bottleneck in population B after the introgression event, starting 1,400 generations ago and finishing 1,200 generations ago.

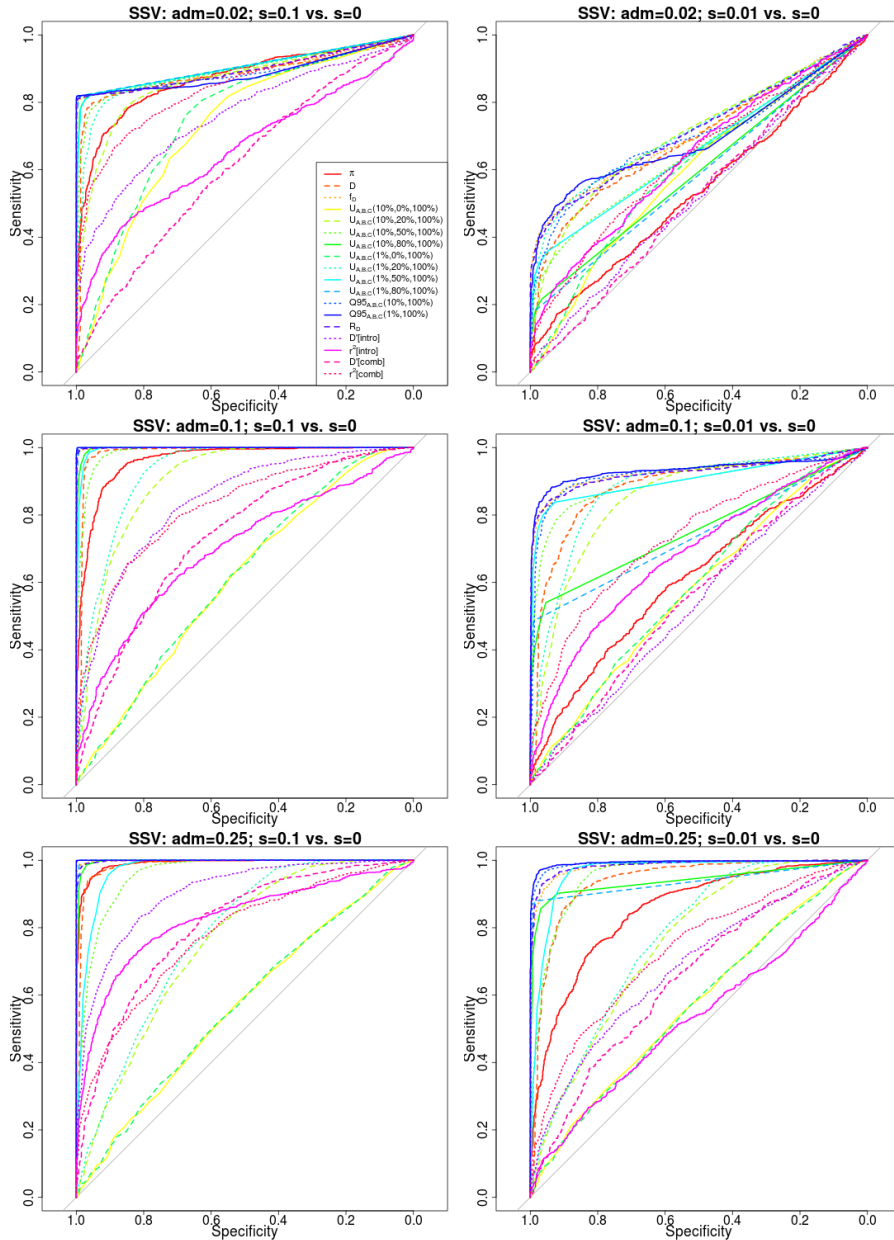


Figure S14: Receiver operating characteristic curves for adaptive introgression with an intermediate neutrality period. We simulated the same demography as in Figure 3, but changed the selection coefficient of the beneficial variant to be 0 right after the introgression event (1,600 generations ago). If still present in population B , the variant regained its original coefficient 800 generations ago.

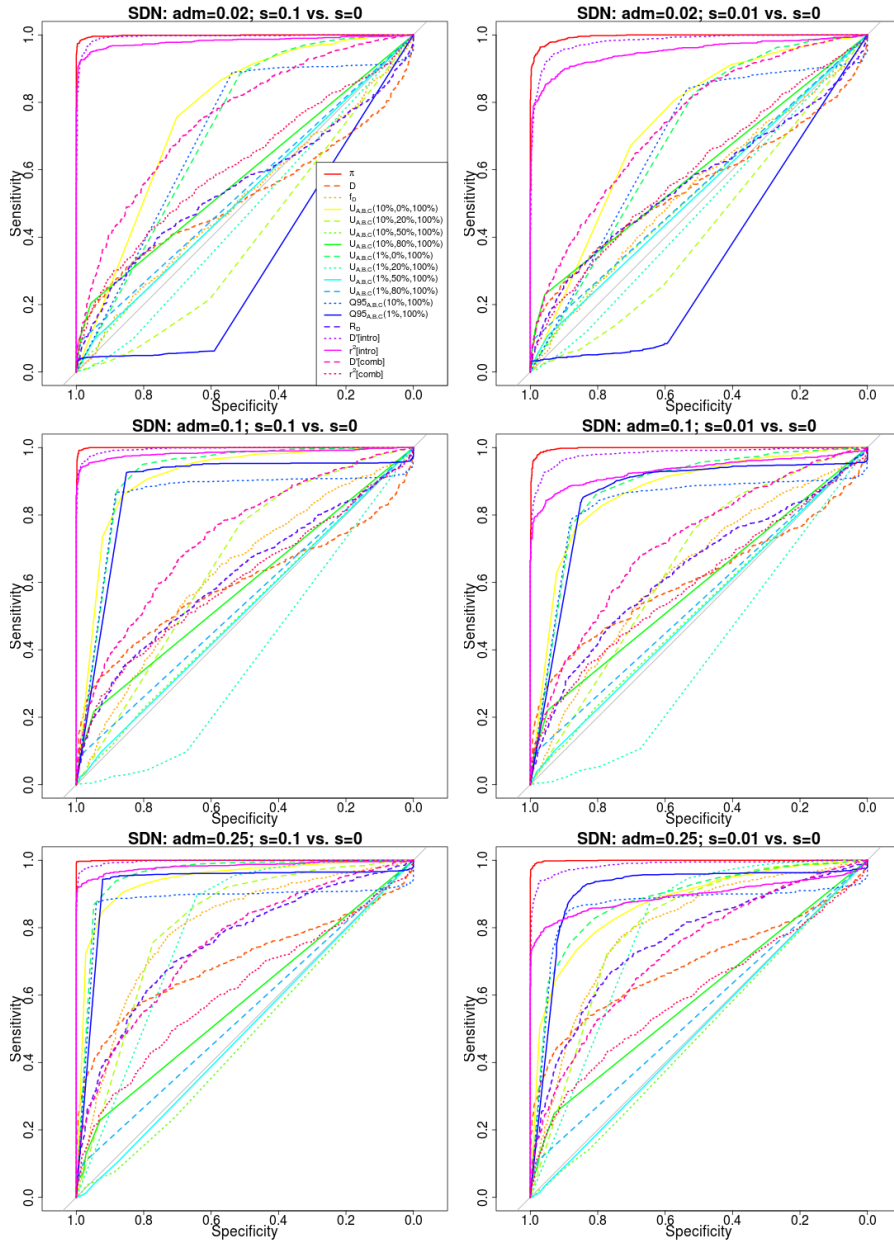


Figure S15: Receiver operating characteristic curves for a selective sweep from de novo mutation. We simulated the same demography as in Figure 3, but rather than introducing the beneficial variant in the introgressed population via admixture from an archaic population, we introduced it by mutation in the introgressed population (B) 3,900 generations ago.

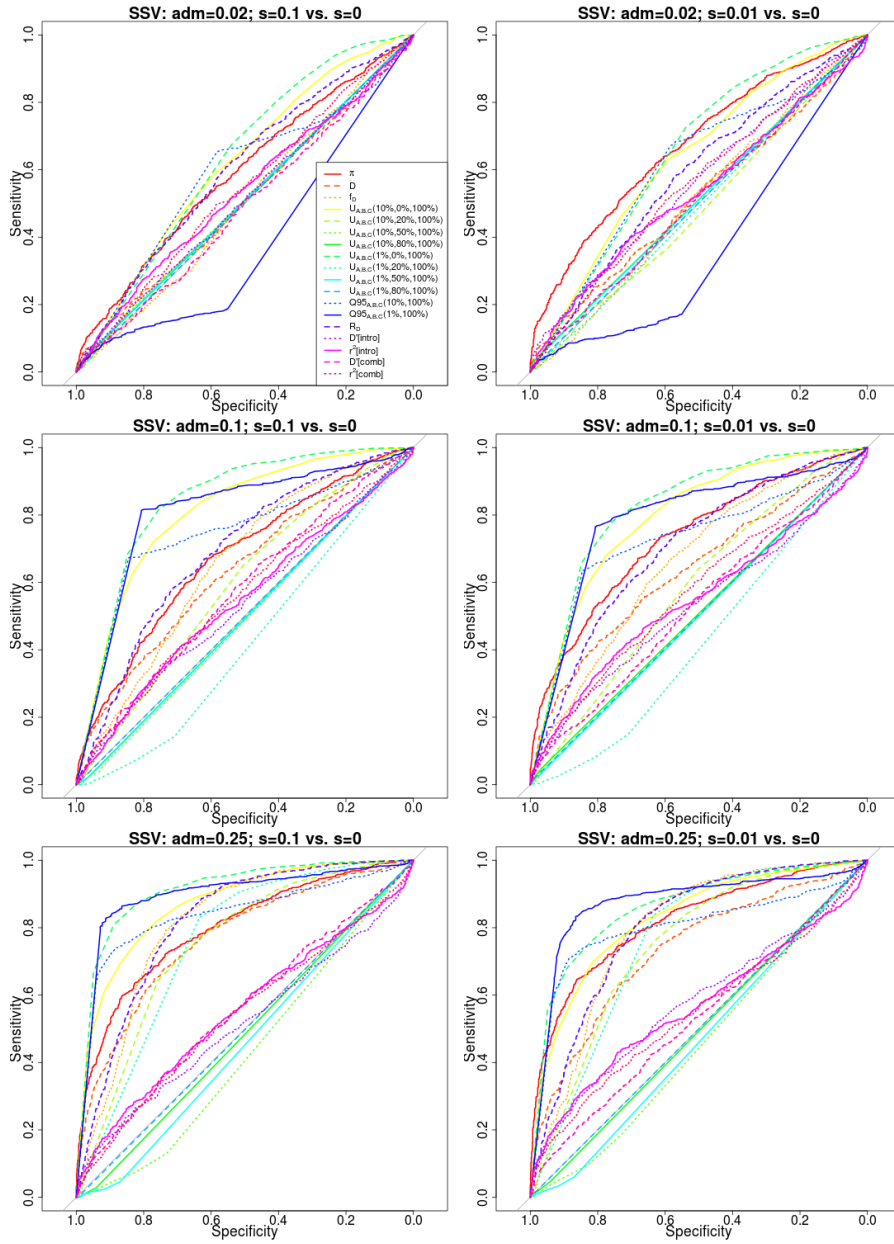


Figure S16: Receiver operating characteristic curves for selection from standing variation. We simulated the same demography as in Figure 3, but rather than introducing the beneficial variant in the introgressed population via admixture from an archaic population, we introduced it with a starting frequency of 20% in the introgressed population (B) 3,900 generations ago.

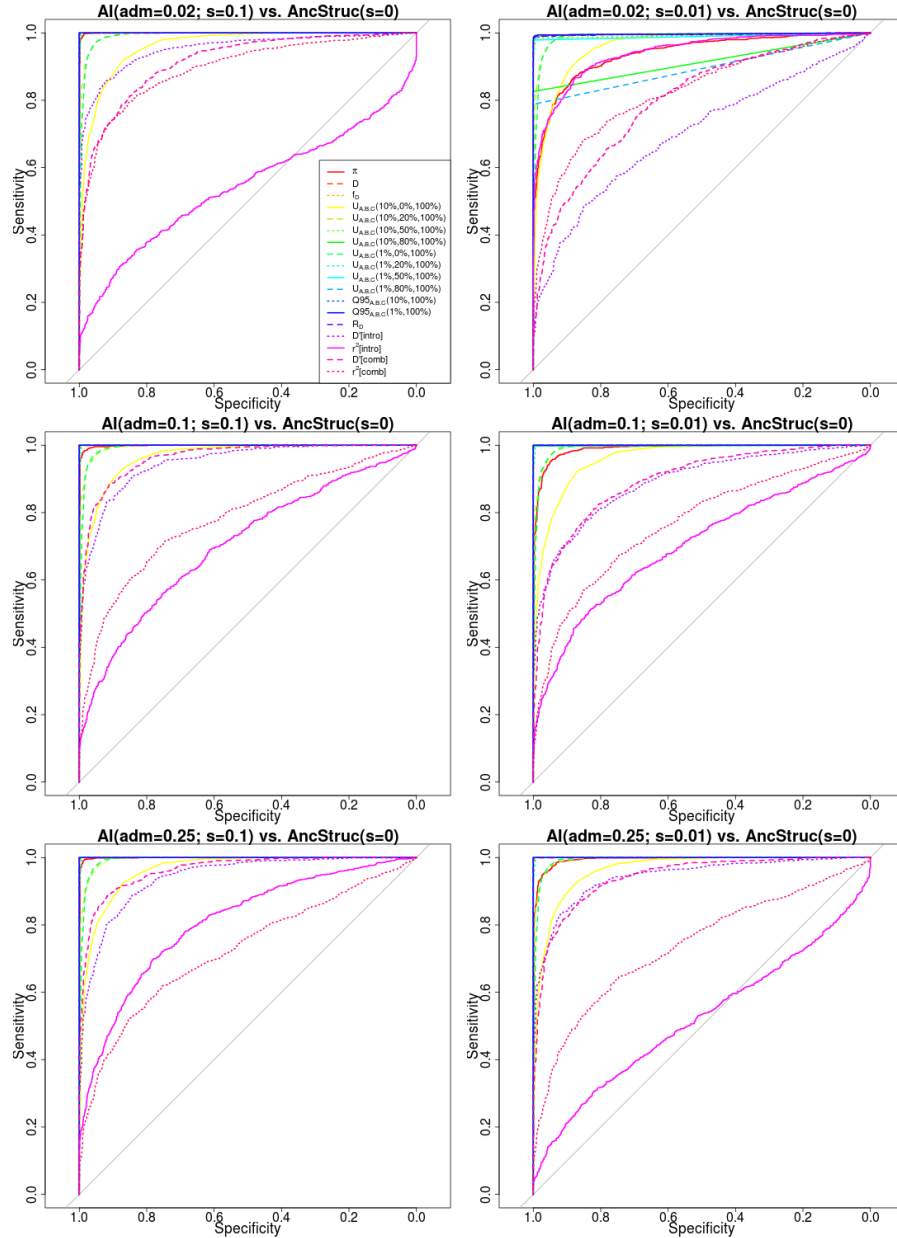


Figure S17: Receiving operating characteristic curves for adaptive introgression against a neutral ancestral structure model with strong migration rates. The demographic scenario for adaptive introgression was the same as in Figure 3. For a description of the ancestral structure model, see main text.

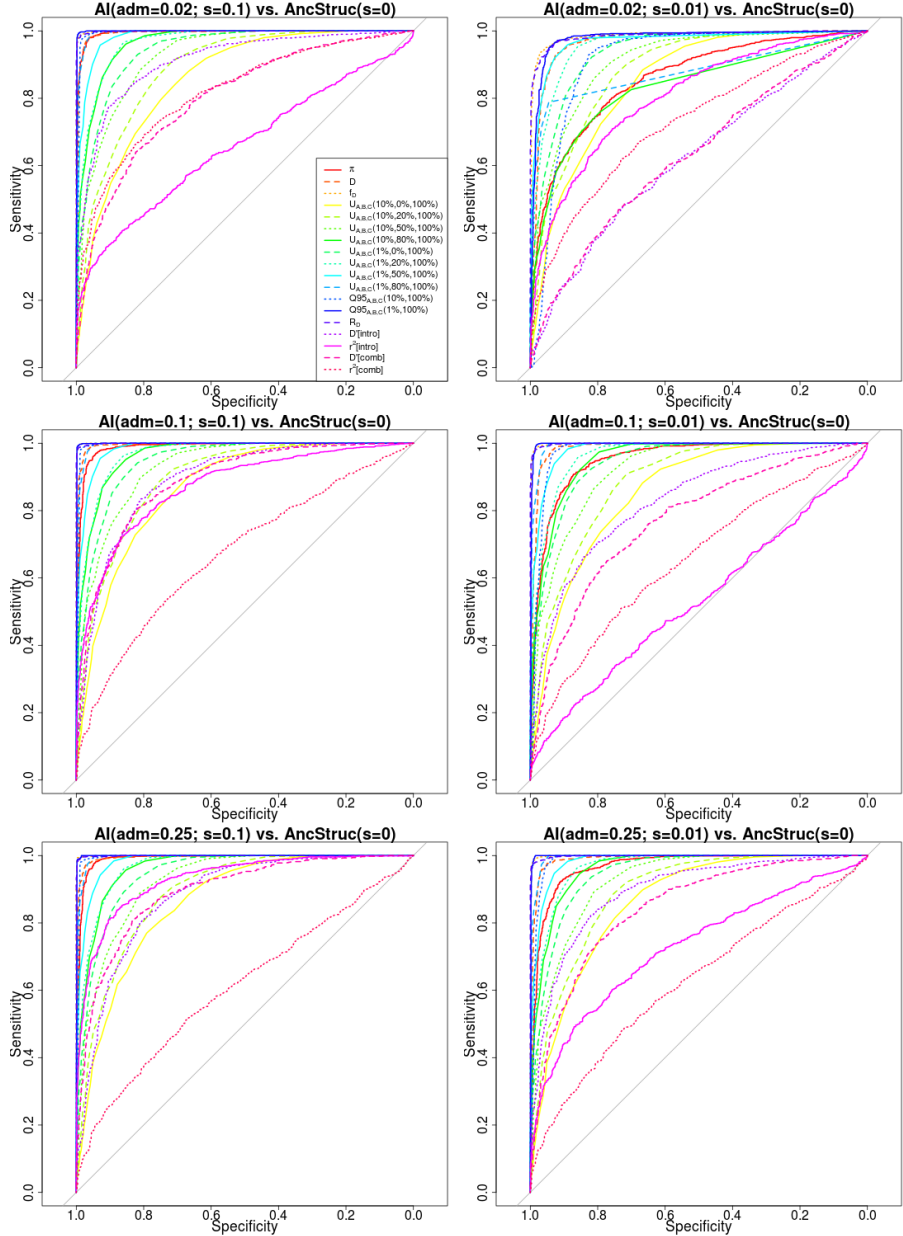


Figure S18: Receiving operating characteristic curves for adaptive introgression against a neutral ancestral structure model with intermediate migration rates. The demographic scenario for adaptive introgression was the same as in Figure 3. For a description of the ancestral structure model, see main text.

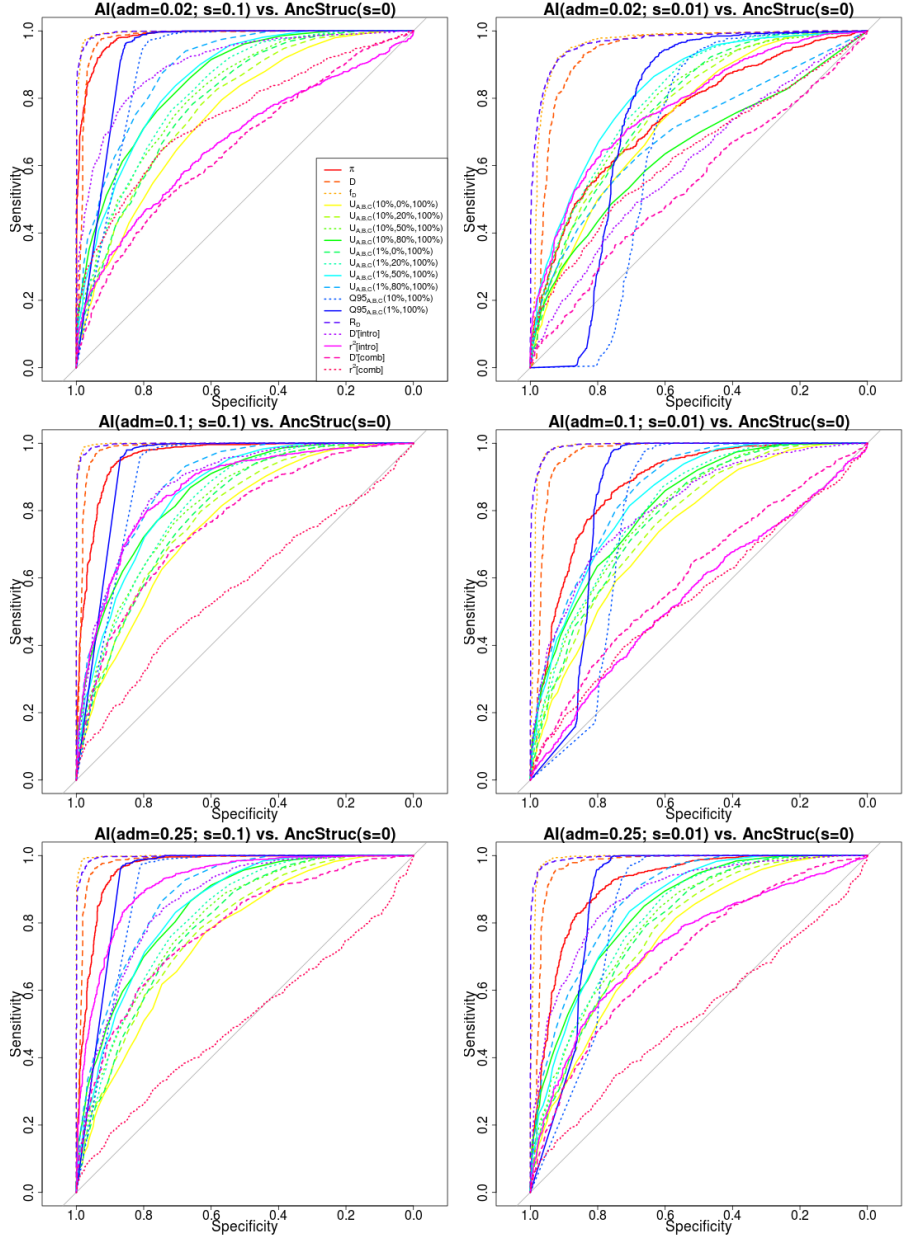


Figure S19: Receiving operating characteristic curves for adaptive introgression against a neutral ancestral structure model with weak migration rates. The demographic scenario for adaptive introgression was the same as in Figure 3. For a description of the ancestral structure model, see main text.

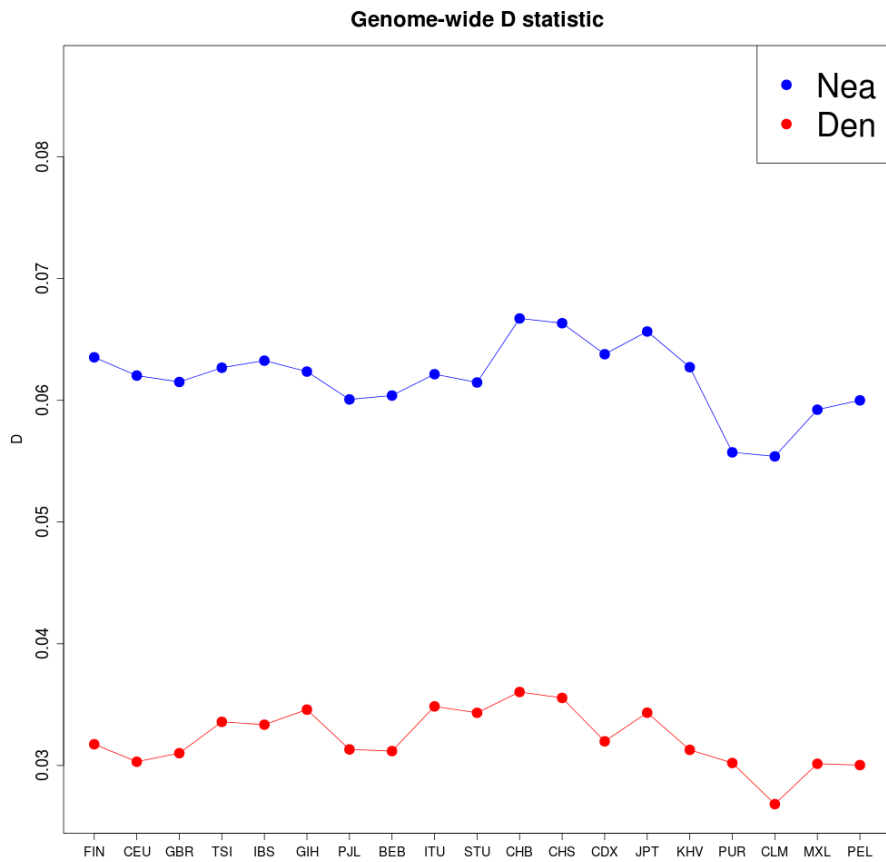


Figure S20: We computed $D(X, YRI, Y, \text{Chimpanzee})$ for different choices of present-day human panels X (x-axis) from phase 3 of the 1000 Genomes Project, and for two high-coverage archaic human genomes Y : Altai Neanderthal (blue) and Denisova (red). The low value of the right-most panel is due to that panel being composed of African-Americans, which have a higher proportion of African ancestry than the other panels.

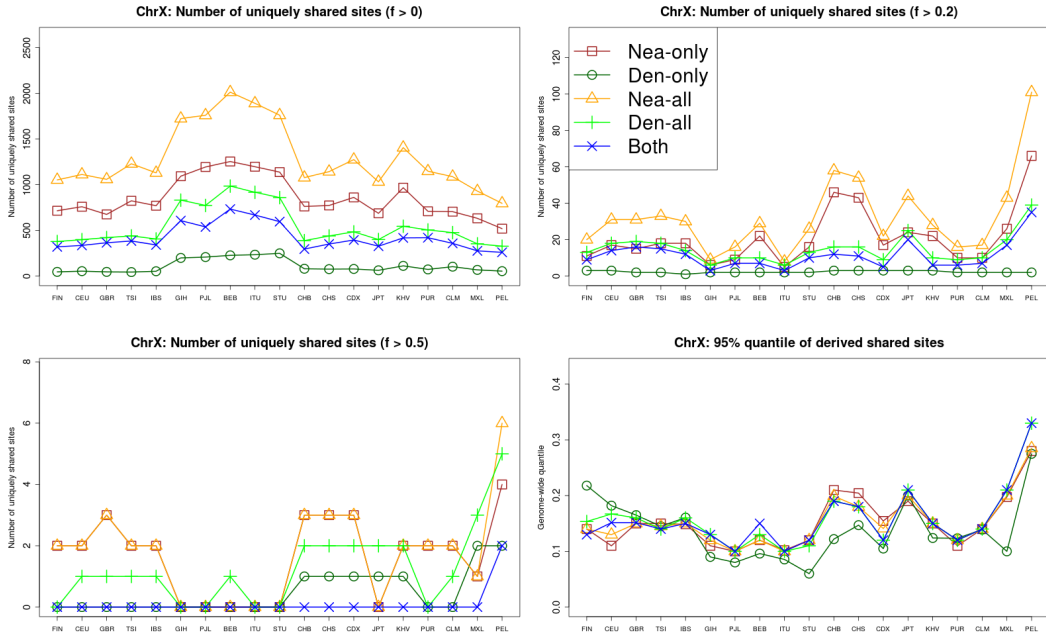


Figure S21: We computed the number of uniquely shared sites in the X chromosome between particular archaic humans genomes and different choices of present-day non-African human panels X (x-axis) from phase 3 of the 1000 Genomes Project, using a shared frequency cutoff of 0% (top-left panel), 20% (top-right panel) and 50% (bottom-left panel). Nea-only = $U_{Afr,X,Nea,Den}(1\%, 20\%, 100\%, 0\%)$. Den-only = $U_{Afr,X,Nea,Den}(1\%, 20\%, 0\%, 100\%)$. Nea-all = $U_{Afr,X,Nea}(1\%, 20\%, 100\%)$. Den-all = $U_{Afr,X,Den}(1\%, 20\%, 100\%)$. Both = $U_{Afr,X,Nea,Den}(1\%, 20\%, 100\%, 100\%)$. We also computed the quantile statistics Q95 for different choices of present-day non-African human panels (x-axis) from phase 3 of the 1000 Genomes Project (bottom-right panel). Nea-only = $Q95_{Afr,X,Nea,Den}(1\%, 100\%, 0\%)$. Den-only = $Q95_{Afr,X,Nea,Den}(1\%, 0\%, 100\%)$. Nea-all = $Q95_{Afr,X,Nea}(1\%, 100\%)$. Den-all = $Q95_{Afr,X,Den}(1\%, 50\%, 100\%)$. Both = $Q95_{Afr,X,Nea,Den}(1\%, 100\%, 100\%)$.

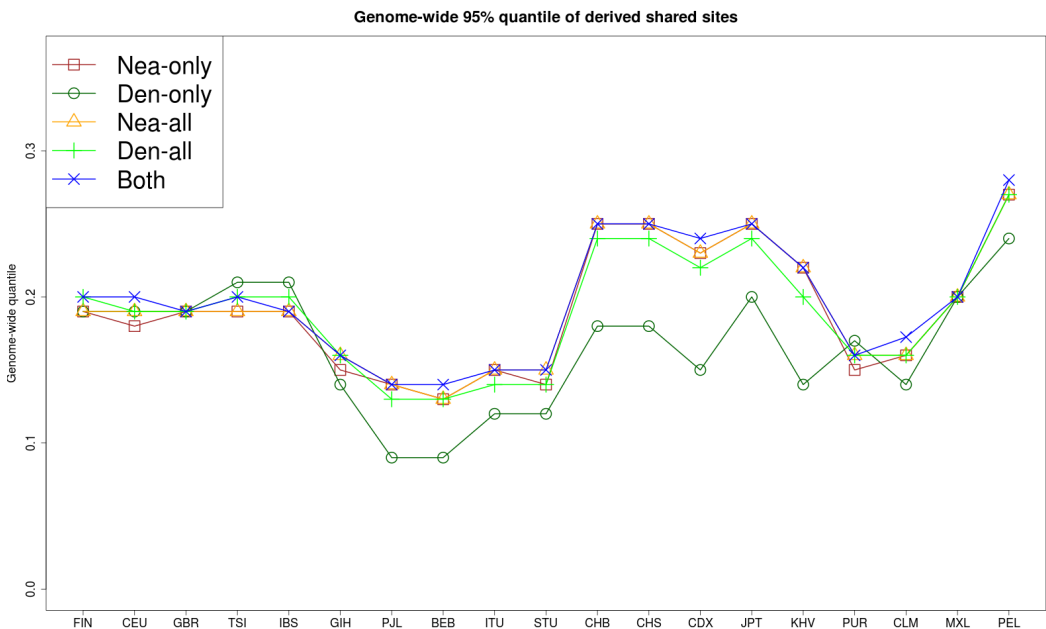


Figure S22: We computed the quantile statistics $Q95$ for different choices of present-day non-African human panels (x-axis) from phase 3 of the 1000 Genomes Project (D). Nea-only = $Q95_{Afr,X,Nea,Den}(1\%, 100\%, 0\%)$. Den-only = $Q95_{Afr,X,Nea,Den}(1\%, 0\%, 100\%)$. Nea-all = $Q95_{Afr,X,Nea}(1\%, 100\%)$. Den-all = $Q95_{Afr,X,Den}(1\%, 100\%)$. Both = $Q95_{Afr,X,Nea,Den}(1\%, 100\%, 100\%)$.

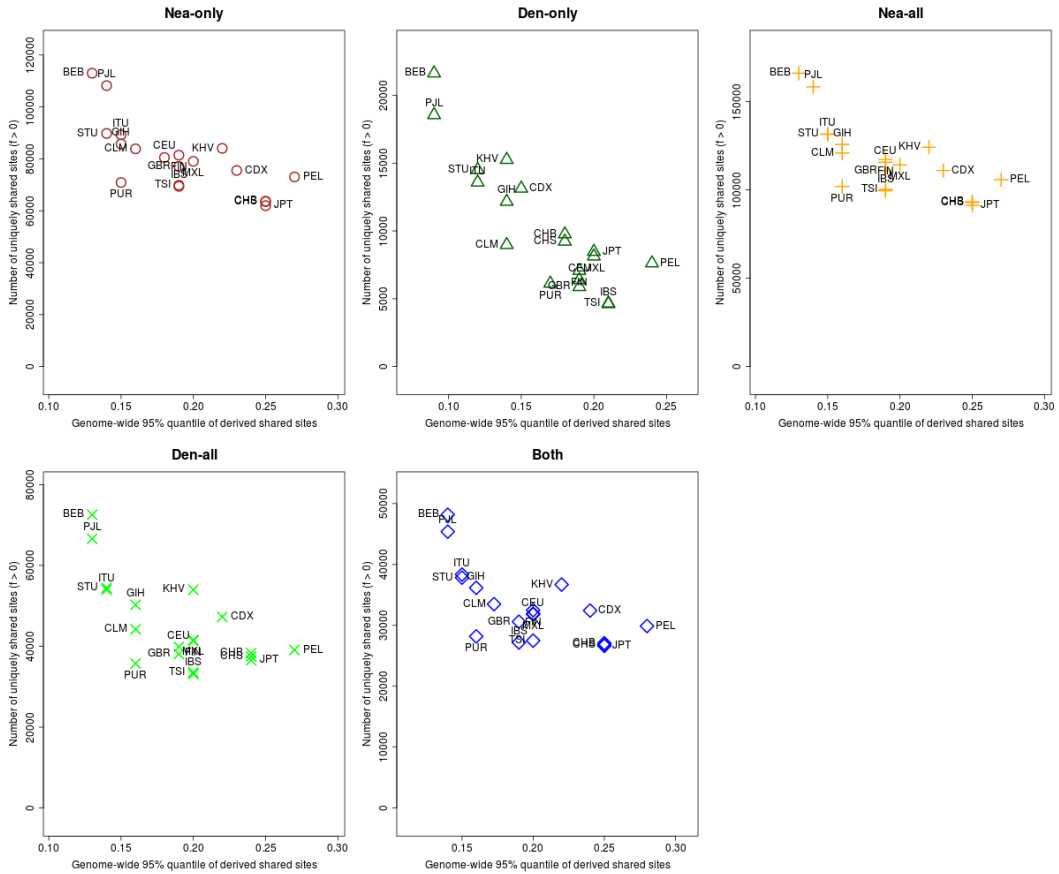


Figure S23: For each population panel from the 1000 Genomes Project, we jointly plotted the U and $Q95$ statistics with an archaic frequency cutoff of $> 0\%$ within each population. Nea-only = $U_{Afr,X,Nea,Den}(1\%, 0\%, 100\%, 0\%)$ and $Q95_{Afr,X,Nea,Den}(1\%, 100\%, 0\%)$. Den-only = $U_{Afr,X,Nea,Den}(1\%, 0\%, 0\%, 100\%)$ and $Q95_{Afr,X,Nea,Den}(1\%, 0\%, 100\%)$. Nea-all = $U_{Afr,X,Nea}(1\%, 0\%, 100\%)$ and $Q95_{Afr,X,Nea}(1\%, 100\%)$. Den-all = $U_{Afr,X,Den}(1\%, 0\%, 100\%)$ and $Q95_{Afr,X,Den}(1\%, 100\%)$. Both = $U_{Afr,X,Nea,Den}(1\%, 0\%, 100\%, 100\%)$ and $Q95_{Afr,X,Nea,Den}(1\%, 100\%, 100\%)$.

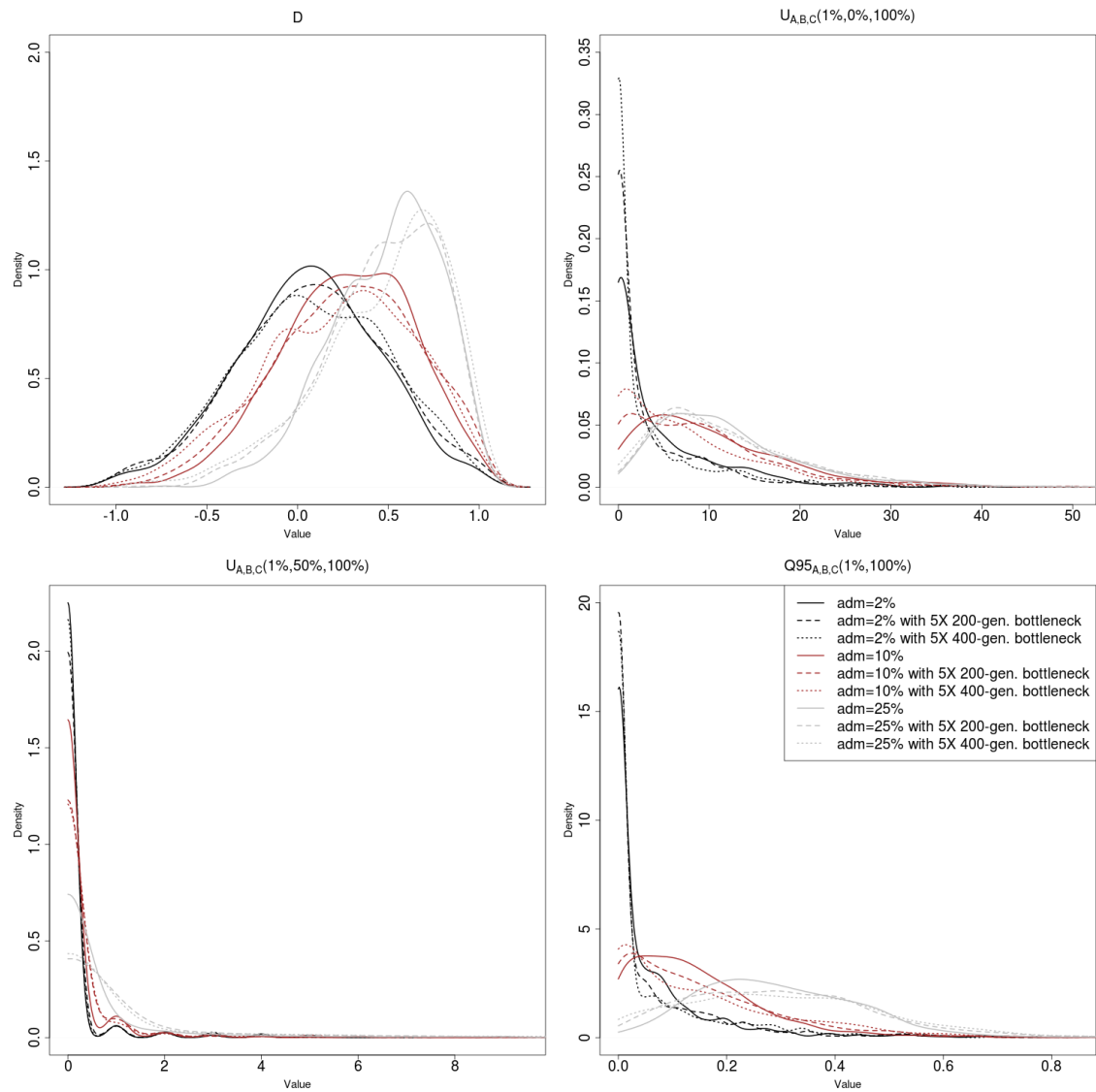


Figure S24: Effect of bottlenecks after the admixture event on the distribution of various statistics under introgression and neutrality.

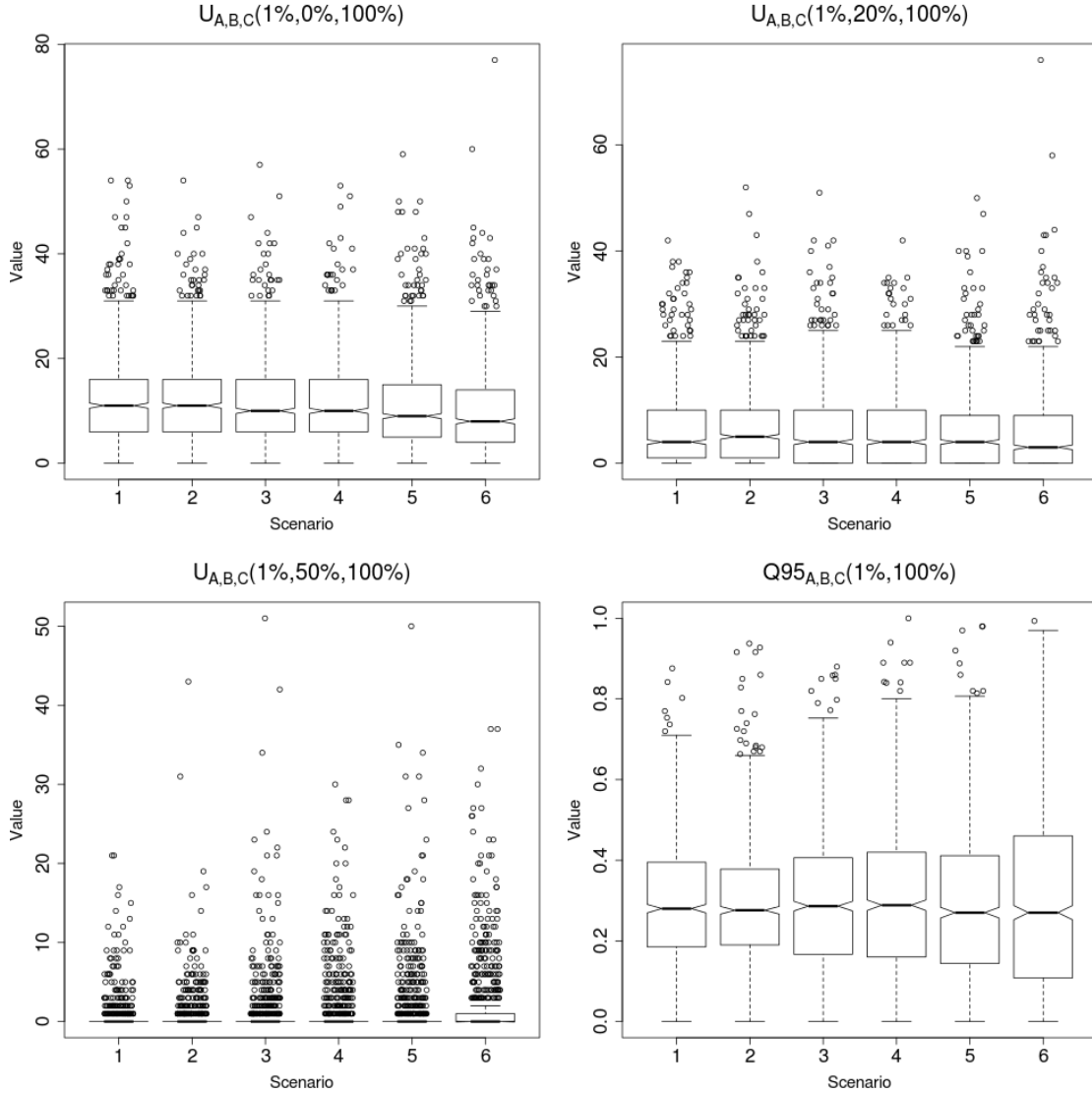


Figure S25: Boxplots showing the effect of different types of bottlenecks on the distribution of U and $Q95$ under neutrality. We performed 1,000 simulations for each of 6 different 3-population scenarios with 25% admixture from population C into population B, following the models described in Figure 2. Scenario 1: Constant population size (Figure 2.A). Scenario 2: Pre-admixture 5X bottleneck for 200 generations (Figure 2.B). Scenario 3: Post-admixture 5X bottleneck for 200 generations (Figure 2.C). Scenario 4: Post-admixture 5X bottleneck for 400 generations. Scenario 5: Post-admixture 10X bottleneck for 200 generations. Scenario 6: Post-admixture 10X bottleneck for 400 generations.

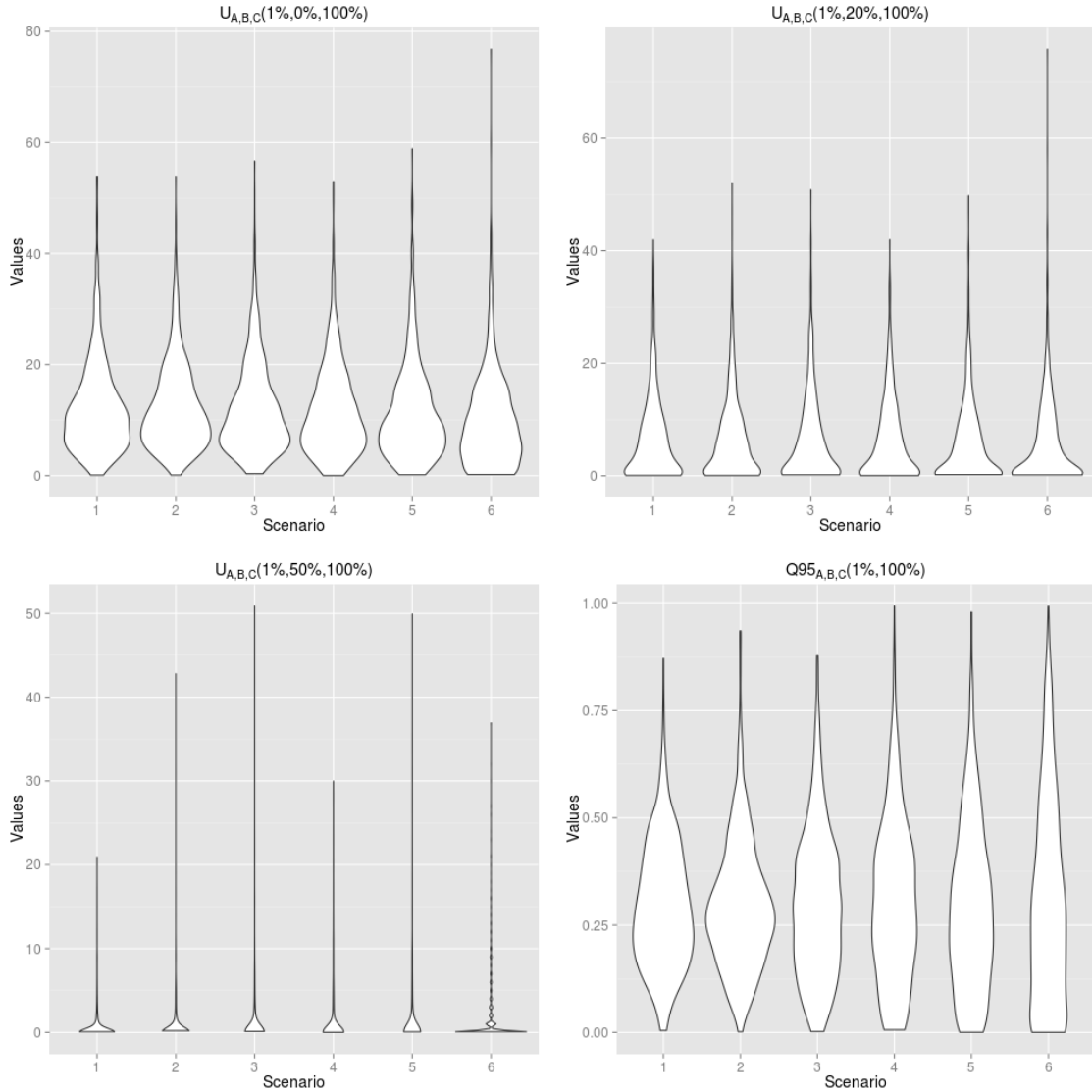


Figure S26: Violin plots showing the effect of different types of bottlenecks on the distribution of U and $Q95$ under neutrality (this is the same data as Figure S25). We performed 1,000 simulations for each of 6 different 3-population scenarios with 25% admixture from population C into population B, following the models described in Figure 2. Scenario 1: Constant population size (Figure 2.A). Scenario 2: Pre-admixture 5X bottleneck for 200 generations (Figure 2.B). Scenario 3: Post-admixture 5X bottleneck for 200 generations (Figure 2.C). Scenario 4: Post-admixture 5X bottleneck for 400 generations. Scenario 5: Post-admixture 10X bottleneck for 200 generations. Scenario 6: Post-admixture 10X bottleneck for 400 generations.

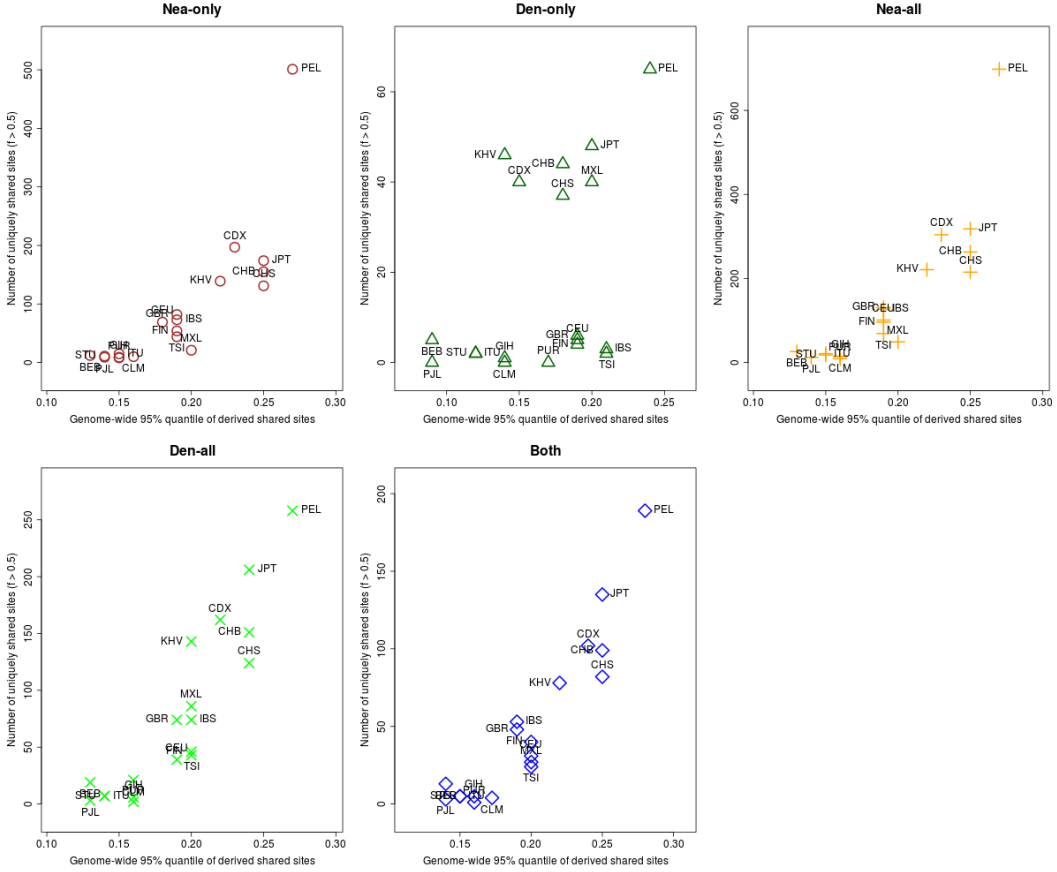


Figure S27: For each population panel from the 1000 Genomes Project, we jointly plotted the U and $Q95$ statistics with an archaic frequency cutoff of $> 50\%$ within each population. $\text{Nea-only} = U_{Afr,X,\text{Nea},\text{Den}}(1\%, 50\%, 100\%, 0\%)$ and $Q95_{Afr,X,\text{Nea},\text{Den}}(1\%, 100\%, 0\%)$. $\text{Den-only} = U_{Afr,X,\text{Nea},\text{Den}}(1\%, 50\%, 0\%, 100\%)$ and $Q95_{Afr,X,\text{Nea},\text{Den}}(1\%, 0\%, 100\%)$. $\text{Nea-all} = U_{Afr,X,\text{Nea}}(1\%, 50\%, 100\%)$ and $Q95_{Afr,X,\text{Nea}}(1\%, 100\%)$. $\text{Den-all} = U_{Afr,X,\text{Den}}(1\%, 50\%, 100\%)$ and $Q95_{Afr,X,\text{Den}}(1\%, 100\%)$. $\text{Both} = U_{Afr,X,\text{Nea},\text{Den}}(1\%, 50\%, 100\%, 100\%)$ and $Q95_{Afr,X,\text{Nea},\text{Den}}(1\%, 100\%, 100\%)$.

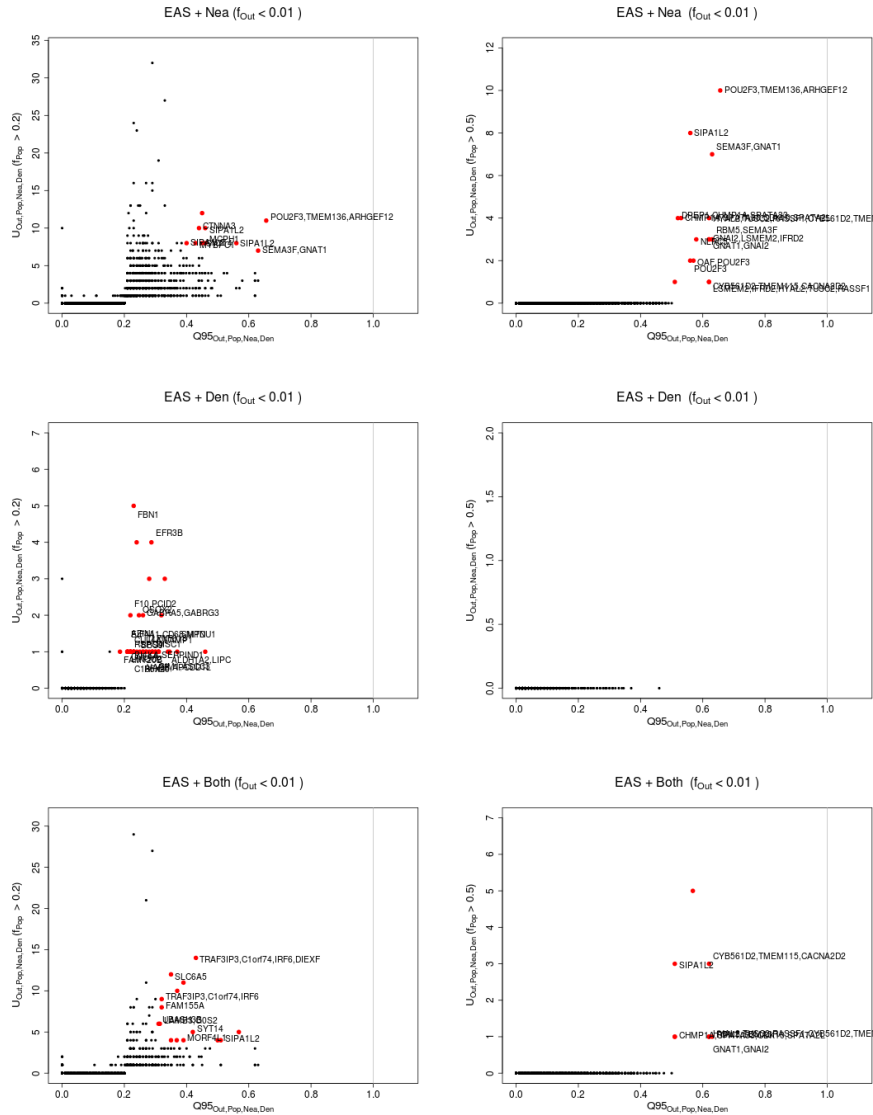


Figure S28: Uniquely shared archaic alleles in an East Asian (EAS) panel. Joint distribution of $Q95_{EUR+AFR,EAS,Nea,Den}(1\%, y, z)$ and $U_{EUR+AFR,EAS,Nea,Den}(1\%, x, y, z)$, for 40kb non-overlapping regions along the genome, using two choices of x (20% in left column panels, 50% in right column panels). Red dots refer to regions that are in the 99.9% quantiles for both statistics. Neanderthal-specific shared alleles are displayed in the top panels, Denisovan-specific shared alleles are displayed in the middle-row panels, and alleles shared with both archaic human genome are displayed in the bottom panels.

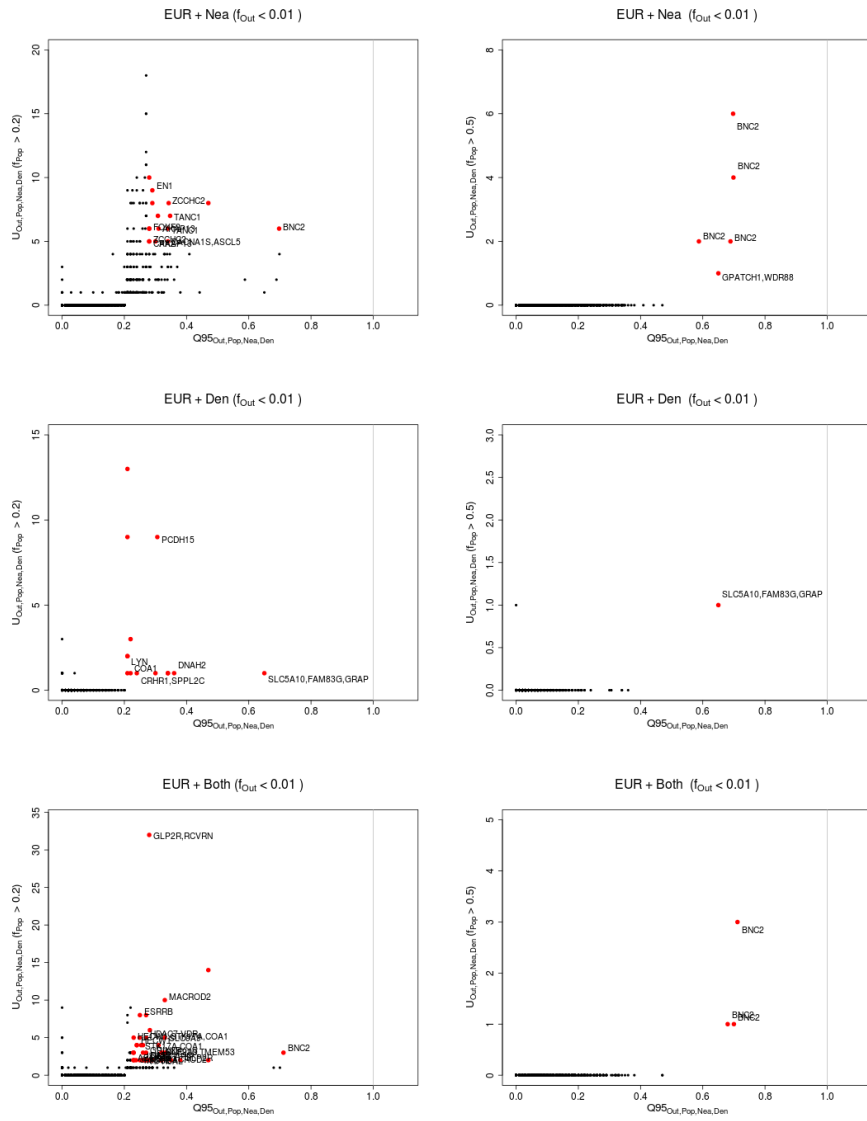


Figure S29: Uniquely shared archaic alleles in an European (EUR) panel. Joint distribution of $Q95_{EAS+AFR,EUR,Nea,Den}(1\%, y, z)$ and $U_{EAS+AFR,EUR,Nea,Den}(1\%, x, y, z)$, for 40kb non-overlapping regions along the genome, using two choices of x (20% in left column panels, 50% in right column panels). Red dots refer to regions that are in the 99.9% quantiles for both statistics. Neanderthal-specific shared alleles are displayed in the top panels, Denisovan-specific shared alleles are displayed in the middle-row panels, and alleles shared with both archaic human genome are displayed in the bottom panels.

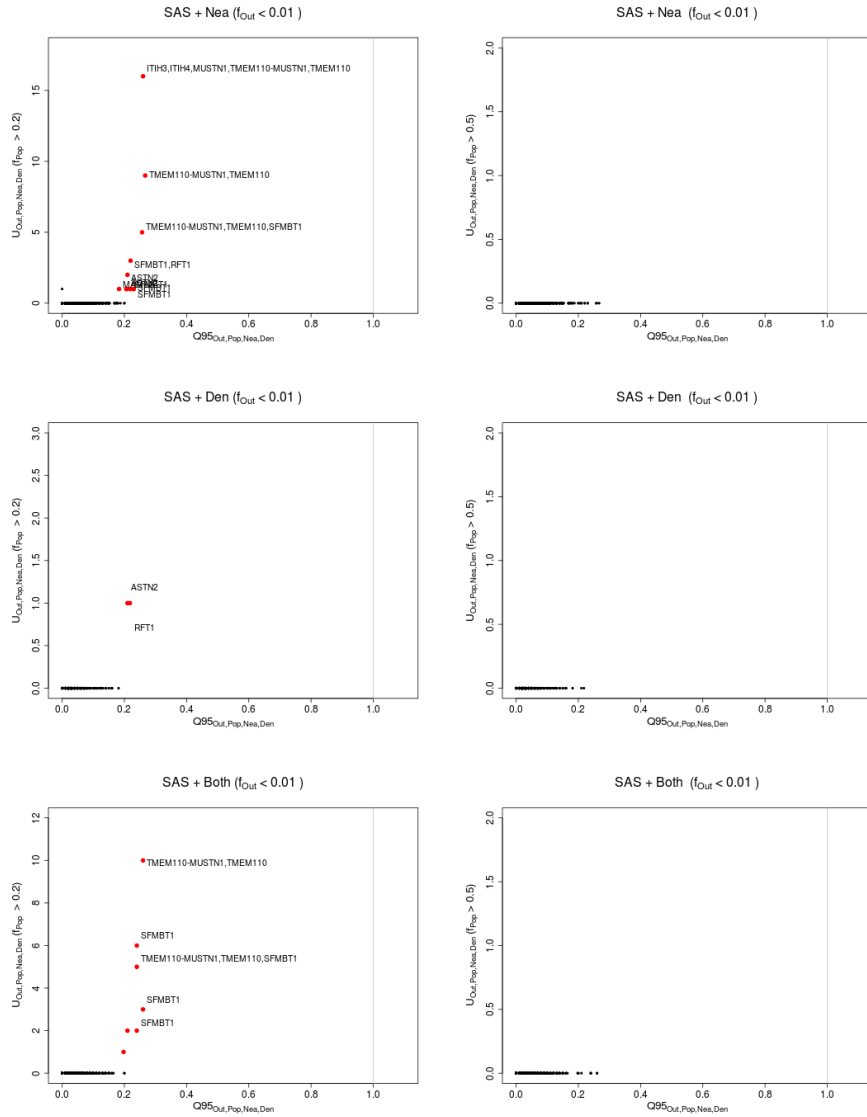


Figure S30: Uniquely shared archaic alleles in a South Asian (SAS) panel. Joint distribution of $Q95_{EAS+EUR+AFR,SAS,Nea,Den}(1\%, y, z)$ and $U_{EAS+EUR+AFR,SAS,Nea,Den}(1\%, x, y, z)$, for 40kb non-overlapping regions along the genome, using two choices of x (20% in left column panels, 50% in right column panels). Red dots refer to regions that are in the 99.9% quantiles for both statistics. Neanderthal-specific shared alleles are displayed in the top panels, Denisovan-specific shared alleles are displayed in the middle-row panels, and alleles shared with both archaic human genome are displayed in the bottom panels.

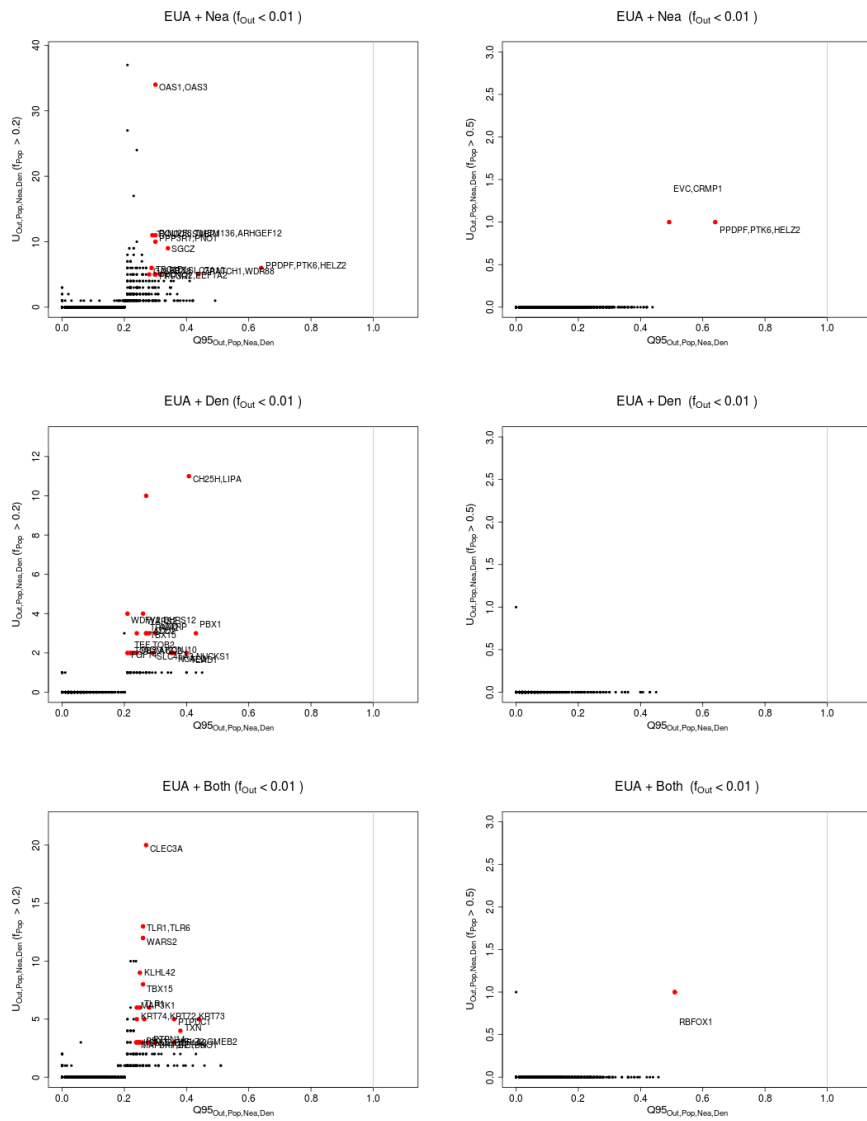


Figure S31: Uniquely shared archaic alleles in a Eurasian (EUA=EUR+SAS+EAS) panel. Joint distribution of $Q95_{AFR,EUR+SAS+EAS,Nea,Den}(1\%,y,z)$ and $U_{AFR,EUR+SAS+EAS,Nea,Den}(1\%,x,y,z)$, for 40kb non-overlapping regions along the genome, using two choices of x (20% in left column panels, 50% in right column panels). Red dots refer to regions that are in the 99.9% quantiles for both statistics. Neanderthal-specific shared alleles are displayed in the top panels, Denisovan-specific shared alleles are displayed in the middle-row panels, and alleles shared with both archaic human genome are displayed in the bottom panels.

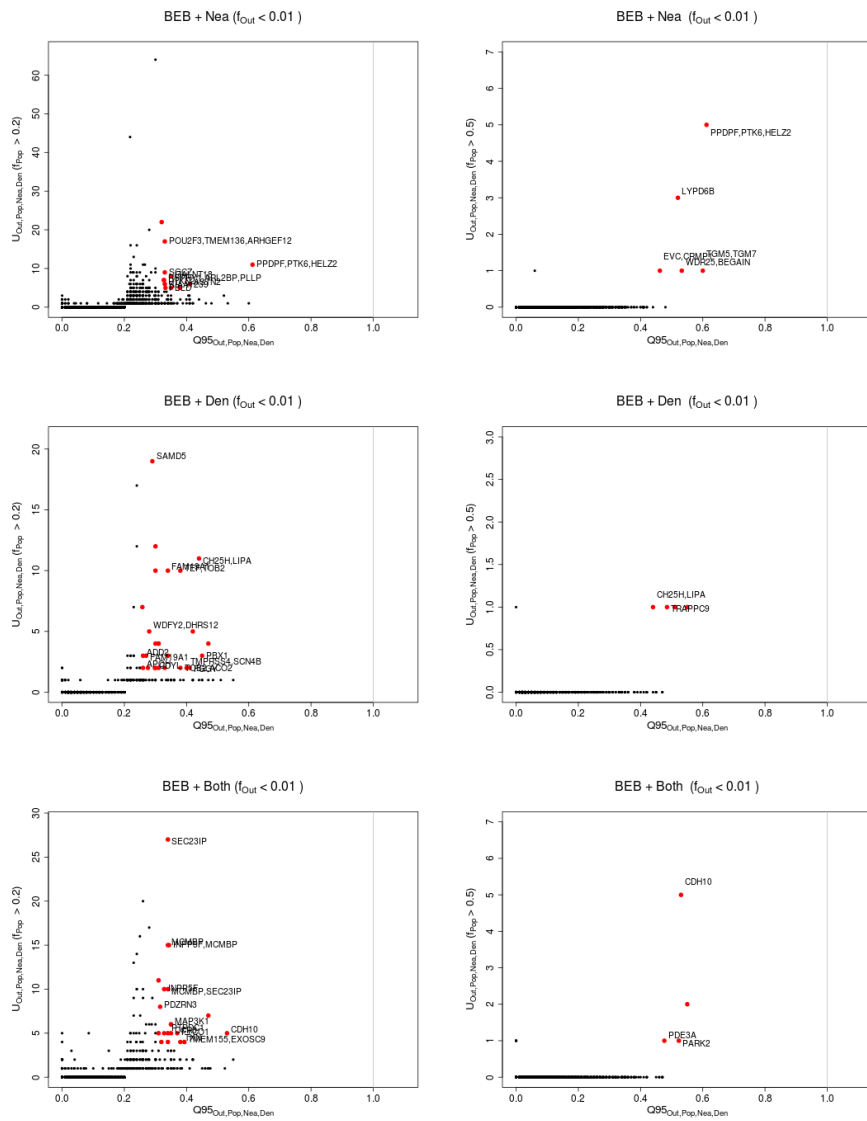


Figure S32: Uniquely shared archaic alleles in a Bengali (BEB) panel. Joint distribution of $Q95_{AFR,BEB,Nea,Den}(1\%, y, z)$ and $U_{AFR,BEB,Nea,Den}(1\%, x, y, z)$, for 40kb non-overlapping regions along the genome, using two choices of x (20% in left column panels, 50% in right column panels). Neanderthal-specific shared alleles are displayed in the top panels, Denisovan-specific shared alleles are displayed in the middle-row panels, and alleles shared with both archaic human genome are displayed in the bottom panels.

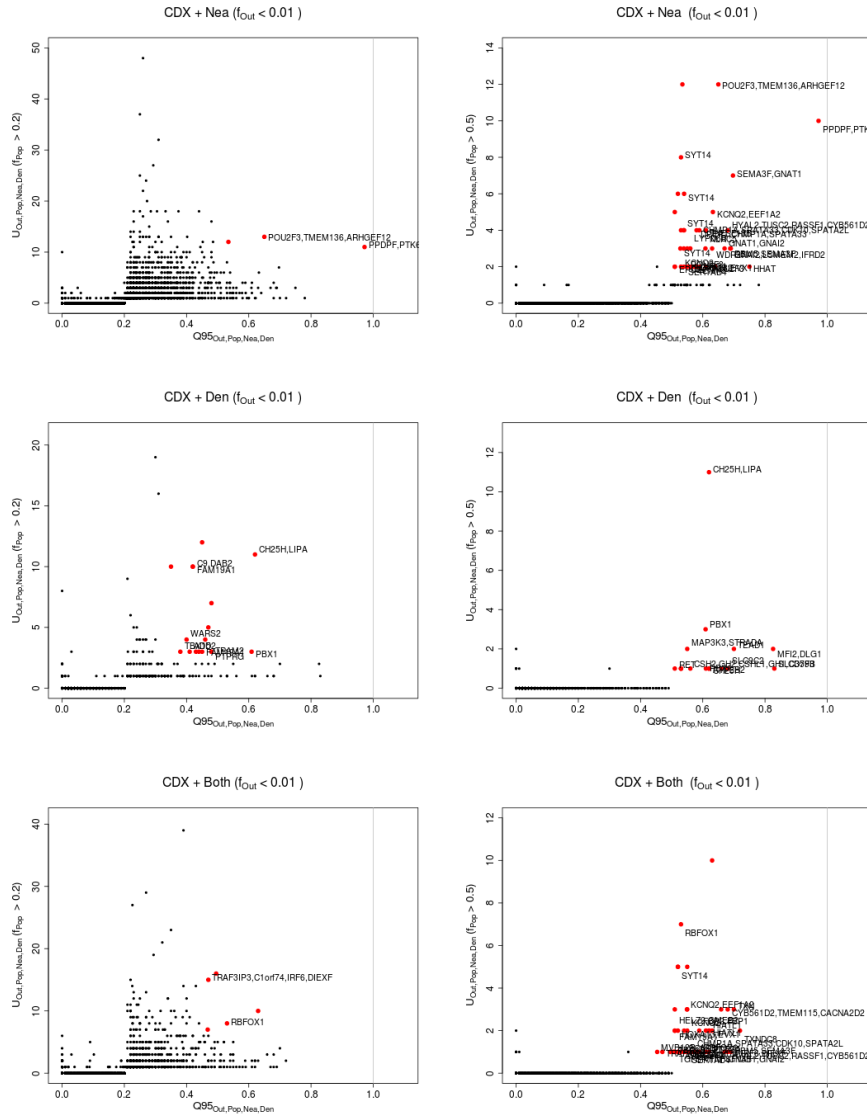


Figure S33: Uniquely shared archaic alleles in a Chinese Dai (CDX) panel. Joint distribution of $Q95_{AFR,CDX,Nea,Den}(1\%,y,z)$ and $U_{AFR,CDX,Nea,Den}(1\%,x,y,z)$, for 40kb non-overlapping regions along the genome, using two choices of x (20% in left column panels, 50% in right column panels). Red dots refer to regions that are in the 99.9% quantiles for both statistics. Neanderthal-specific shared alleles are displayed in the top panels, Denisovan-specific shared alleles are displayed in the middle-row panels, and alleles shared with both archaic human genome are displayed in the bottom panels.

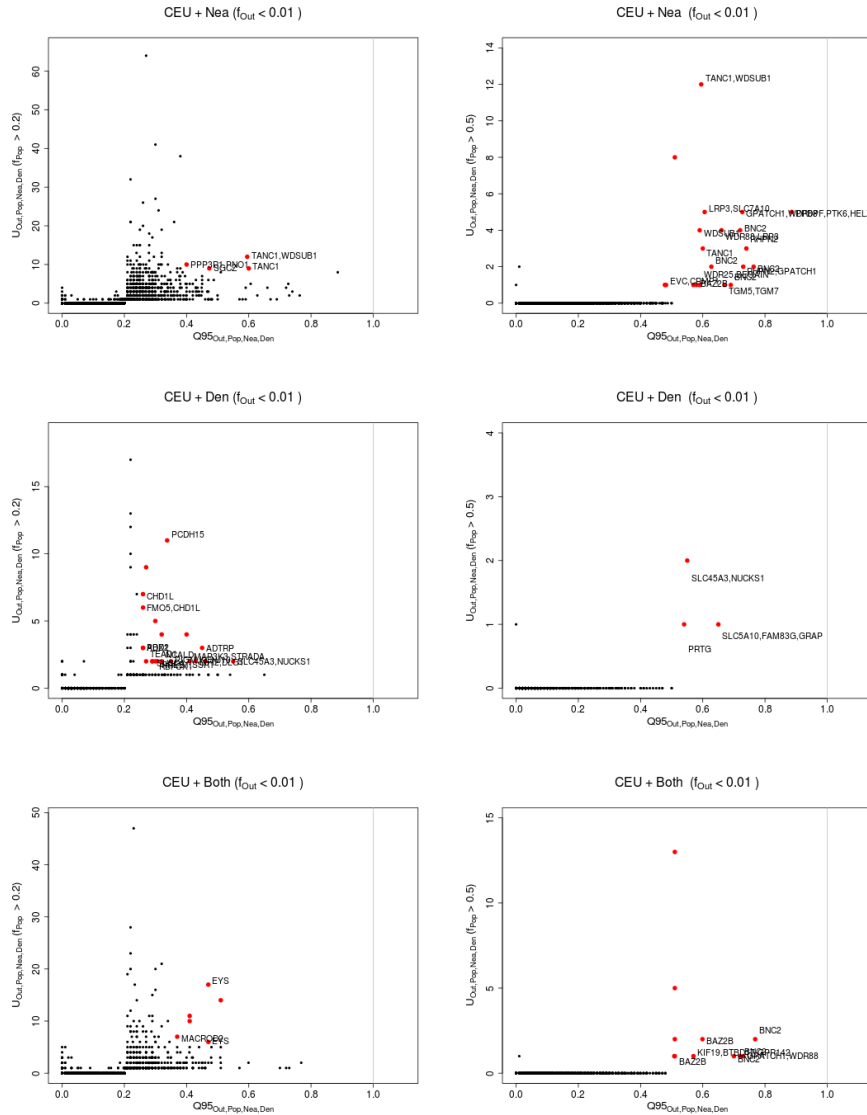


Figure S34: Uniquely shared archaic alleles in a Central European (CEU) panel. Joint distribution of $Q95_{AFR,CEU,Nea,Den}(1\%, y, z)$ and $U_{AFR,CEU,Nea,Den}(1\%, x, y, z)$, for 40kb non-overlapping regions along the genome, using two choices of x (20% in left column panels, 50% in right column panels). Red dots refer to regions that are in the 99.9% quantiles for both statistics. Neanderthal-specific shared alleles are displayed in the top panels, Denisovan-specific shared alleles are displayed in the middle-row panels, and alleles shared with both archaic human genome are displayed in the bottom panels.

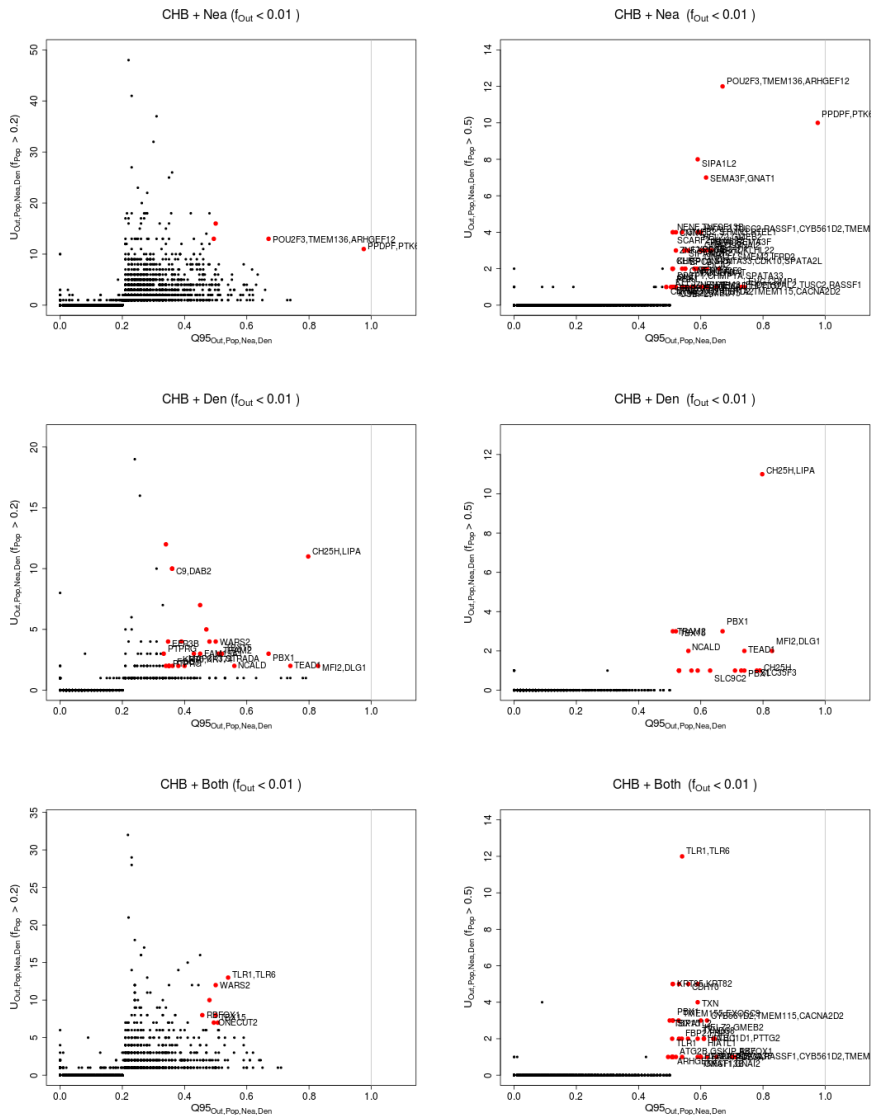


Figure S35: Uniquely shared archaic alleles in a Han Chinese (CHB) panel. Joint distribution of $Q95_{AFR,CHB,Nea,Den}(1\%, y, z)$ and $U_{AFR,CHB,Nea,Den}(1\%, x, y, z)$, for 40kb non-overlapping regions along the genome, using two choices of x (20% in left column panels, 50% in right column panels). Red dots refer to regions that are in the 99.9% quantiles for both statistics. Neanderthal-specific shared alleles are displayed in the top panels, Denisovan-specific shared alleles are displayed in the middle-row panels, and alleles shared with both archaic human genome are displayed in the bottom panels.

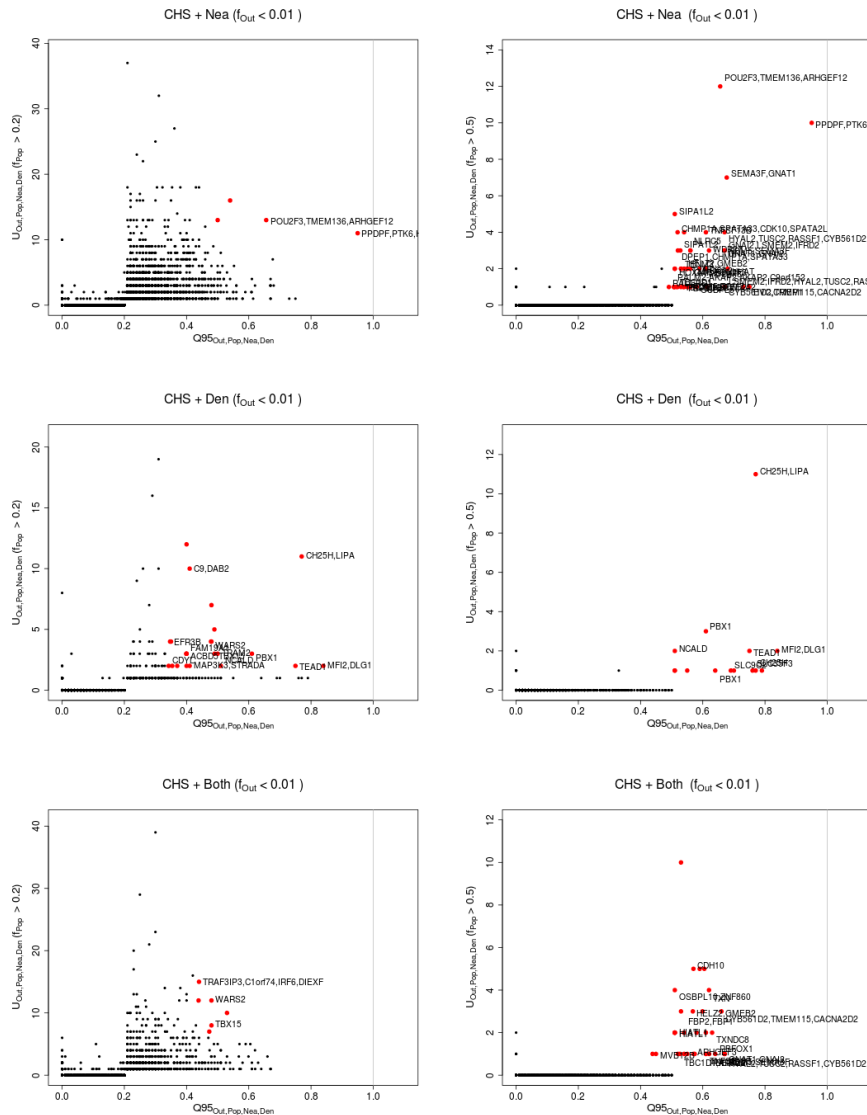


Figure S36: Uniquely shared archaic alleles in a Southern Han Chinese (CHS) panel. Joint distribution of $Q95_{AFR,BEB,Nea,Den}(1\%, y, z)$ and $U_{AFR,CHS,Nea,Den}(1\%, x, y, z)$, for 40kb non-overlapping regions along the genome, using two choices of x (20% in left column panels, 50% in right column panels). Red dots refer to regions that are in the 99.9% quantiles for both statistics. Neanderthal-specific shared alleles are displayed in the top panels, Denisovan-specific shared alleles are displayed in the middle-row panels, and alleles shared with both archaic human genome are displayed in the bottom panels.

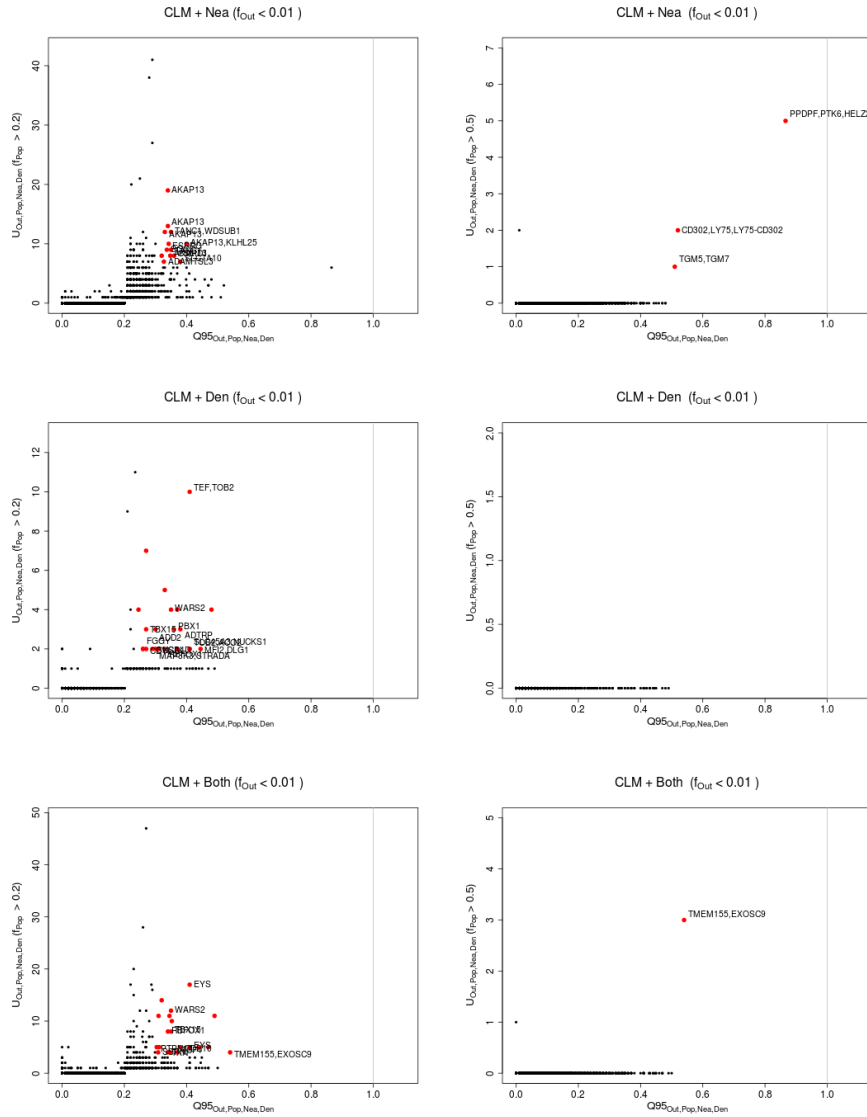


Figure S37: Uniquely shared archaic alleles in a Colombian (CLM) panel. Joint distribution of $Q95_{AFR, CLM, Nea, Den}(1\%, y, z)$ and $U_{AFR, CLM, Nea, Den}(1\%, x, y, z)$, for 40kb non-overlapping regions along the genome, using two choices of x (20% in left column panels, 50% in right column panels). Red dots refer to regions that are in the 99.9% quantiles for both statistics. Neanderthal-specific shared alleles are displayed in the top panels, Denisovan-specific shared alleles are displayed in the middle-row panels, and alleles shared with both archaic human genome are displayed in the bottom panels.

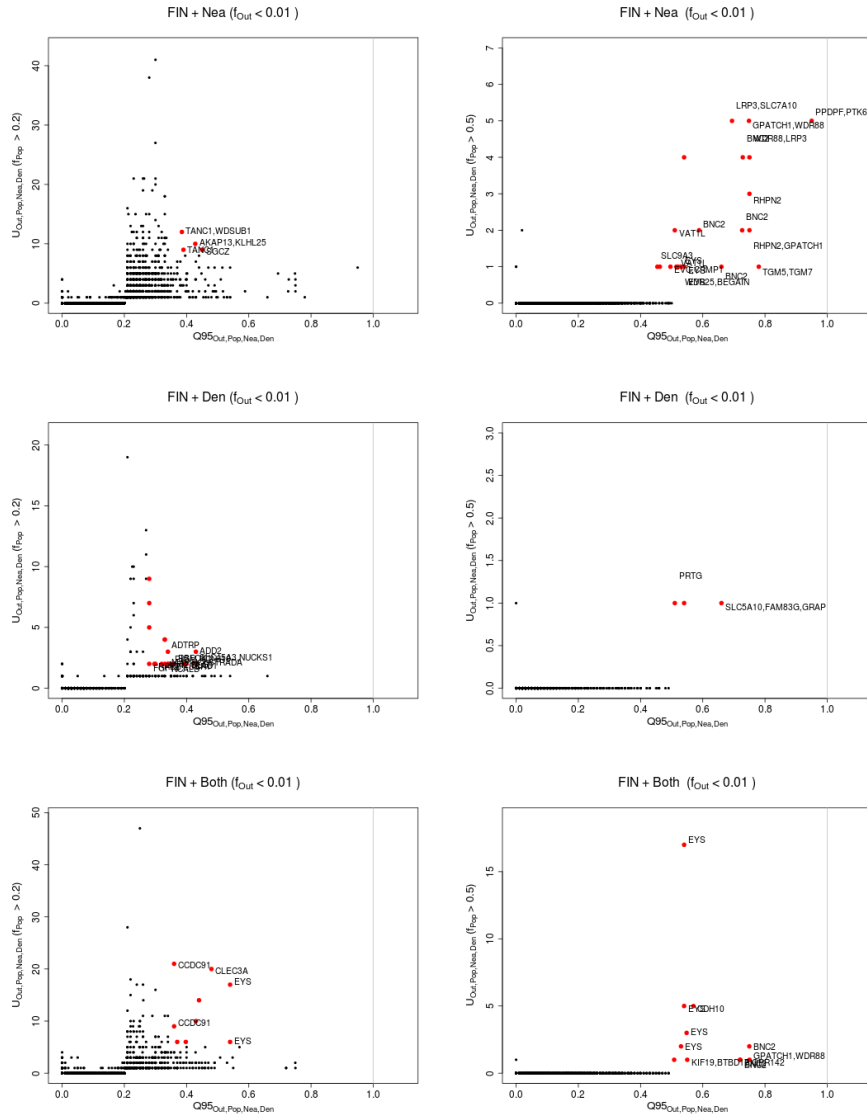


Figure S38: Uniquely shared archaic alleles in a Finnish (FIN) panel. Joint distribution of $Q95_{AFR,FIN,Nea,Den}(1\%, y, z)$ and $U_{AFR,FIN,Nea,Den}(1\%, x, y, z)$, for 40kb non-overlapping regions along the genome, using two choices of x (20% in left column panels, 50% in right column panels). Red dots refer to regions that are in the 99.9% quantiles for both statistics. Neanderthal-specific shared alleles are displayed in the top panels, Denisovan-specific shared alleles are displayed in the middle-row panels, and alleles shared with both archaic human genome are displayed in the bottom panels.

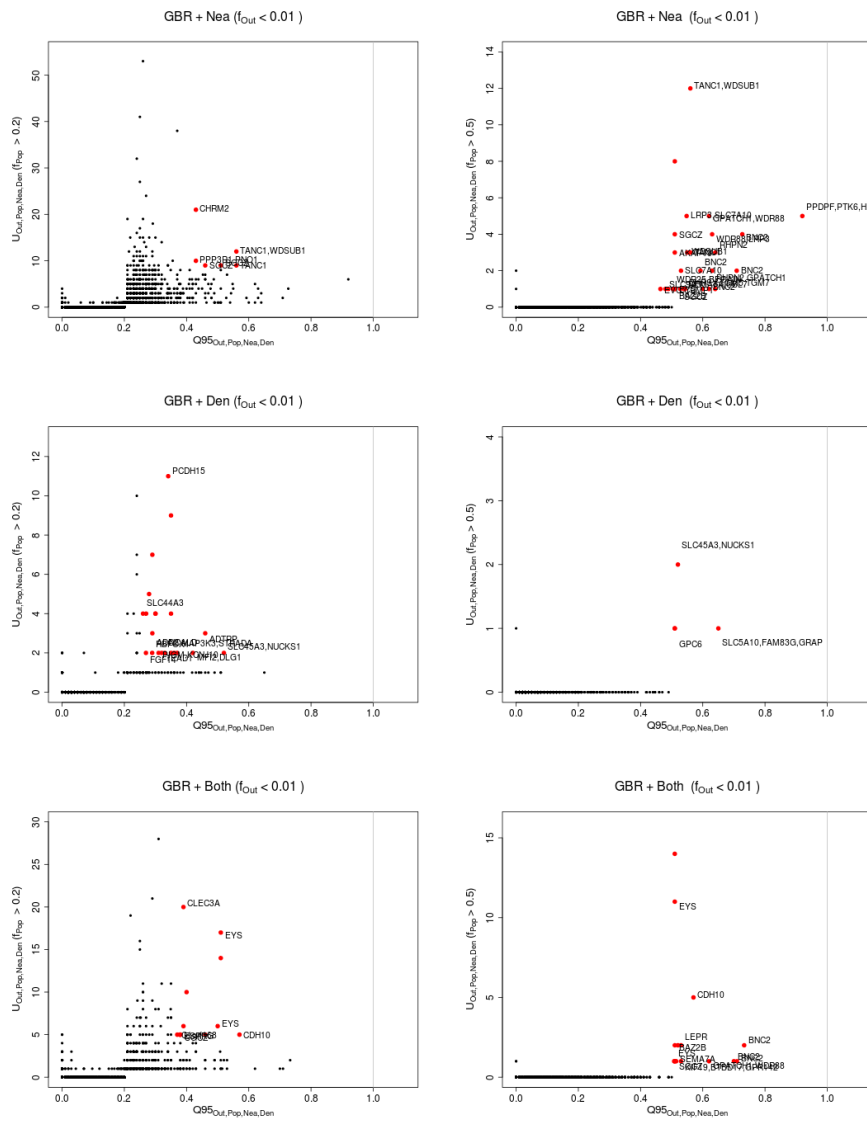


Figure S39: Uniquely shared archaic alleles in a British (GBR) panel. Joint distribution of $Q95_{AFR,GBR,Nea,Den}(1\%, y, z)$ and $U_{AFR,GBR,Nea,Den}(1\%, x, y, z)$, for 40kb non-overlapping regions along the genome, using two choices of x (20% in left column panels, 50% in right column panels). Red dots refer to regions that are in the 99.9% quantiles for both statistics. Neanderthal-specific shared alleles are displayed in the top panels, Denisovan-specific shared alleles are displayed in the middle-row panels, and alleles shared with both archaic human genome are displayed in the bottom panels.

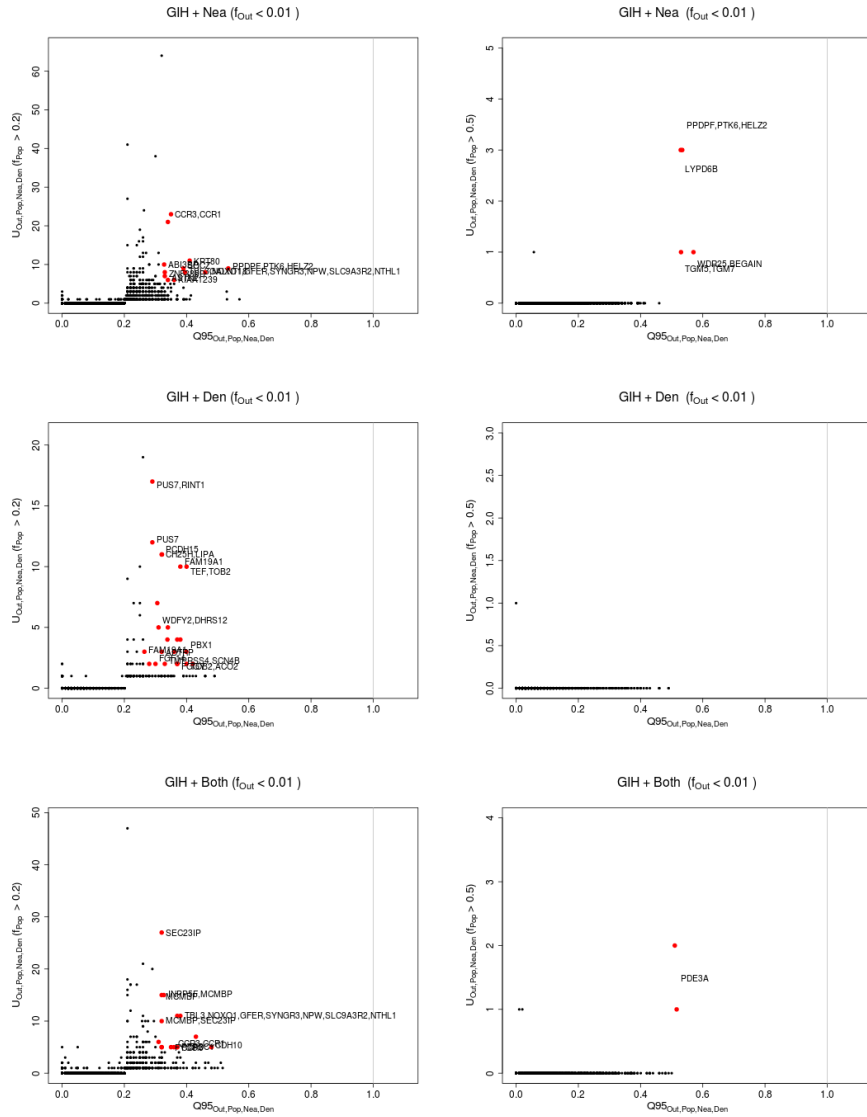


Figure S40: Uniquely shared archaic alleles in a Gujarati Indian (GIH) panel. Joint distribution of $Q95_{AFR, GIH, Nea, Den}(1\%, y, z)$ and $U_{AFR, GIH, Nea, Den}(1\%, x, y, z)$, for 40kb non-overlapping regions along the genome, using two choices of x (20% in left column panels, 50% in right column panels). Red dots refer to regions that are in the 99.9% quantiles for both statistics. Neanderthal-specific shared alleles are displayed in the top panels, Denisovan-specific shared alleles are displayed in the middle-row panels, and alleles shared with both archaic human genome are displayed in the bottom panels.

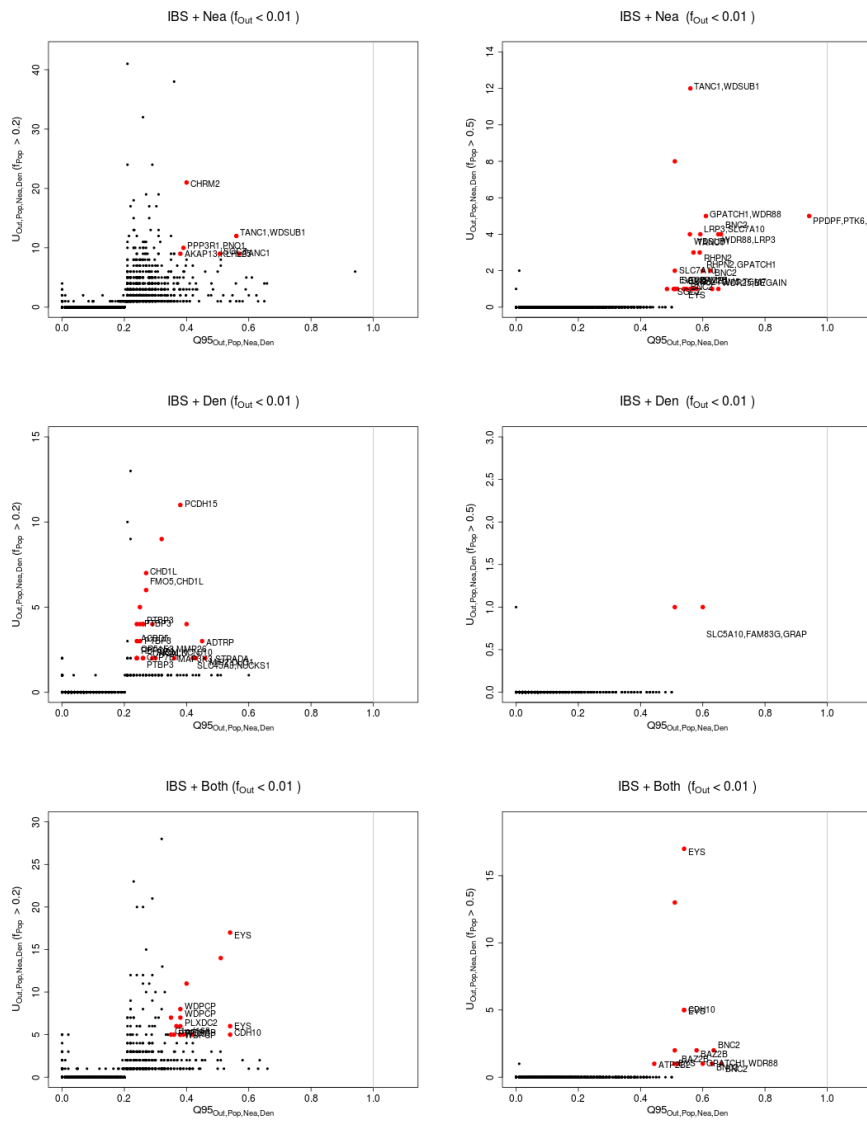


Figure S41: Uniquely shared archaic alleles in an Iberian (IBS) panel. Joint distribution of $Q95_{AFR,IBS,Nea,Den}(1\%,y,z)$ and $U_{AFR,IBS,Nea,Den}(1\%,x,y,z)$, for 40kb non-overlapping regions along the genome, using two choices of x (20% in left column panels, 50% in right column panels). Red dots refer to regions that are in the 99.9% quantiles for both statistics. Neanderthal-specific shared alleles are displayed in the top panels, Denisovan-specific shared alleles are displayed in the middle-row panels, and alleles shared with both archaic human genome are displayed in the bottom panels.

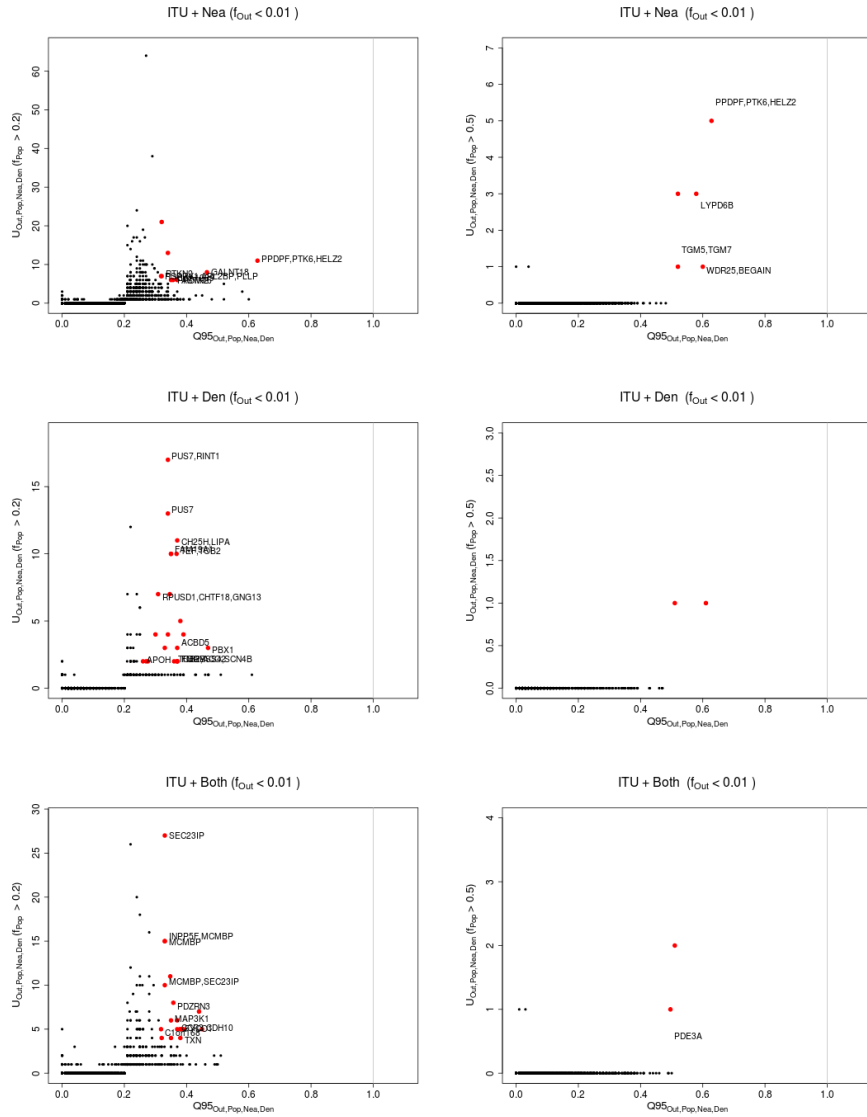


Figure S42: Uniquely shared archaic alleles in an Indian Telugu (ITU) panel. Joint distribution of $Q95_{AFR,ITU,Nea,Den}(1\%, y, z)$ and $U_{AFR,ITU,Nea,Den}(1\%, x, y, z)$, for 40kb non-overlapping regions along the genome, using two choices of x (20% in left column panels, 50% in right column panels). Red dots refer to regions that are in the 99.9% quantiles for both statistics. Neanderthal-specific shared alleles are displayed in the top panels, Denisovan-specific shared alleles are displayed in the middle-row panels, and alleles shared with both archaic human genome are displayed in the bottom panels.

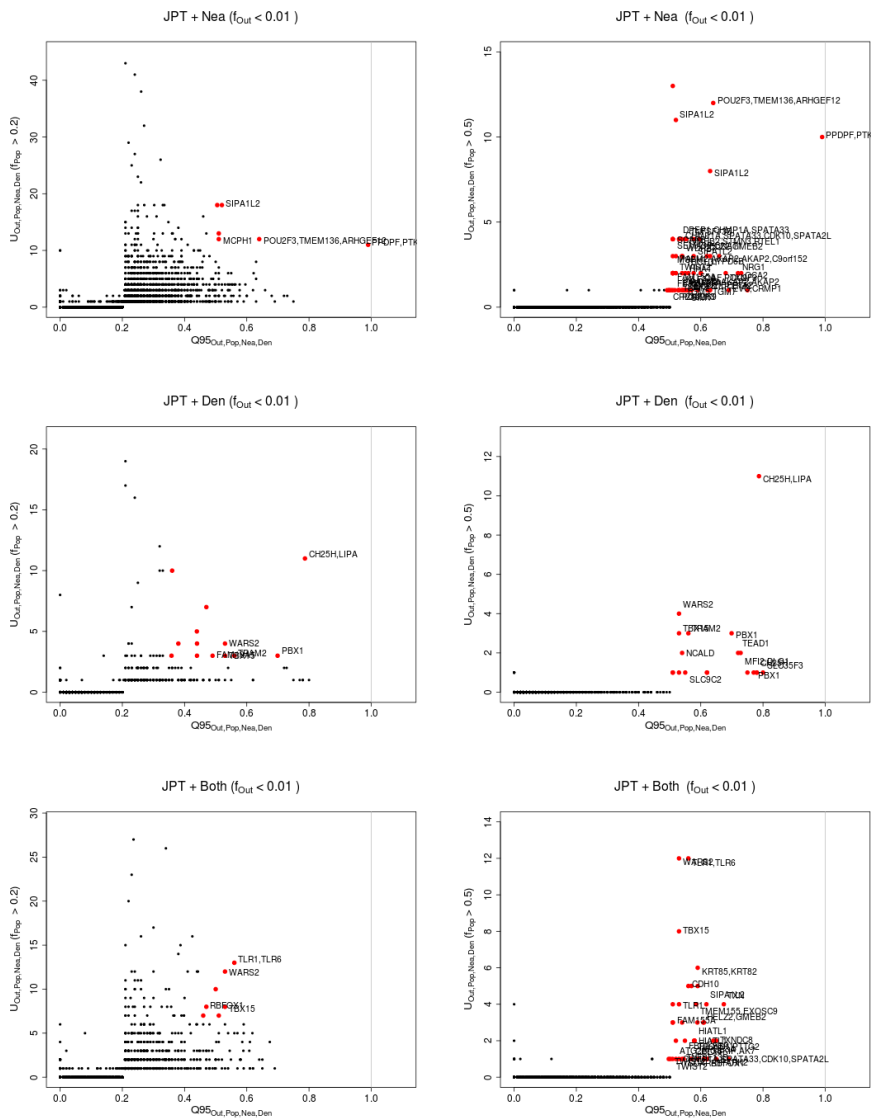


Figure S43: Uniquely shared archaic alleles in a Japanese (JPT) panel. Joint distribution of $Q95_{AFR,JPT,Nea,Den}(1\%, y, z)$ and $U_{AFR,JPT,Nea,Den}(1\%, x, y, z)$, for 40kb non-overlapping regions along the genome, using two choices of x (20% in left column panels, 50% in right column panels). Red dots refer to regions that are in the 99.9% quantiles for both statistics. Neanderthal-specific shared alleles are displayed in the top panels, Denisovan-specific shared alleles are displayed in the middle-row panels, and alleles shared with both archaic human genome are displayed in the bottom panels.

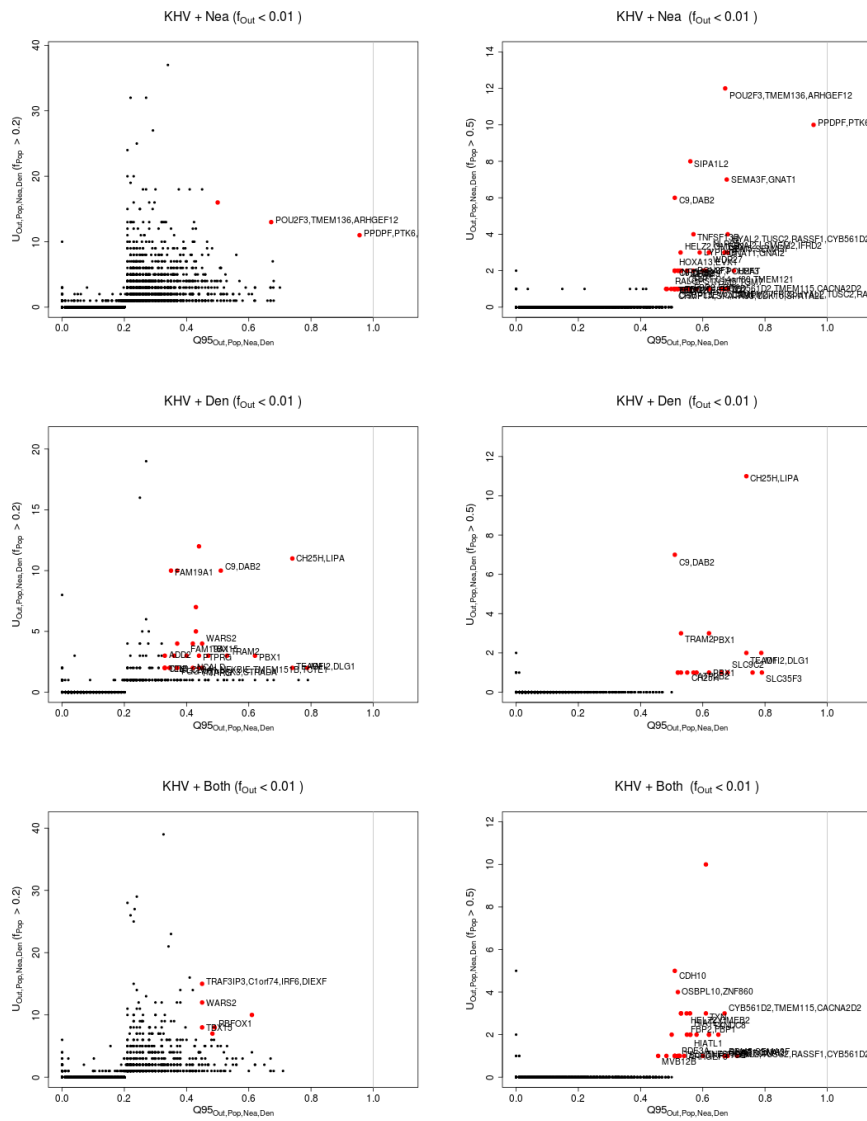


Figure S44: Uniquely shared archaic alleles in a Kinh (KHV) panel. Joint distribution of $Q95_{AFR,KHV,Nea,Den}(1\%, y, z)$ and $U_{AFR,KHV,Nea,Den}(1\%, x, y, z)$, for 40kb non-overlapping regions along the genome, using two choices of x (20% in left column panels, 50% in right column panels). Red dots refer to regions that are in the 99.9% quantiles for both statistics. Neanderthal-specific shared alleles are displayed in the top panels, Denisovan-specific shared alleles are displayed in the middle-row panels, and alleles shared with both archaic human genome are displayed in the bottom panels.

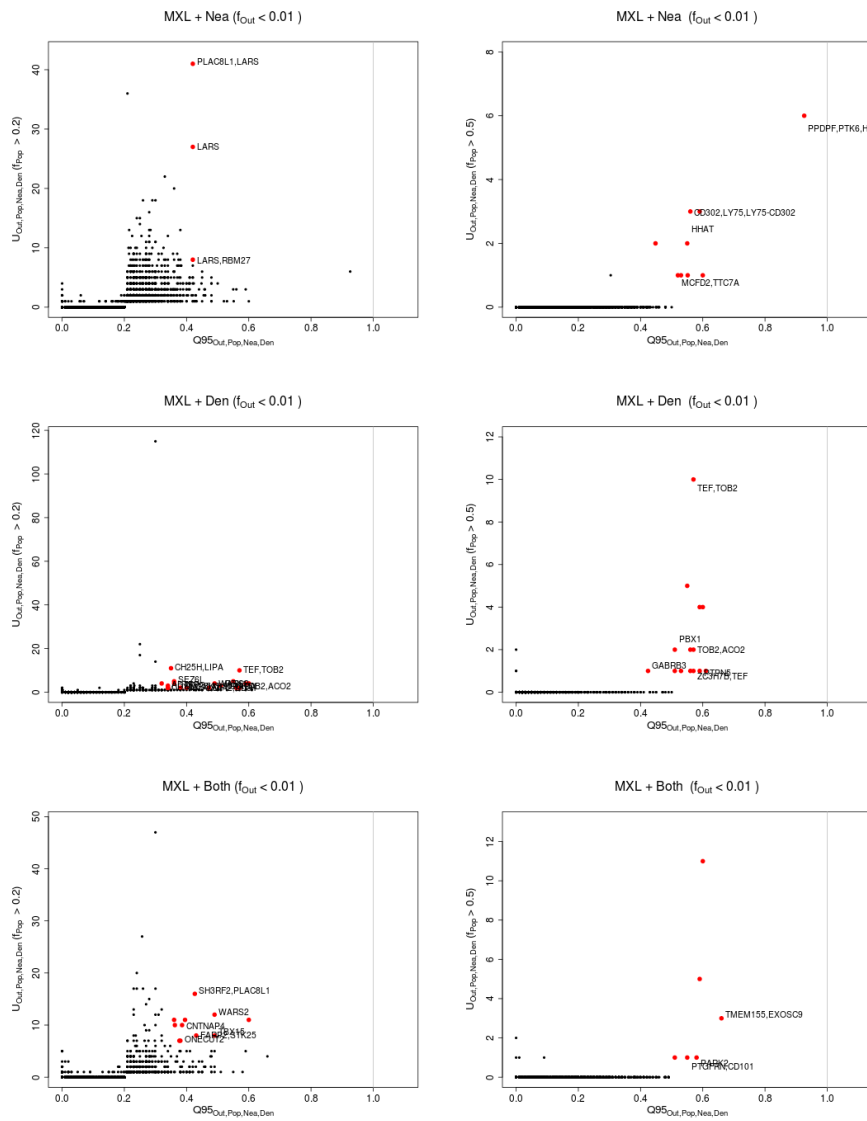


Figure S45: Uniquely shared archaic alleles in a Mexican (MXL) panel. Joint distribution of $Q95_{AFR,MXL,Nea,Den}(1\%, y, z)$ and $U_{AFR,MXL,Nea,Den}(1\%, x, y, z)$, for 40kb non-overlapping regions along the genome, using two choices of x (20% in left column panels, 50% in right column panels). Red dots refer to regions that are in the 99.9% quantiles for both statistics. Neanderthal-specific shared alleles are displayed in the top panels, Denisovan-specific shared alleles are displayed in the middle-row panels, and alleles shared with both archaic human genome are displayed in the bottom panels.

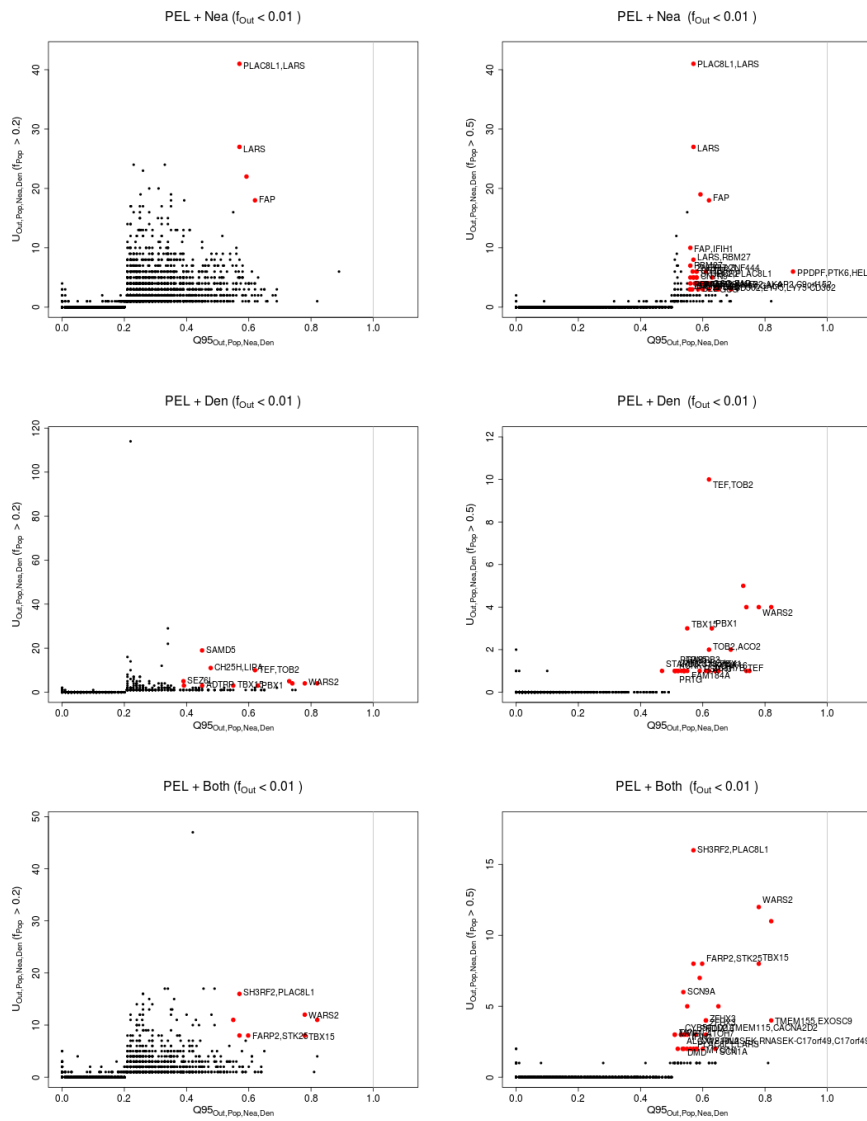


Figure S46: Uniquely shared archaic alleles in a Peruvian (PEL) panel. Joint distribution of $Q95_{AFR,PEL,Nea,Den}(1\%,y,z)$ and $U_{AFR,PEL,Nea,Den}(1\%,x,y,z)$, for 40kb non-overlapping regions along the genome, using two choices of x (20% in left column panels, 50% in right column panels). Red dots refer to regions that are in the 99.9% quantiles for both statistics. Neanderthal-specific shared alleles are displayed in the top panels, Denisovan-specific shared alleles are displayed in the middle-row panels, and alleles shared with both archaic human genome are displayed in the bottom panels.

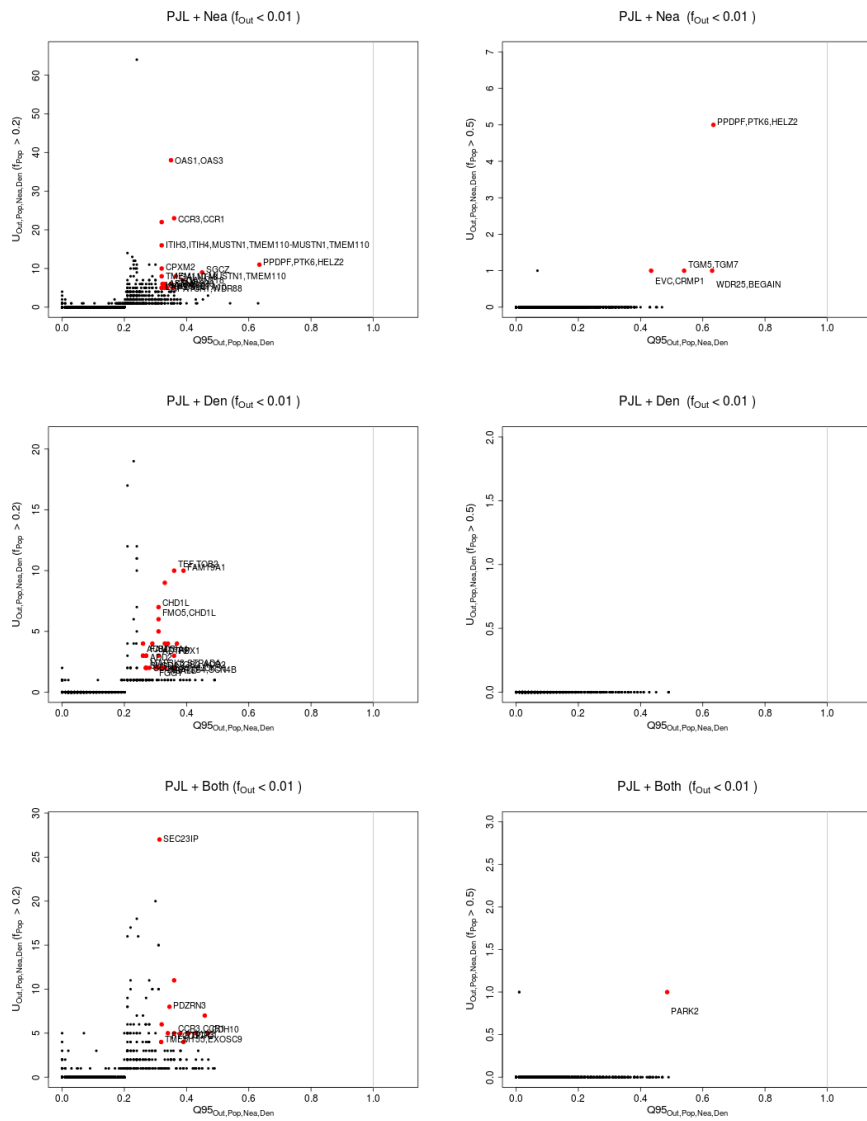


Figure S47: Uniquely shared archaic alleles in a Punjabi (PJL) panel. Joint distribution of $Q95_{AFR,PJL,Nea,Den}(1\%,y,z)$ and $U_{AFR,PJL,Nea,Den}(1\%,x,y,z)$, for 40kb non-overlapping regions along the genome, using two choices of x (20% in left column panels, 50% in right column panels). Red dots refer to regions that are in the 99.9% quantiles for both statistics. Neanderthal-specific shared alleles are displayed in the top panels, Denisovan-specific shared alleles are displayed in the middle-row panels, and alleles shared with both archaic human genome are displayed in the bottom panels.

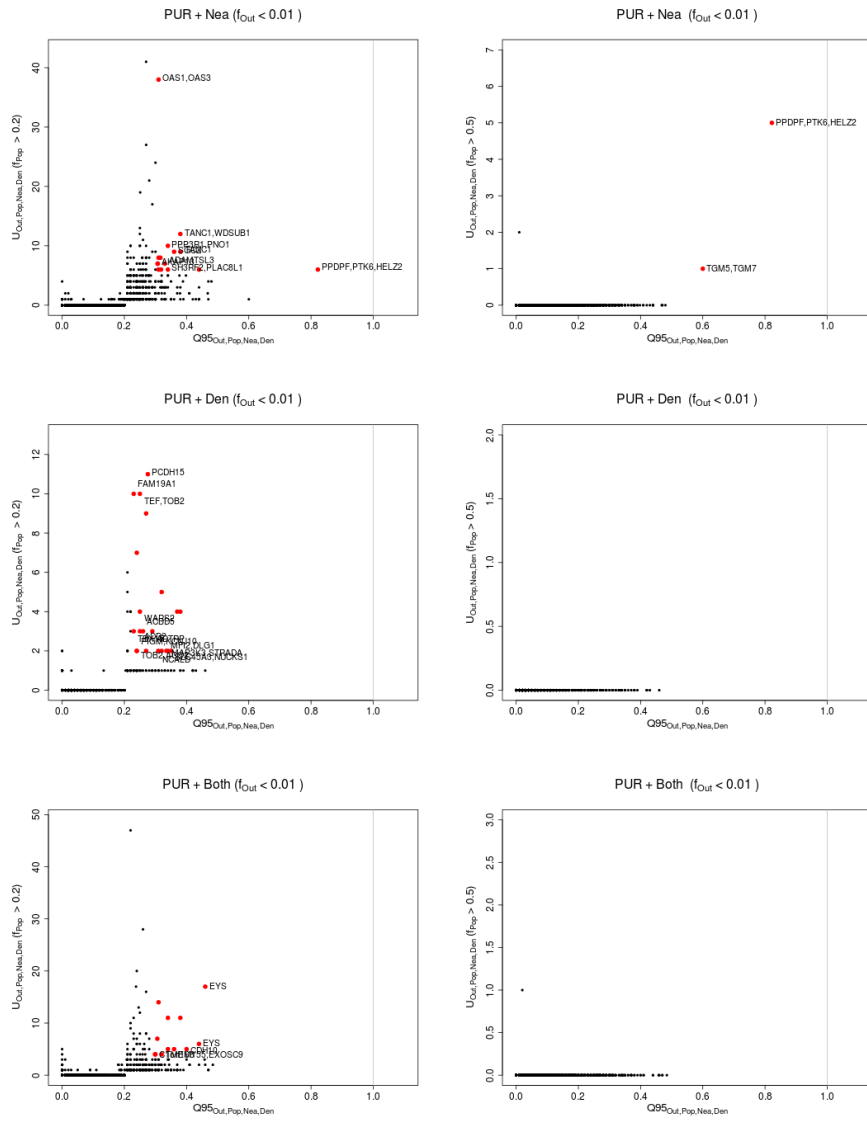


Figure S48: Uniquely shared archaic alleles in a Puerto Rican (PUR) panel. Joint distribution of $Q95_{AFR,PUR,Nea,Den}(1\%, y, z)$ and $U_{AFR,PUR,Nea,Den}(1\%, x, y, z)$, for 40kb non-overlapping regions along the genome, using two choices of x (20% in left column panels, 50% in right column panels). Red dots refer to regions that are in the 99.9% quantiles for both statistics. Neanderthal-specific shared alleles are displayed in the top panels, Denisovan-specific shared alleles are displayed in the middle-row panels, and alleles shared with both archaic human genome are displayed in the bottom panels.

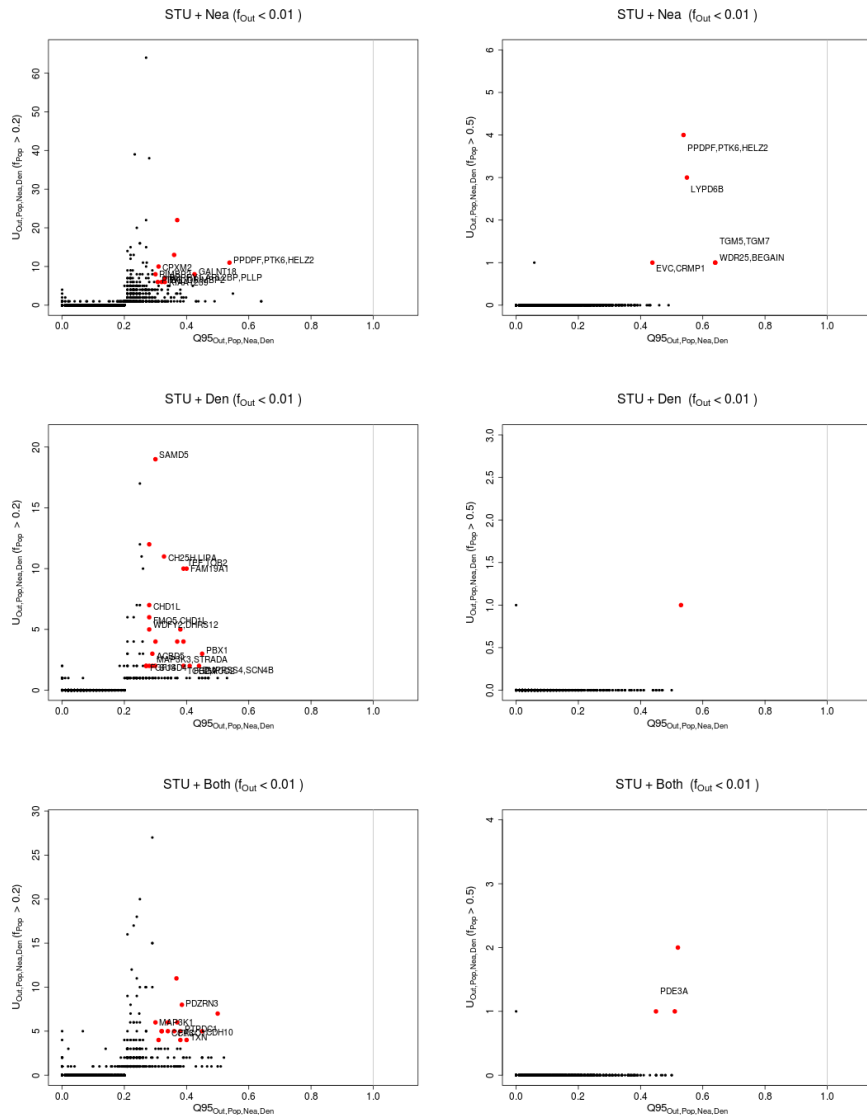


Figure S49: Uniquely shared archaic alleles in a Sri Lankan Tamil (STU) panel. Joint distribution of $Q95_{AFR,STU,Nea,Den}(1\%, y, z)$ and $U_{AFR,STU,Nea,Den}(1\%, x, y, z)$, for 40kb non-overlapping regions along the genome, using two choices of x (20% in left column panels, 50% in right column panels). Red dots refer to regions that are in the 99.9% quantiles for both statistics. Neanderthal-specific shared alleles are displayed in the top panels, Denisovan-specific shared alleles are displayed in the middle-row panels, and alleles shared with both archaic human genome are displayed in the bottom panels.

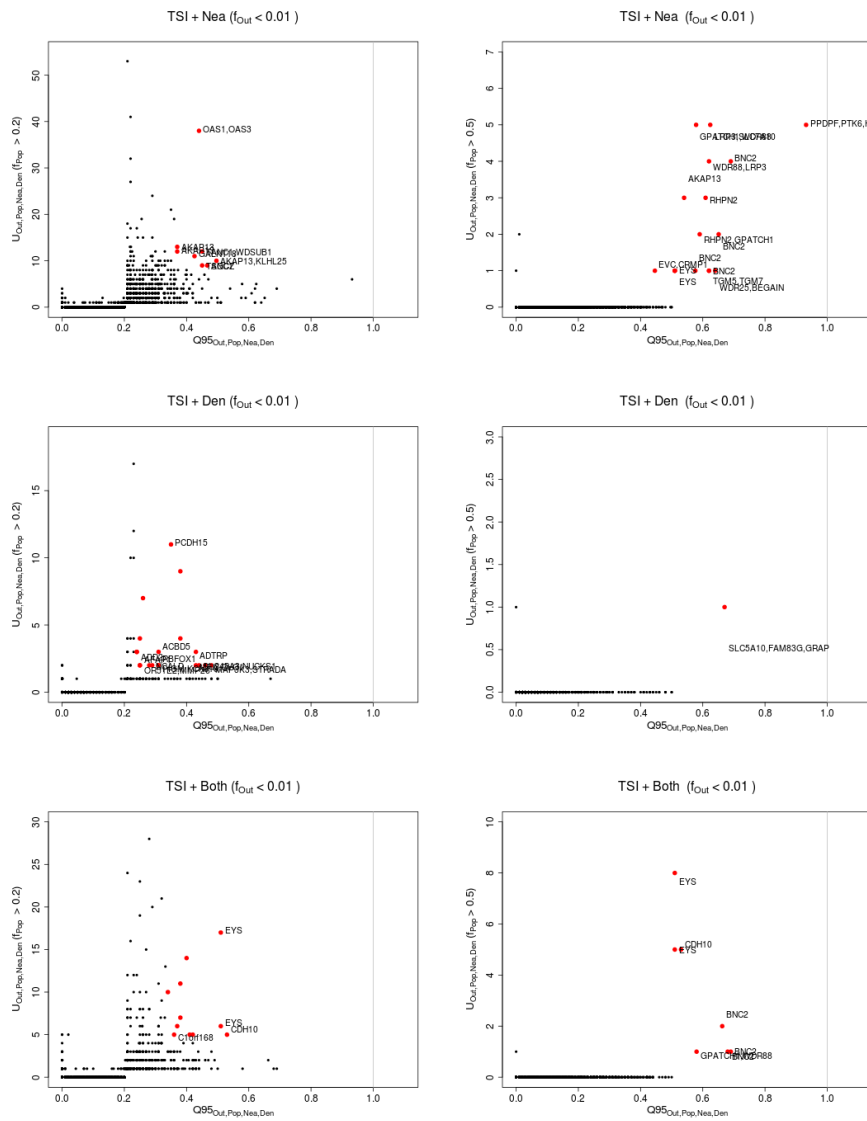


Figure S50: Uniquely shared archaic alleles in a Toscani (TSI) panel. Joint distribution of $Q95_{AFR,TSI,Nea,Den}(1\%,y,z)$ and $U_{AFR,TSI,Nea,Den}(1\%,x,y,z)$, for 40kb non-overlapping regions along the genome, using two choices of x (20% in left column panels, 50% in right column panels). Red dots refer to regions that are in the 99.9% quantiles for both statistics. Neanderthal-specific shared alleles are displayed in the top panels, Denisovan-specific shared alleles are displayed in the middle-row panels, and alleles shared with both archaic human genome are displayed in the bottom panels.

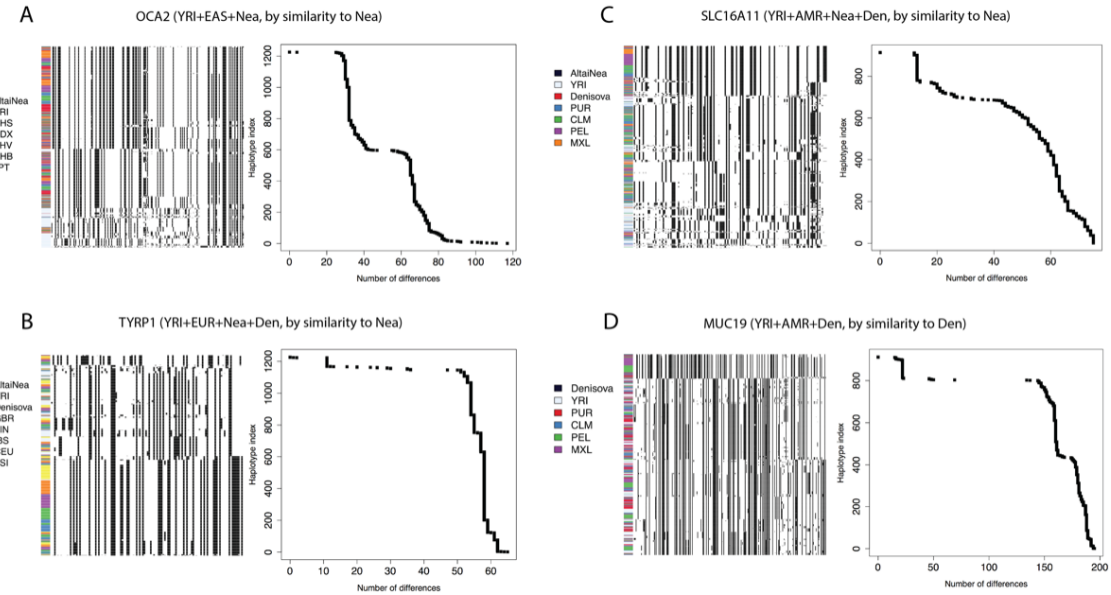


Figure S51: We explored the haplotype structure of *OCA2*, *TYRP1*, *SLC16A11* and *MUC19*. We applied a clustering algorithm to the haplotypes of particular human populations and then ordered the clusters by decreasing similarity to the archaic human genome with the larger number of uniquely shared sites. We also plotted the number of differences to the closest archaic haplotype for each human haplotype and sorted them simply by decreasing similarity. Note that, in the latter case, no clustering was performed, so the rows in the cumulative difference plots do not necessarily correspond to the rows in the adjacent haplotype structure plots. *OCA2*: chr15:28160001-28200000. *TYRP1*: chr9:12680001-12720000. *SLC16A11*: chr17:6880001-6960000. *MUC19*: chr12:40800001-40840000.

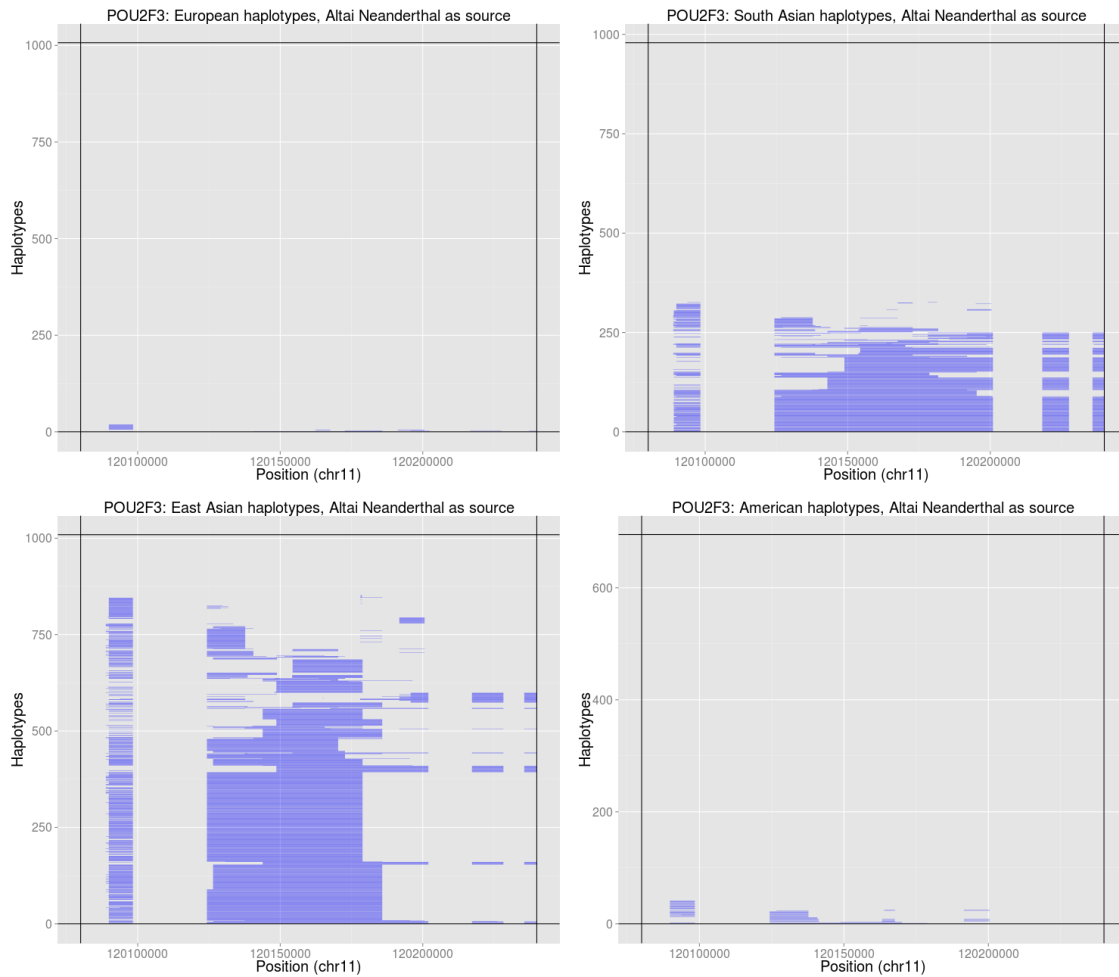


Figure S52: Introgressed tracks inferred in the four Non-African 1000 Genomes continental panels by an HMM [21] in the *POU2F3* region, using the Altai Neanderthal genome as the archaic source.

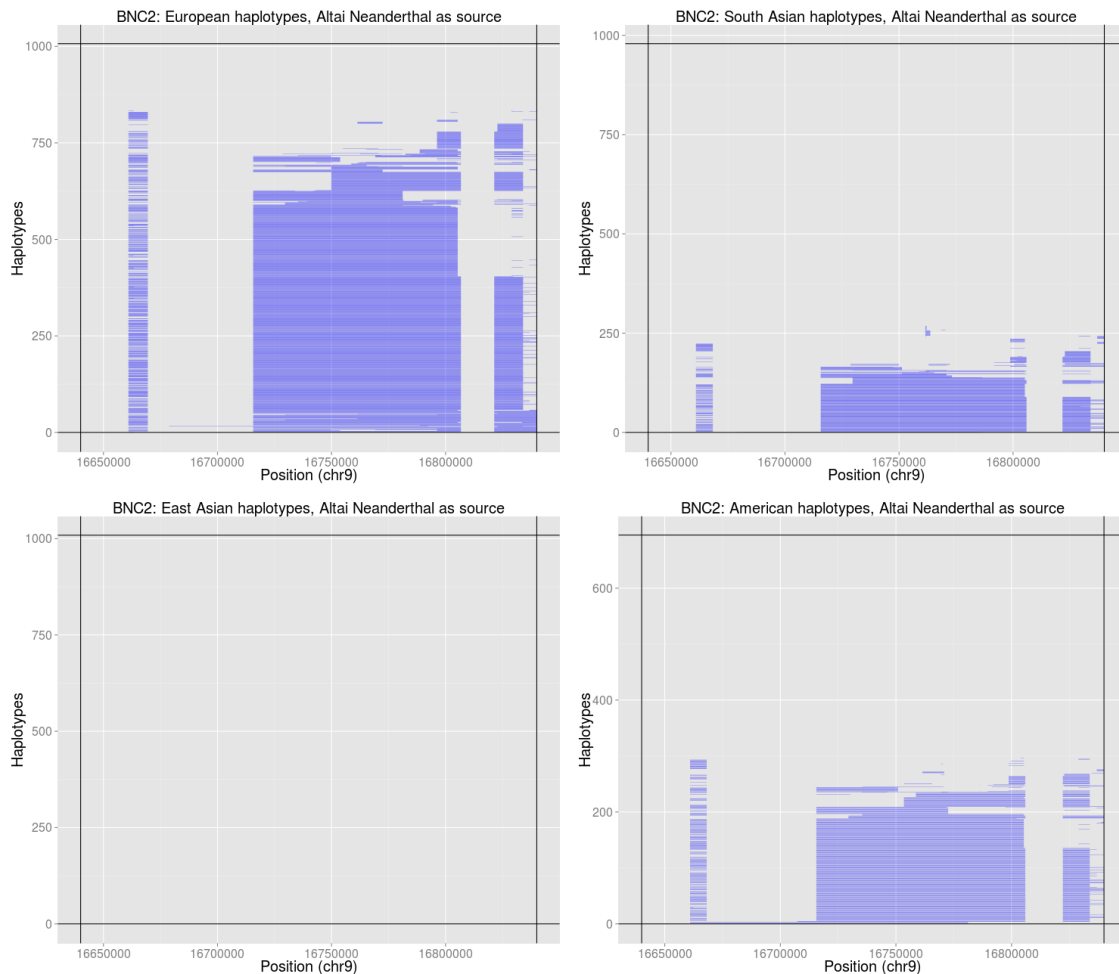


Figure S53: Introgressed tracks inferred in the four Non-African 1000 Genomes continental panels by an HMM [21] in the *BNC2* region, using the Altai Neanderthal genome as the archaic source.

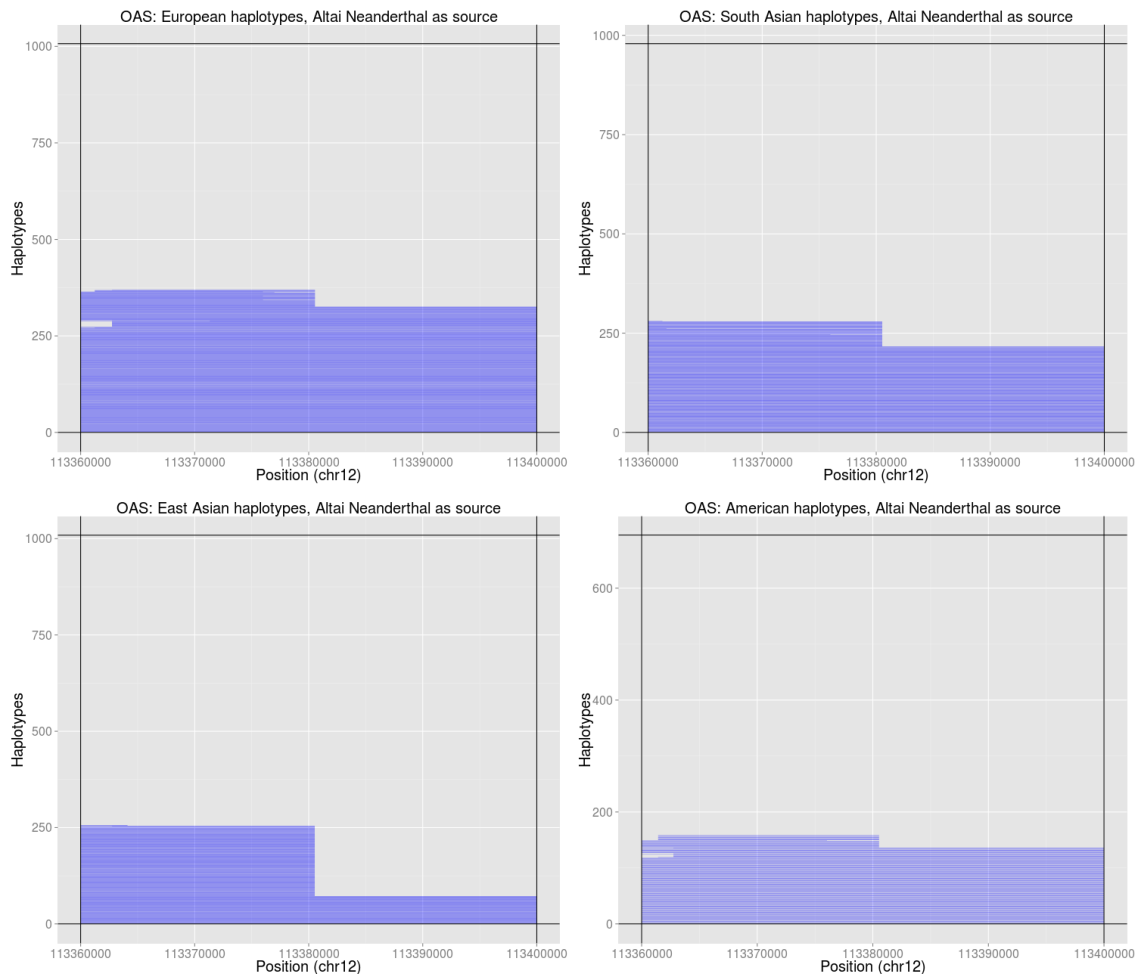


Figure S54: Introgressed tracks inferred in the four Non-African 1000 Genomes continental panels by an HMM [21] in the OAS region, using the Altai Neanderthal genome as the archaic source.

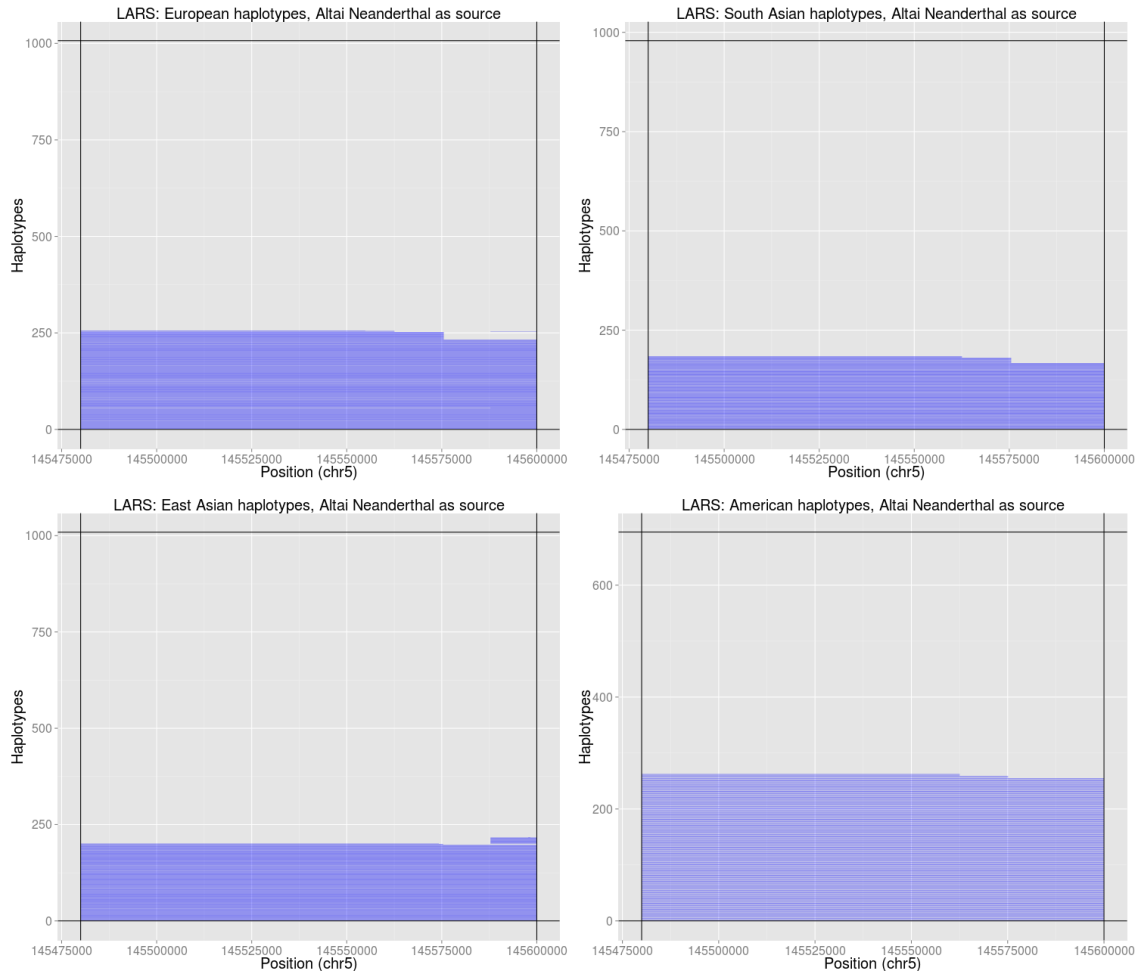


Figure S55: Introgressed tracks inferred in the four Non-African 1000 Genomes continental panels by an HMM [21] in the *LARS* region, using the Altai Neanderthal genome as the archaic source.

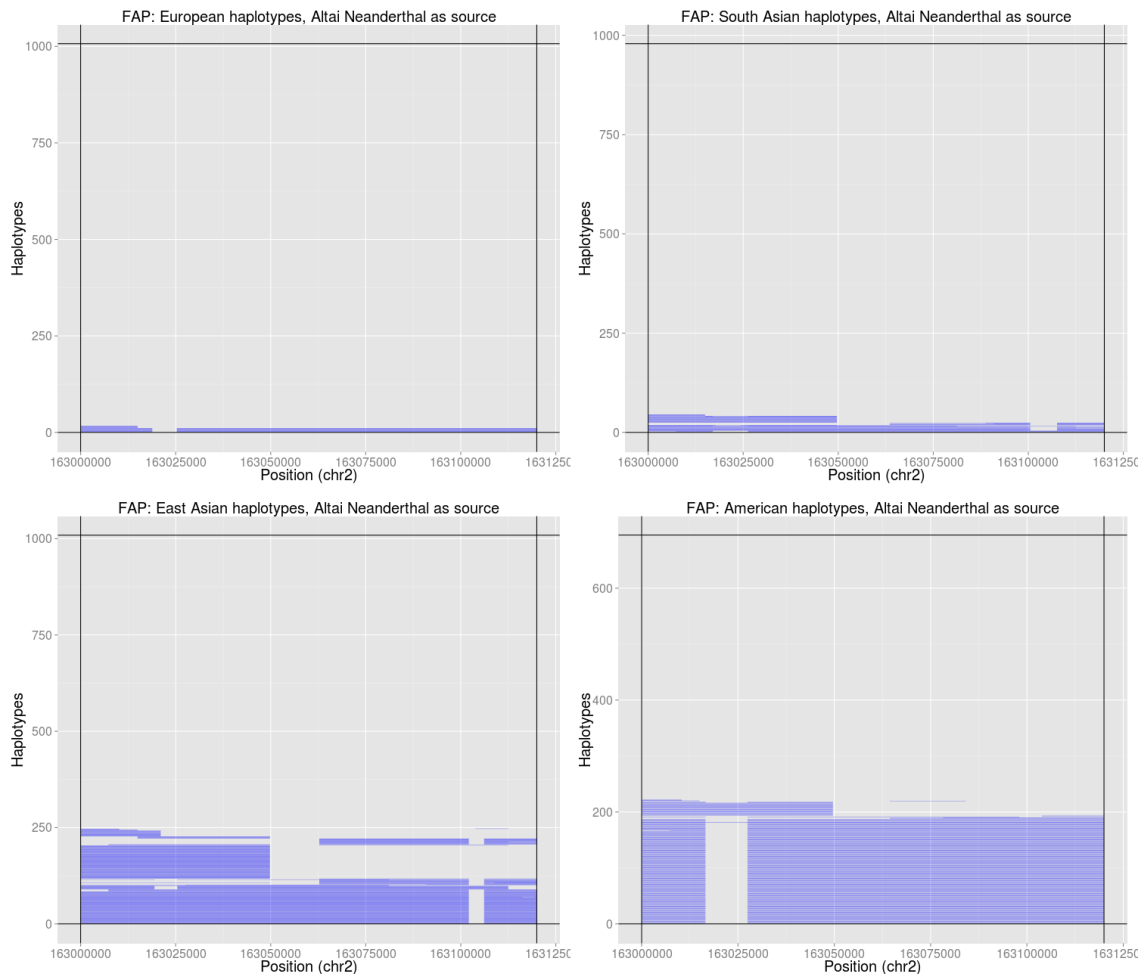


Figure S56: Introgressed tracks inferred in the four Non-African 1000 Genomes continental panels by an HMM [21] in the *FAP/IFIH1* region, using the Altai Neanderthal as the archaic source.

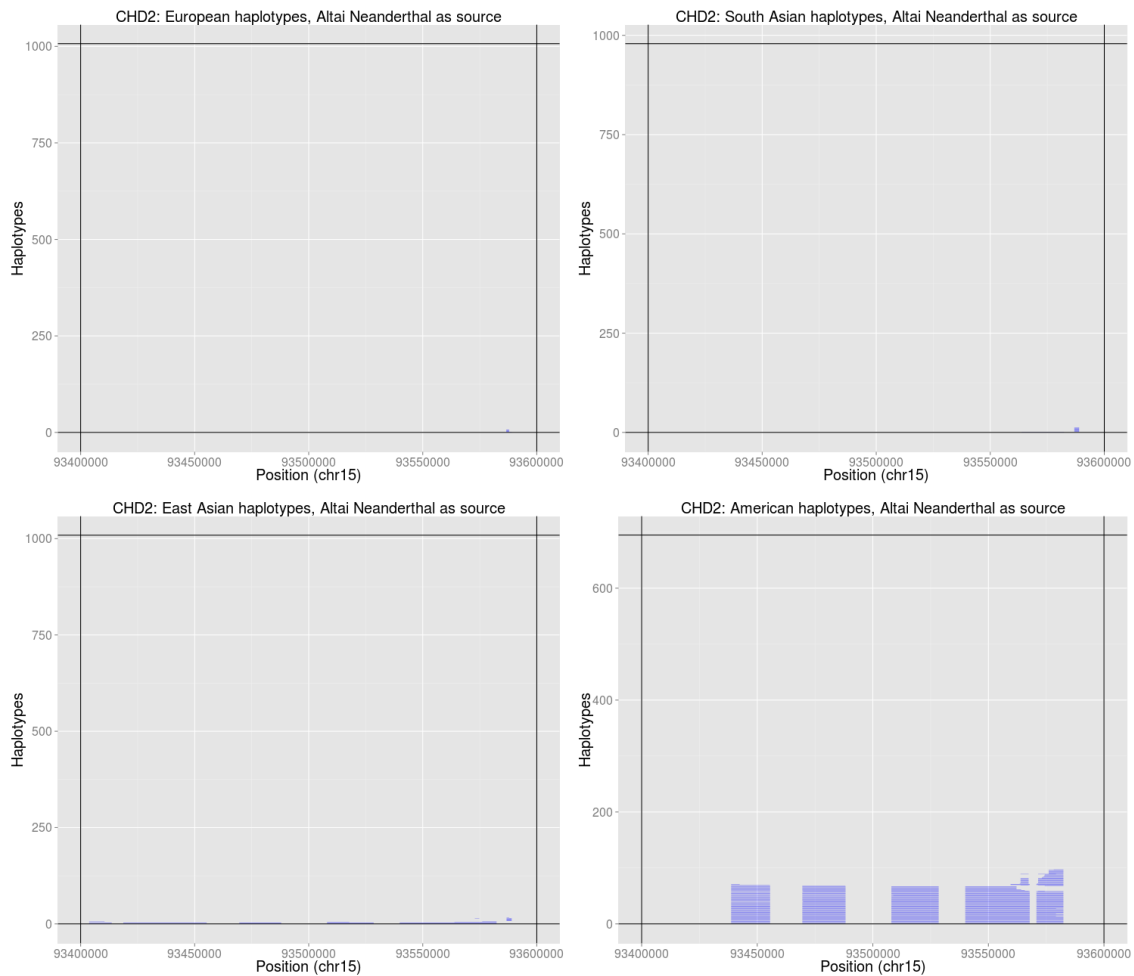


Figure S57: Introgressed tracks inferred in the four Non-African 1000 Genomes continental panels by an HMM [21] in the *CHD2* region, using the Altai Neanderthal genome as the archaic source.

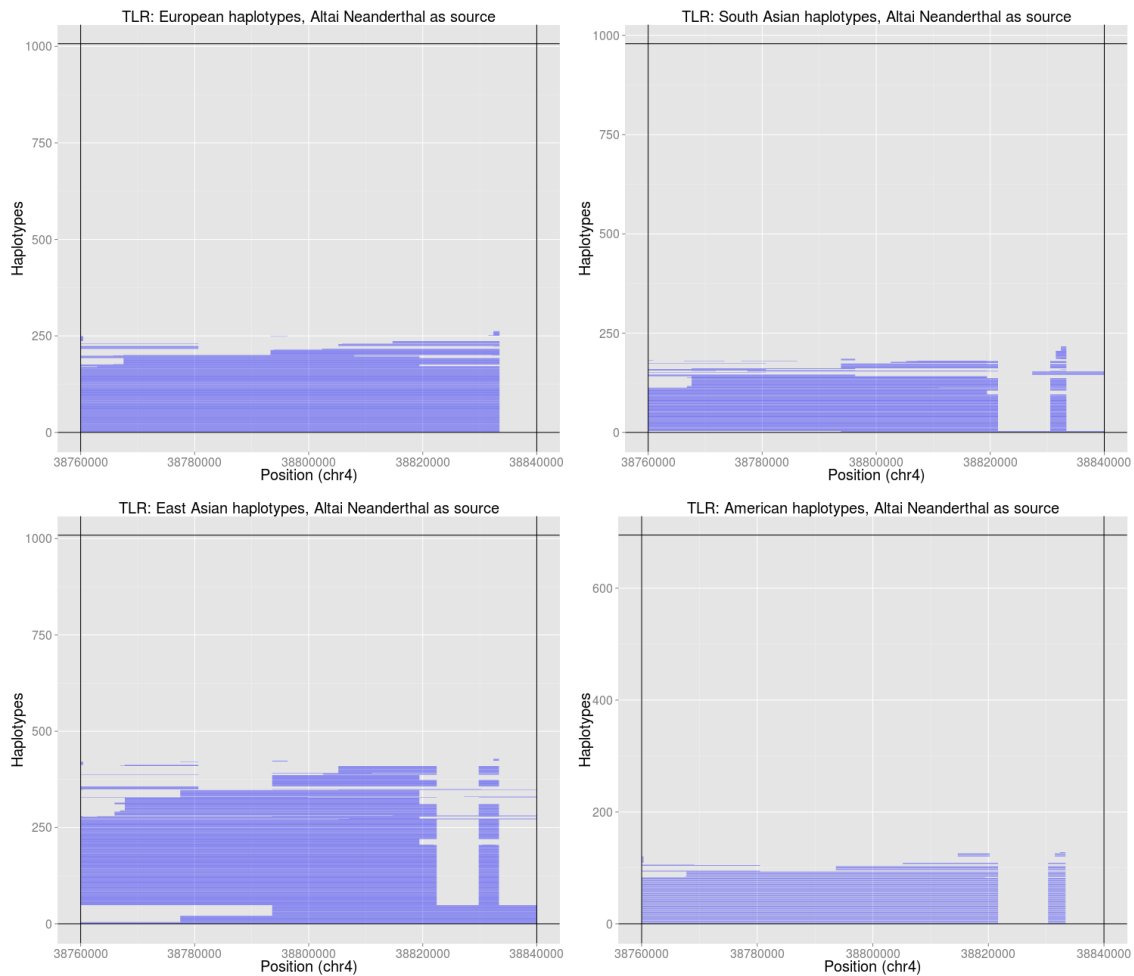


Figure S58: Introgressed tracks inferred in the four Non-African 1000 Genomes continental panels by an HMM [21] in the *TLR1-6* region, using the Altai Neanderthal genome as the archaic source.

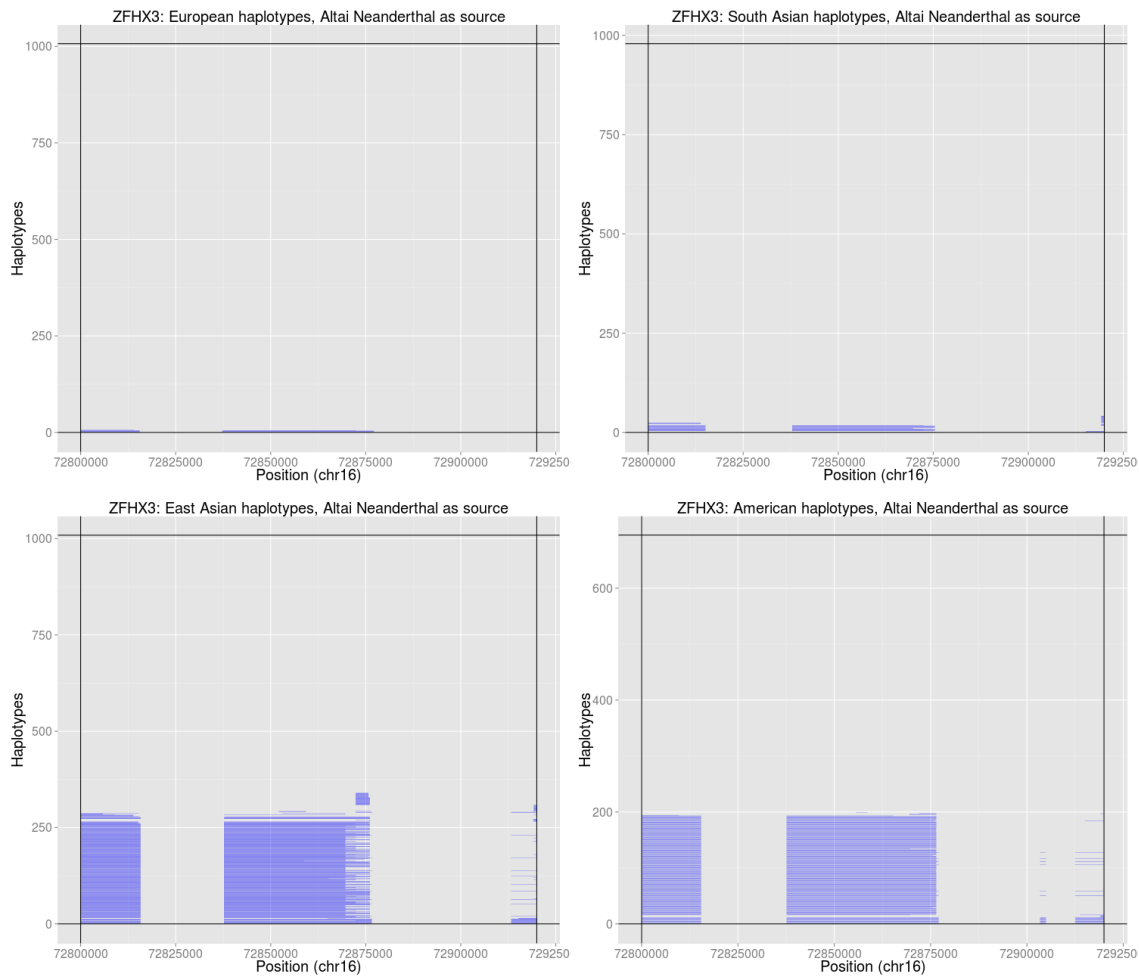


Figure S59: Introgressed tracks inferred in the four Non-African 1000 Genomes continental panels by an HMM [21] in the *ZFHX3* region, using the Altai Neanderthal genome as the archaic source.

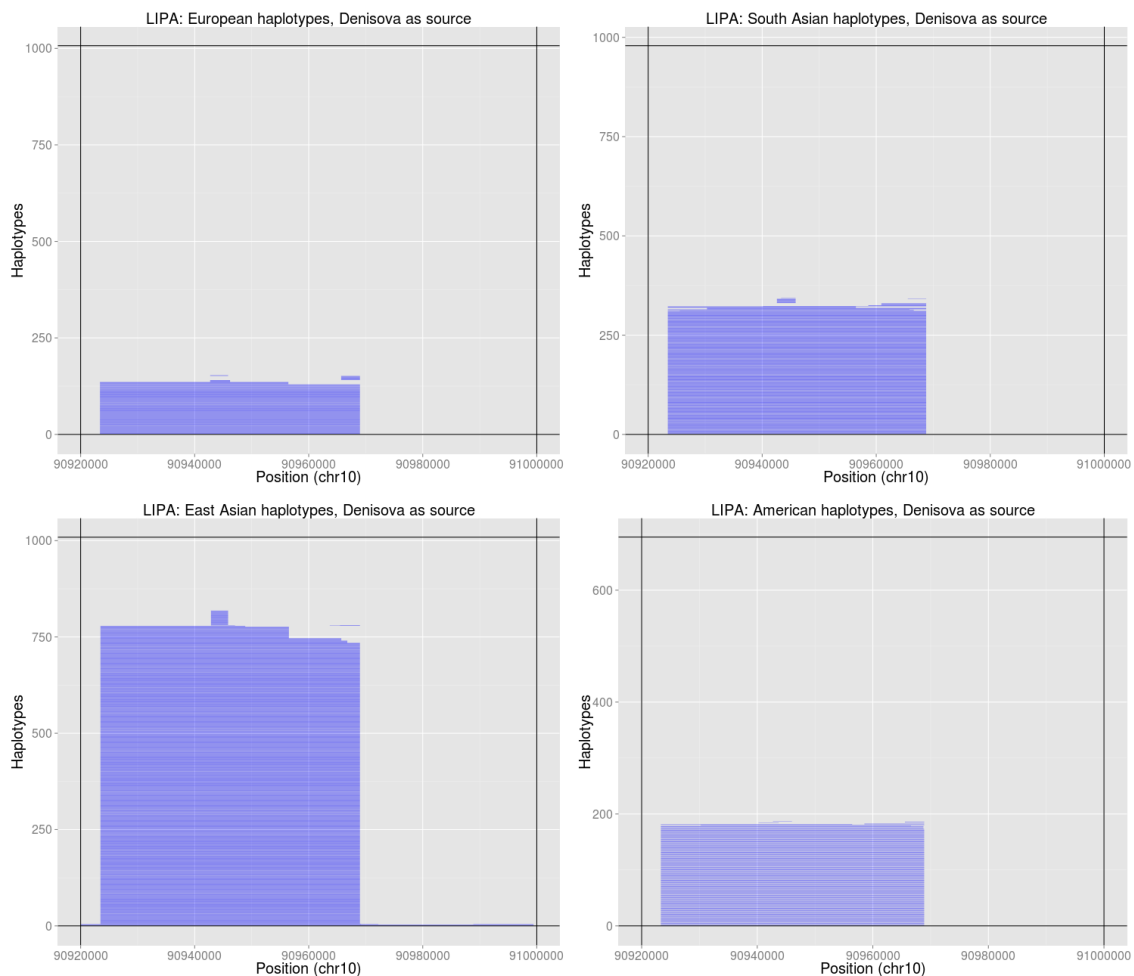


Figure S60: Introgressed tracks inferred in the four Non-African 1000 Genomes continental panels by an HMM [21] in the *LIPA* region, using the Denisova genome as the archaic source.

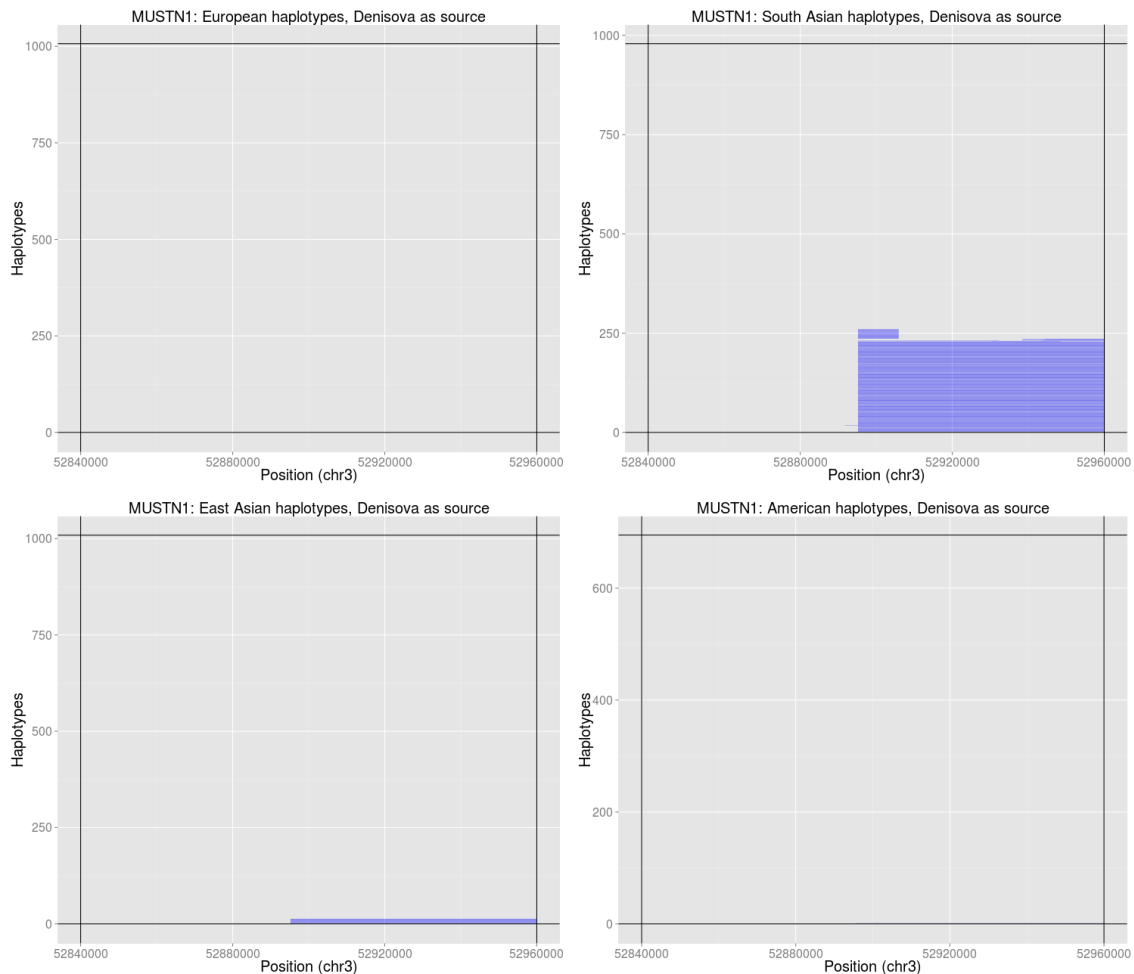


Figure S61: Introgressed tracks inferred in the four Non-African 1000 Genomes continental panels by an HMM [21] in the *MUSTN1* region, using the Denisova genome as the archaic source.